General Disclaimer

One or more of the Following Statements may affect this Document

- This document has been reproduced from the best copy furnished by the organizational source. It is being released in the interest of making available as much information as possible.

- This document may contain data, which exceeds the sheet parameters. It was furnished in this condition by the organizational source and is the best copy available.

- This document may contain tone-on-tone or color graphs, charts and/or pictures, which have been reproduced in black and white.

- This document is paginated as submitted by the original source.

- Portions of this document are not fully legible due to the historical nature of some of the material. However, it is the best reproduction available from the original submission.

WHOI-75-14

Woods Hole Oceanographic Institution

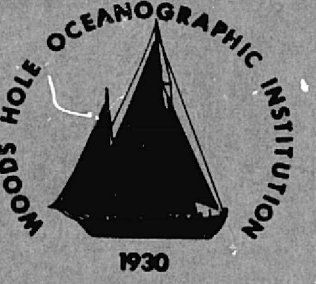

CATALOGUE OF GEOIDAL VARIATIONS FOR SIMPLE SEAFLOOR TOPOGRAPHIC FEATURES

By

Carl Bowin

February 1975

TECHNICAL REPORT

Prepared for the National Aeronautics and Space Administration under NASA contract number NAS6-2585.

WOODS HOLE, MASSACHUSETTS 02543

WHOI-75-14

CATALOGUE OF GEOIDAL VARIATIONS FOR SIMPLE SEAFLOOR TOPOGRAPHIC FEATURES

By

Carl Bowin

WOODS HOLE OCEANOGRAPHIC INSTITUTION
Woods Hole, Massachusetts 02543

February 1975

TECHNICAL REPORT

Prepared for the National Aeronautics and Space Administration under NASA contract number NAS6-2585.

Approved for Distribution J. R. Heirtzler

J. R. Heirtzler, Chairman
Department of Geology & Geophysics

ABSTRACT

This report presents a catalogue of theoretical geoidal variations for three types of structural features common to the earth's surface: seamounts, submarine ridges, and submarine trenches. These structures have been simulated by simple geometric shapes modeled in three-dimensions. A computer program calculated the potential and gravitational variations over the models. Profile plots of geoidal variations and free-air gravity anomalies are presented over cross-sections of the structures. The purpose of this catalogue is to provide a ready reference information set for comparison with satellite altimeter data for ocean areas.

TABLE OF CONTENTS

	Page No.
INTRODUCTION	1
METHOD	2
RESULTS	3
ACKNOWLEDGEMENTS	8
REFERENCES CITED	9
TABLE 1: INDEX TO SEAMOUNT MODELS	10
TABLE 2: INDEX TO RIDGE MODELS	11
TABLE 3: " " " "	12
TABLE 4: PARAMETERS FOR SEAMOUNT MODELS	13
TABLE 5: " " RIDGE MODELS	14
TABLE 6: " " TRENCH MODELS	15
TABLE 7: " " TOPOGRAPHY MODELS	16
TABLE 8: " " COMPENSATION MODELS	17
MODELS IN NUMERIC ORDER	following 17

INTRODUCTION

The accurate delineation of large scale topography of the sea surface is equivalent to surface gravity measurements and hence can be useful for determining mass anomalies in the earth's crust. Satellite altimeter data offers two advantages over normal shipboard gravity observations. First, large scale features of several hundred to several thousand kilometer width are traversed quickly by a satellite pass, and hence problems of datum levels and instrument drift tend to be minimized. Secondly, orbiting satellites easily cross regions of the earth's surface that are remote and hazardous for surface travel. The southern oceans and the Arctic Ocean are particularly obvious regions in point. The radar altimeter information obtained during the SKYLAB mission instrument testing has already provided useful data on the marine geoid (McGoogan, et al, 1974; Leitao and McGoogan, in press; Hoge, 1974; Bowin, 1974).

In order to assist in the evaluation and interpretation of the SKYLAB radar altimeter data, as well as that from future missions, a catalogue of theoretical geoidal variations has been prepared for three types of structural features: seamounts, submarine ridges, and submarine trenches. The purpose of this catalogue is to provide a ready reference information set for comparison with satellite altimeter data.

METHOD

For several years the gravity group at the Woods Hole Oceanographic Institution has been computing the gravitational attraction of models of crustal structure in their analyses of earth features. Recently a computer program (G3DC) was developed (Bowin et al, in press) to permit the rapid computation of the gravitational attraction of three dimensional models which take into account the curvature of a planetary surface. This program was needed particularly for studies of the gravity field of the moon, because the moon has a much smaller radius than the earth and because gravity observations are available at several heights above the lunar surface. Both these factors make it important to take into account the curvature of the moon's surface.

The potential of a mass varies inversely as the distance, whereas gravitational attraction varies inversely as the square of the distance. Accordingly, program logic was added to the three-dimensional gravity computation program mentioned above to compute the potential of each element of the model in addition to gravitational attraction. At each field point for which the computations are made, the potential and gravitational attraction are calculated for each body of the model as well as for the complete model. If the densities used in the model calculations are those corresponding to mass anomalies from homogeneous spherical shells, then the potential

values are those resulting from the anomalous mass and can be used directly in examining geoidal perturbations. If the full rock densities are used in the model, then the potential values obtained must be referenced to the potential value at some location where it is known or assumed. The results given in this catalogue were determined by the first method.

Use of the computer program described above allows geoidal variations to be determined directly for any given model without the need to first compute a gravity field, and then from that field calculate geoidal variations.

RESULTS

The crustal structure models constructed for this catalogue are in complete isostatic equilibrium, since that is generally the condition of the earth's surface. For some of the models we present the potential and gravity anomalies separately for the topography and for its compensating mass at depth. In that way the effect of the topography can be seen as if the topography were a load (in the case of seamounts and ridges) or deficiency (in the case of trenches) on the earth's crust. Such results are labeled with a suffix T (for topography) or C (for compensation). These results, of course, have larger magnitude variations of potential and gravity anomalies than do the models in isostatic equilibrium.

Three types of structures are presented: seamounts, simulated by vertical cones; ridges, simulated by horizontal triangular prisms; and trenches, also simulated by horizontal triangular prisms, but with the apex pointing downward rather than upward. All of these models are constructed from polygonal laminae which stack one upon the other to comprise the bodies of the model. The technique of this type of model construction is described by Talwani and Ewing (1960). If the laminae are thick, and the edges of the laminae are close to computation points, then the anomalies may show irregularities corresponding to the stair step edges of the three-dimensional model.

Seamount models are labeled with the letter S, ridge models with the letter H, and trench models with the letter D. A summary tabulation in numeric order is given in Tables 4,5,6,7, and 8.

To help the reader more easily assimilate the results, three tables have been prepared to suggest some ways by which the models might be examined. The models shown in Table 1 help demonstrate the results for varying crustal density and height of the seamount. Ridge models having the same base width, crustal density, and height are indicated by the model numbers in parentheses. Thus the same table also aids an understanding of the difference in anomalies resulting from linear and circular features.

For the seamount models of Table 1, it is seen that the maximum free-air gravity anomaly and the maximum geoid rise increases with increasing height of the seamount and increasing crustal density as would be expected. The same relations are true for the ridges. The magnitudes of these variations can be read from the model plots. A comparison of S-11 (water depth 4 km) with S-2 (water depth 5 km) and S-12 with S-3 shows that decreasing the depth of the mass anomalies affects more the free-air anomaly than the potential (geoid).

For seamounts with a crustal density of 2.8 g/cm^3, a base width of 80 km, and water depth of 4 km, the following models show the effect of different seamount heights: S-10 (5 km height, island with 1 km relief), S-11 (4 km height), and S-12 (2 km height). The magnitude of the gravity and geoid anomalies increases with increased height of the seamount. Note in S-10 that the anomalies plotted are for a line tangent to the shore of the island, not over the center of the feature. For seamounts with a constant height (5 km), water depth of 5 km, and a crustal density of 2.8 g/cm^3, the following models show the effect of different base width: S-15 (40 km width), S-13 (60 km width), S-14 (100 km width), and S-16 (120 km width). As the width increases, the geoid rise increases in magnitude, but the free-air anomaly decreases.

The effect of varying crustal density and base width for ridges

having a constant height (4 km) in water 5 km deep can be studied by examining the models given in Table 2. Free-air and geoid anomalies increase with increasing crustal density, but again, the free-air anomalies decrease whereas the geoid anomalies increase with increasing width of a ridge. Table 3 is an index to ridge models of constant crustal density (2.8 g/cm^3) and constant water depth (5 km) but with varying ridge height and width. As the reader now has learned, the magnitude of both the anomalies increases with increasing height, but different relationships occur with increasing width. Although the maximum free-air anomaly value decreases with increasing width, the integral of the positive portion of the free-air anomaly curve increases with increasing width. Models with varying width but a different water depth (2 km) are also indexed in Table 3.

The trench model numbers correspond directly with the ridge model numbers except that heights for the ridges are depths for trenches. Thus Tables 1, 2, and 3 serve also as indexes to the trench models if the H prefix is changed to D. The trenches have a 25 km thick normal crust instead of 5 km as in the seamount and ridge models, in order to avoid having the compensation mass penetrate through the bottom of some of the trench models. The relations of free-air and geoid anomalies described previously apply also to the trench models but with the anomalies being negative instead of positive features.

The isostatically compensated trench model structure is not characteristic of the deep-sea trenches associated with island arcs. These trenches are not in isostatic equilibrium, are sites of considerable mass deficiency, and hence are closer to the models with trench topography only (such as D-7T).

A comparison of the seamount and ridge models identified in Table 1 shows an interesting relation. For features of the same width and height, the ridge has a lower free-air gravity anomaly maximum but a higher geoidal rise than those of the seamount. This seemingly anomalous situation results from the greater gravitational effect of the compensation mass for the ridge than that for the seamount. It is only the vertical component of the gravitational attraction of anomalous masses in the model that contributes to the computed gravity anomaly values. Thus the greater effective mass deficiency of the compensation for ridge topography more than offsets the effect of its being at greater depth below sea level than the mass of the ridge topography. The free-air anomaly, therefore, is lower over the isostatically compensated ridge than over the isostatically compensated seamount of the same width even though the mass of the ridge is greater than that of the seamount.

ACKNOWLEDGEMENTS

I thank Joseph McGoogan and Samir Vincent for introducing me to SKYLAB radar altimeter data. Bruce Simon assisted in adding the potential calculations to the three-dimensional model program, Leon Gove helped in preparing the models for input to the program, and Gove and Edward Scheer plotted the results. This study was supported by the National Aeronautics and Space Administration under NASA Contract No. NAS6-2585.

REFERENCES CITED

McGoogan, J.T., C.D. Leitao, and W.T. Wells, 1974, SKYLAB Altimeter Applications, paper presented at Union of Radio Science International (URSI), Microwave Scattering and Emission Meeting, September 23-26, 1974.

Leitao, C.D., and J.T. McGoogan, in press, SKYLAB Radar Altimeter: Ocean Surface and Ocean Bottom Topography Correlation, Science.

Hoge, F.E., 1974, Expected SEASAT-A Scientific Results, SEASAT-A Scientific Contributions, NASA, Washington, p. 57-69.

Bowin, C., 1974, Comment on Sattelite Altimeter Data, SEASAT-A Scientific Contributions, NASA, Washington, p. 38.

Bowin, C., B. Simon, and W. Wollenhaupt, in press, Mascons, a Two Body Solution, Jour. Geophys. Res.

Talwani, M., and M. Ewing, 1960, Rapid Computation of Gravitational Attraction of Three Dimensional Bodies of Arbitrary Shape, Geophysics, v. 25, p. 203-225.

TABLE 1

INDEX TO SEAMOUNT MODELS

Seamount Height (km)

Crustal density (g/cm^3)	5	4	2
2.7	S - 7	S - 8 (H-17)	S - 9
2.8	S - 1 (H-4)	S - 2 (H-3)	S - 3 (H-1)
2.9	S - 4	S - 5 (H-21)	S - 6

Water depth = 5 km
Base width = 80 km

Corresponding ridge model numbers in parentheses

TABLE 2

INDEX TO RIDGE MODELS

Crustal density (g/cm^3)	Base Width (km) 80	100	200	500
2.7	H - 17	H - 20	H - 18	H - 19
2.8	H - 3	H - 15	H - 7	H - 11
2.9	H - 21	H - 24	H - 22	H - 23

Water depth = 5 km
Ridge height = 4 km

TABLE 3

INDEX TO RIDGE MODELS

Water depth (km)	5	5	5	2
Ridge height (km)	5	4	2	2
Base width (km) 80	H - 4	H - 3	H - 1	H - 2
100	H - 16	H - 15	H - 13	H - 14
200	H - 8	H - 7	H - 5	H - 6
500	H - 12	H - 11	H - 9	H - 10

Crustal density = 2.8 g/cm^3

TABLE 4

PARAMETERS FOR SEAMOUNT MODELS

Model #	Base Width	Height	Water Depth	Crust Thick.	Density (g/cm^3) Water	Crust	Mantle
S-1	80	5	5	5	1.03	2.8	3.3
S-2	80	4	5	5	"	"	"
S-3	80	2	5	5	"	"	"
S-4	80	5	5	5	1.03	2.9	3.3
S-5	80	4	5	5	"	"	"
S-6	80	2	5	5	"	"	"
S-7	80	5	5	5	1.03	2.7	3.3
S-8	80	4	5	5	"	"	"
S-9	80	2	5	5	"	"	"
S-10	80	5	4	5	1.03	2.8	3.3
S-11	80	4	4	5	"	"	"
S-12	80	2	4	5	"	"	"
S-13	60	5	5	5	1.03	2.8	3.3
S-14	100	5	5	5	"	"	"
S-15	40	5	5	5	"	"	"
S-16	120	5	5	5	"	"	"

TABLE 5

PARAMETERS FOR RIDGE MODELS

Model #	Base Width	Height	Water Depth	Crust Thick.	Density (g/cm^3) Water	Crust	Mantle
H-1	80	2	5	5	1.03	2.8	3.3
H-2	80	2	2	5	"	"	"
H-3	80	4	5	5	"	"	"
H-4	80	5	5	5	"	"	"
H-5	200	2	5	5	1.03	2.8	3.3
H-6	200	2	2	5	"	"	"
H-7	200	4	5	5	"	"	"
H-8	200	5	5	5	"	"	"
H-9	500	2	5	5	1.03	2.8	3.3
H-10	500	2	2	5	"	"	"
H-11	500	4	5	5	"	"	"
H-12	500	5	5	5	"	"	"
H-13	100	2	5	5	1.03	2.8	3.3
H-14	100	2	2	5	"	"	"
H-15	100	4	5	5	"	"	"
H-16	100	5	5	5	"	"	"
H-17	80	4	5	5	1.03	2.7	3.3
H-18	200	4	5	5	"	"	"
H-19	500	4	5	5	"	"	"
H-20	100	4	5	5	"	"	"
H-21	80	4	5	5	1.03	2.9	3.3
H-22	200	4	5	5	"	"	"
H-23	500	4	5	5	"	"	"
H-24	100	4	5	5	"	"	"

TABLE 6

PARAMETERS FOR TRENCH MODELS

Model #	Trench Width	Trench Depth	Water Depth	Crust Thick.	Density (g/cm^3) Water	Crust	Mantle
D-1	80	2	5	25	1.03	2.8	3.3
D-2	80	2	2	25	"	"	"
D-3	80	4	5	25	"	"	"
D-4	80	5	5	25	"	"	"
D-5	200	2	5	25	1.03	2.8	3.3
D-6	200	2	2	25	"	"	"
D-7	200	4	5	25	"	"	"
D-8	200	5	5	25	"	"	"
D-9	500	2	5	25	1.03	2.8	3.3
D-10	500	2	2	25	"	"	"
D-11	500	4	5	25	"	"	"
D-12	500	5	5	25	"	"	"
D-13	100	2	5	25	1.03	2.8	3.3
D-14	100	2	2	25	"	"	"
D-15	100	4	5	25	"	"	"
D-16	100	5	5	25	"	"	"
D-17	80	4	5	25	1.03	2.7	3.3
D-18	200	4	5	25	"	"	"
D-19	500	4	5	25	"	"	"
D-20	100	4	5	25	"	"	"
D-21	80	4	5	25	1.03	2.9	3.3
D-22	200	4	5	25	"	"	"
D-23	500	4	5	25	"	"	"
D-24	100	4	5	25	"	"	"

TABLE 7

PARAMETERS FOR TOPOGRAPHY MODELS

SEAMOUNTS

Model #	Base Width	Height	Water Depth	Crust Thick.	Density (g/cm^3) Water	Crust	Mantle
S-1T	80	5	5	5	1.03	2.8	3.3
S-4T	80	5	5	5	1.03	2.9	3.3
S-7T	80	5	5	5	1.03	2.7	3.3
S-10T1	80	5	4	5	1.03	2.8	3.3
	(portion above sea level)						
S-10T2	80	5	4	5	1.03	2.8	3.3
	(portion below sea level)						
S-13T	60	5	5	5	1.03	2.8	3.3
S-14T	100	5	5	5	1.03	2.8	3.3
S-15T	40	5	5	5	1.03	2.8	3.3
S-16T	120	5	5	5	1.03	2.8	3.3

RIDGES

H-1T	80	2	5	5	1.03	2.8	3.3
H-2T	80	2	2	5	"	"	"
H-3T	80	4	5	5	"	"	"
H-4T	80	5	5	5	"	"	"

TRENCHES

		Depth					
D-1T	80	2	5	25	1.03	2.8	3.3
D-2T	80	2	2	25	"	"	"
D-3T	80	4	4	25	"	"	"
D-4T	80	5	5	25	"	"	"
D-7T	200	4	5	25	"	"	"
D-11T	500	4	5	25	"	"	"
D-23T	500	4	5	25	1.03	2.9	3.3

TABLE 8

PARAMETERS FOR COMPENSATION MODELS

SEAMOUNTS

Model #	Base Width	Height	Water Depth	Crust Thick.	Density (g/cm^3) Water	Crust	Mantle
S-1C	80	5	5	5	1.03	2.8	3.3
S-4C	80	5	5	5	1.03	2.9	3.3
S-7C	80	5	5	5	1.03	2.7	3.3
S-10C	80	5	4	5	1.03	2.8	3.3
S-13C	60	5	5	5	1.03	2.8	3.3
S-14C	100	5	5	5	1.03	2.8	3.3
S-15C	40	5	5	5	1.03	2.8	3.3
S-16C	120	5	5	5	1.03	2.8	3.3

RIDGES

H-4C	80	5	5	5	1.03	2.8	3.3

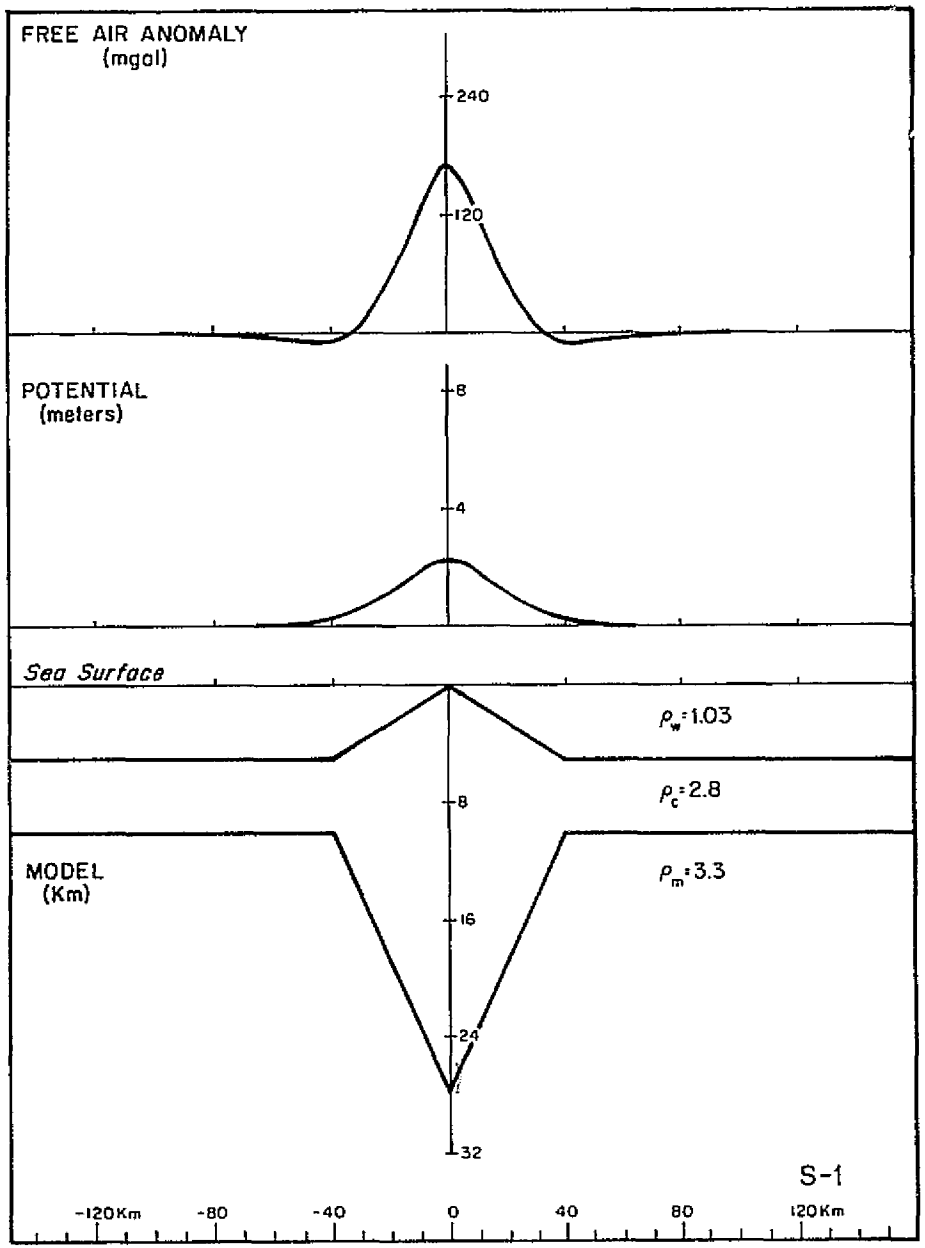
FREE AIR ANOMALY
(mgal)
240
120
POTENTIAL
(meters)
8
4
Sea Surface
ρ_w=1.03
ρ_c=2.8
MODEL
(Km)
ρ_m=3.3
8
16
24
32
S-1
-120Km
-80
-40
0
40
80
120Km

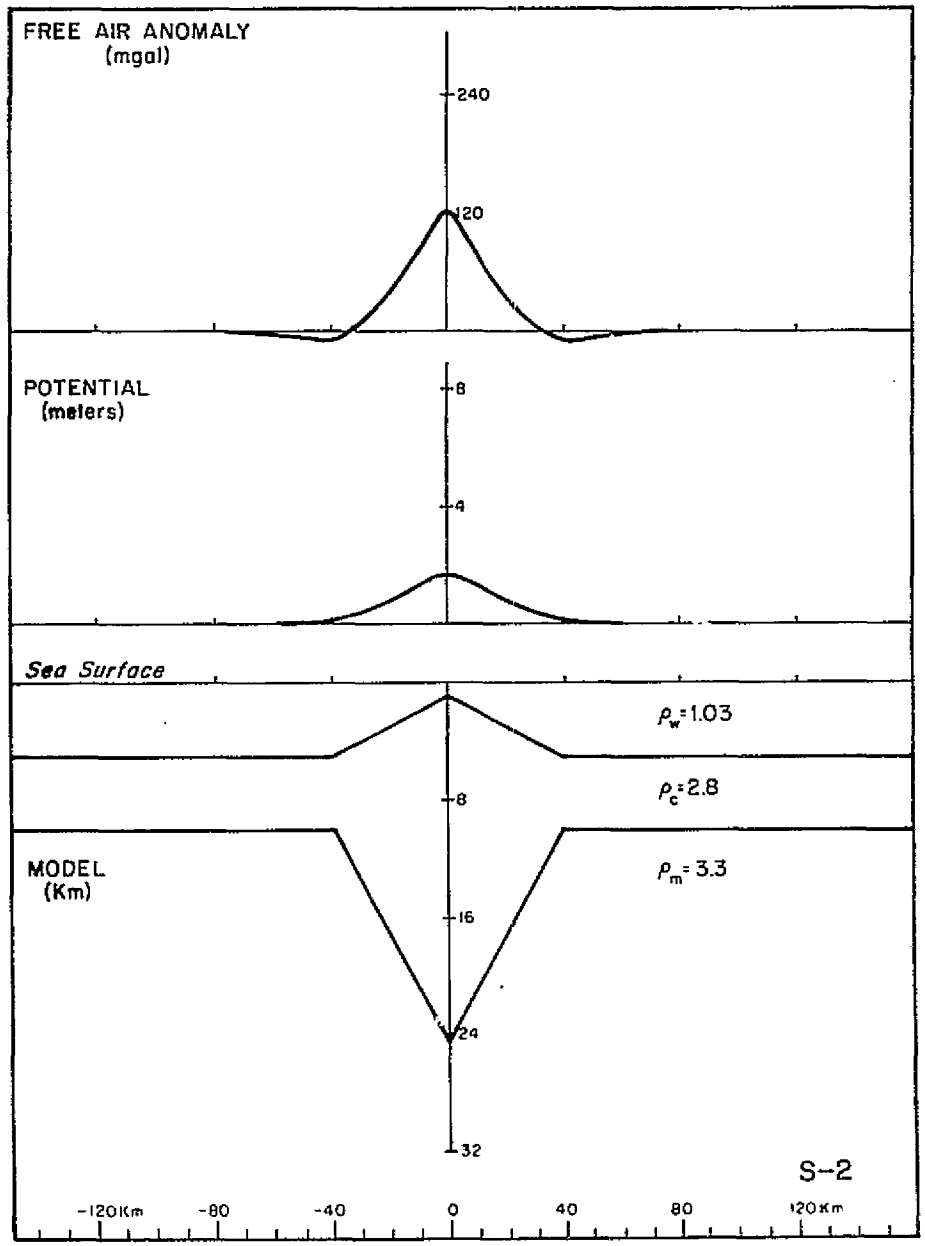
FREE AIR ANOMALY
(mgal)
240
120
POTENTIAL
(meters)
8
4
Sea Surface
ρ_w=1.03
ρ_c=2.8
MODEL
(Km)
ρ_m=3.3
8
16
24
32
S-2
-120Km
-80
-40
0
40
80
120Km

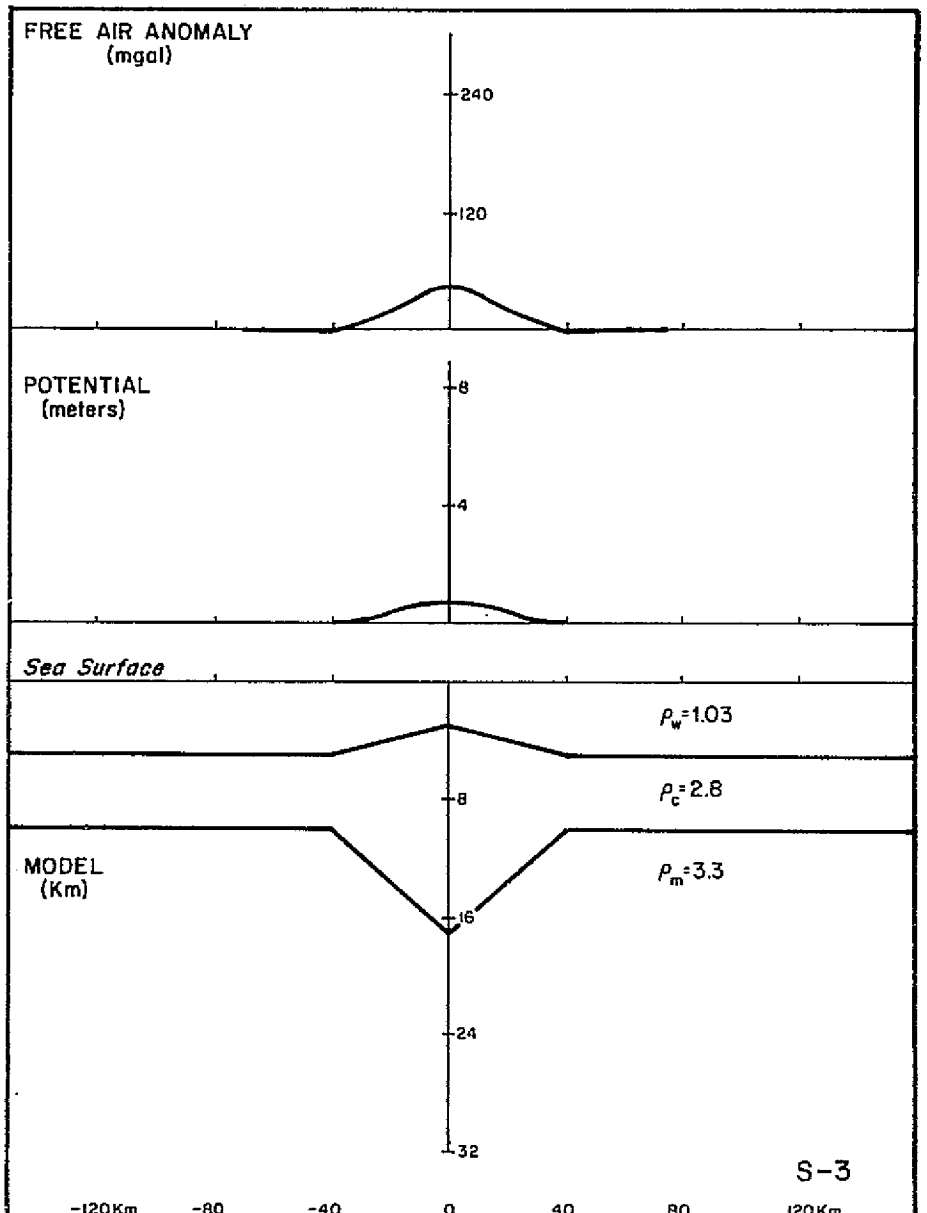
FREE AIR ANOMALY
(mgal)
240
120
POTENTIAL
(meters)
8
4
Sea Surface
ρ_w=1.03
ρ_c=2.8
8
MODEL
(Km)
ρ_m=3.3
16
24
32
S-3
-120Km
-80
-40
0
40
80
120Km

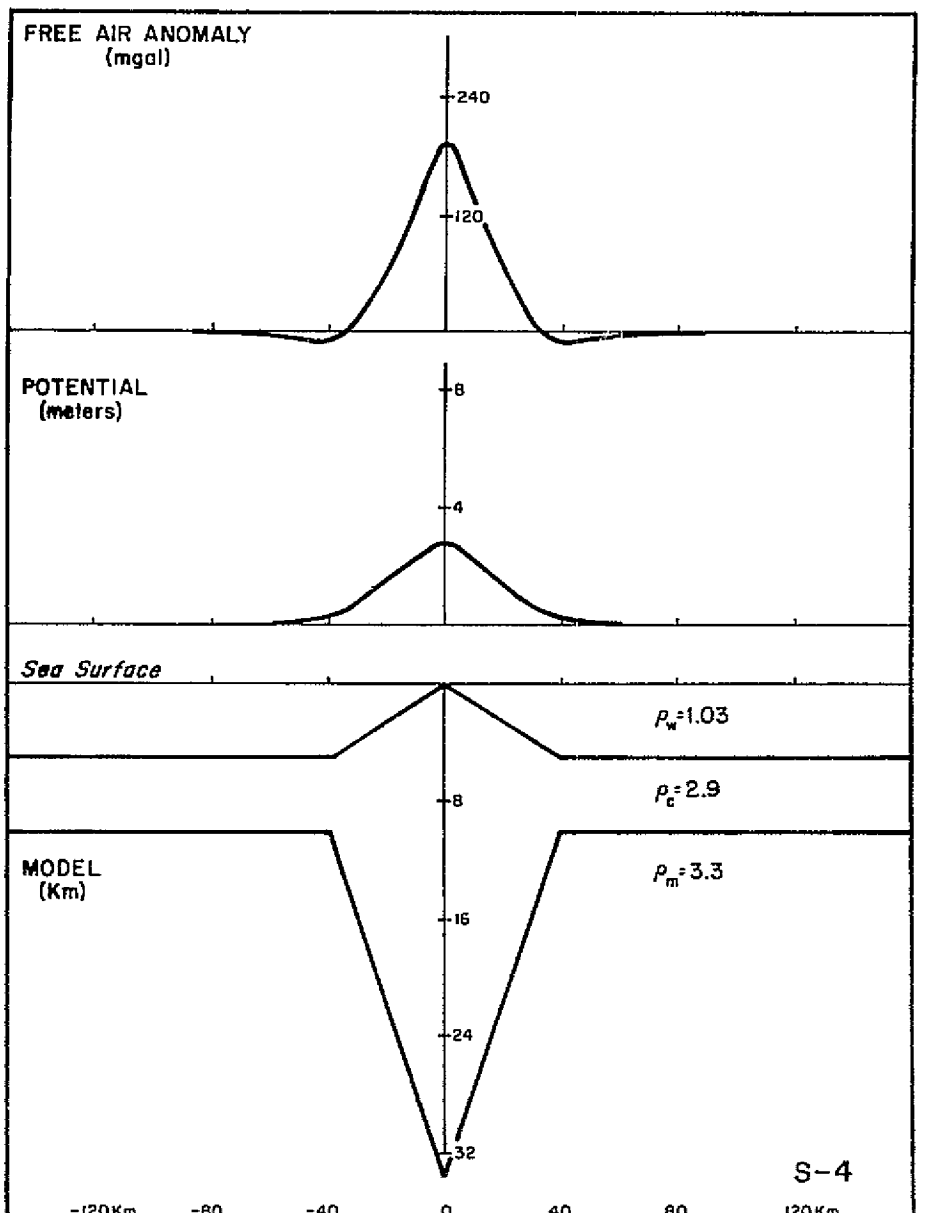
FREE AIR ANOMALY
(mgal)
240
120
POTENTIAL
(meters)
8
4
Sea Surface
ρ_w=1.03
ρ_c=2.9
8
MODEL
(Km)
ρ_m=3.3
16
24
32
S-4
-120Km
-80
-40
0
40
80
120Km

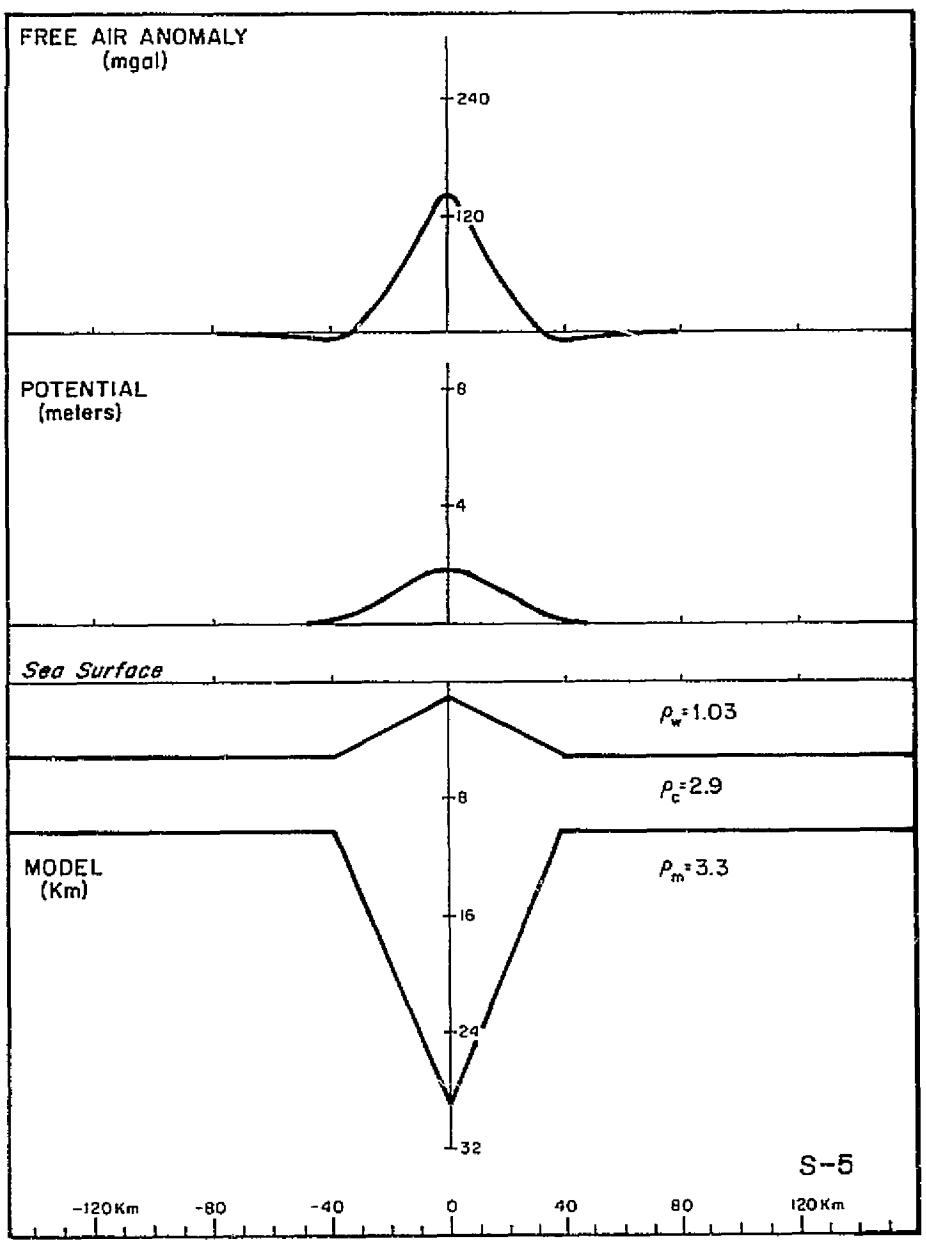
FREE AIR ANOMALY
(mgal)
240
120
POTENTIAL
(meters)
8
4
Sea Surface
ρ_w=1.03
ρ_c=2.9
8
MODEL
(Km)
ρ_m=3.3
16
24
32
S-5
-120Km
-80
-40
0
40
80
120Km

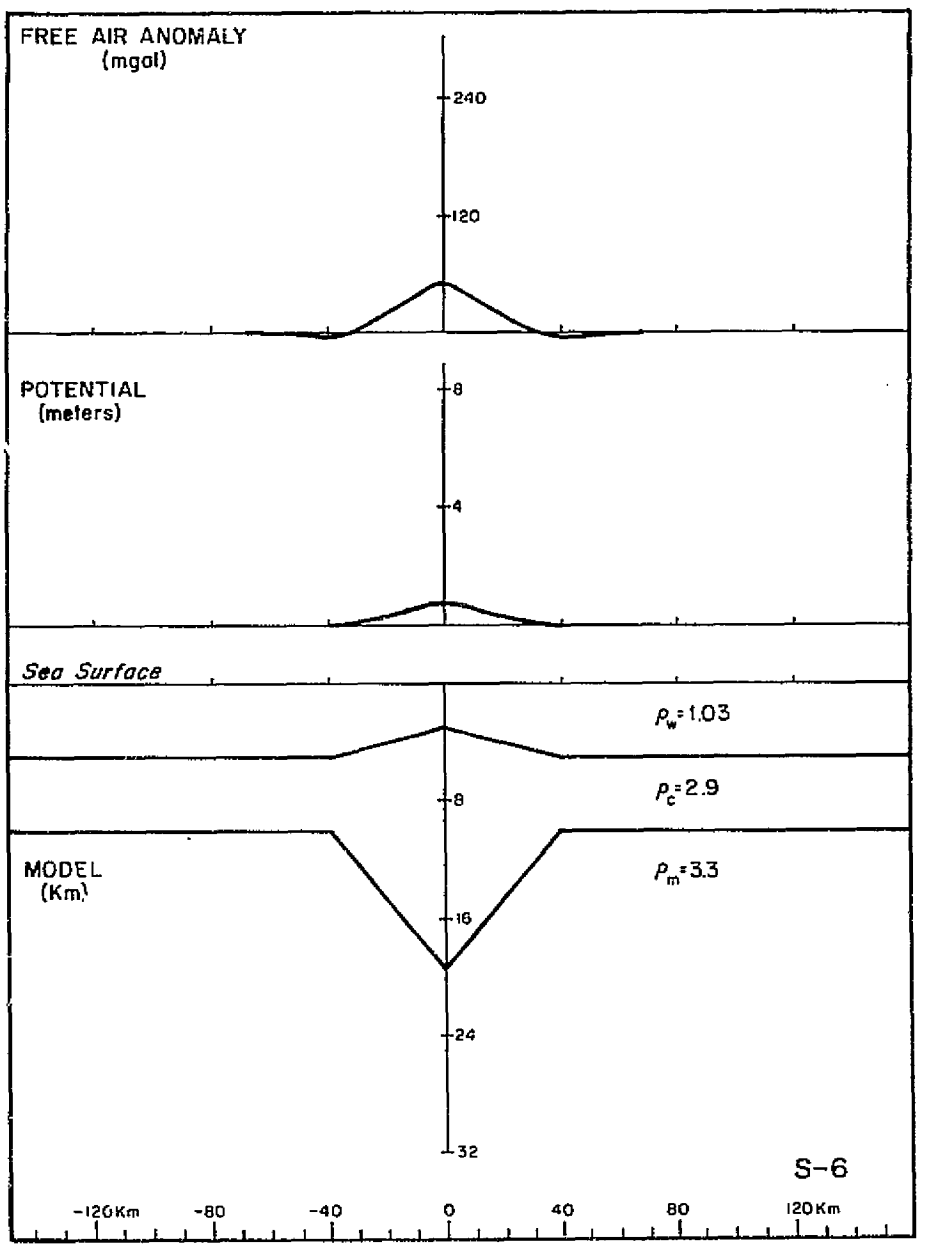
FREE AIR ANOMALY
(mgal)
240
120
POTENTIAL
(meters)
8
4
Sea Surface
ρ_w=1.03
ρ_c=2.9
8
MODEL
(Km)
ρ_m=3.3
16
24
32
S-6
-120Km
-80
-40
0
40
80
120Km

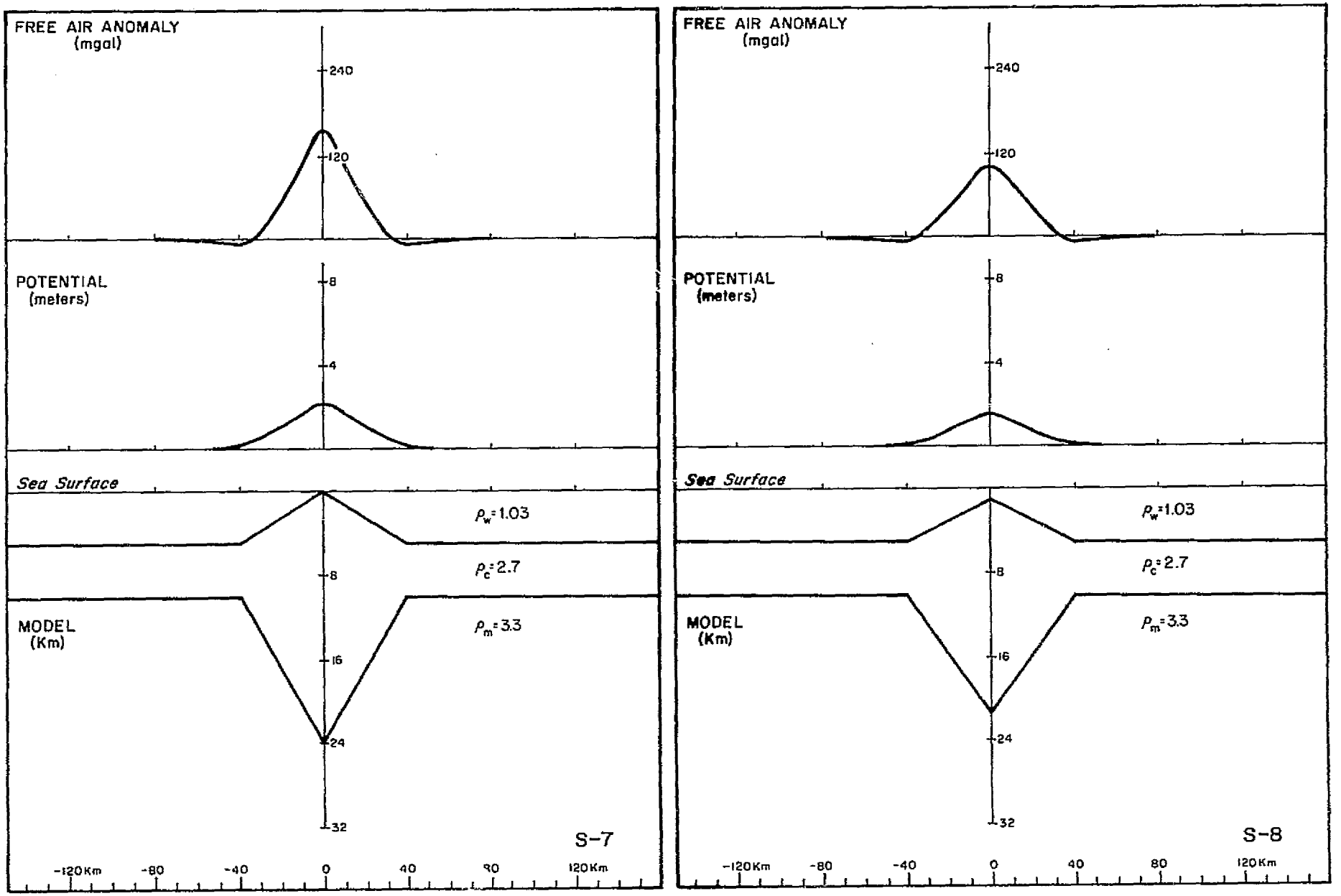
FREE AIR ANOMALY
(mgal)
240
120
POTENTIAL
(meters)
8
4
Sea Surface
ρ_w=1.03
ρ_c=2.7
ρ_m=3.3
MODEL
(Km)
8
16
24
32
S-7
-120Km
-80
-40
0
40
80
120Km
FREE AIR ANOMALY
(mgal)
240
120
POTENTIAL
(meters)
8
4
Sea Surface
ρ_w=1.03
ρ_c=2.7
ρ_m=3.3
MODEL
(Km)
8
16
24
32
S-8
-120Km
-80
-40
0
40
80
120Km

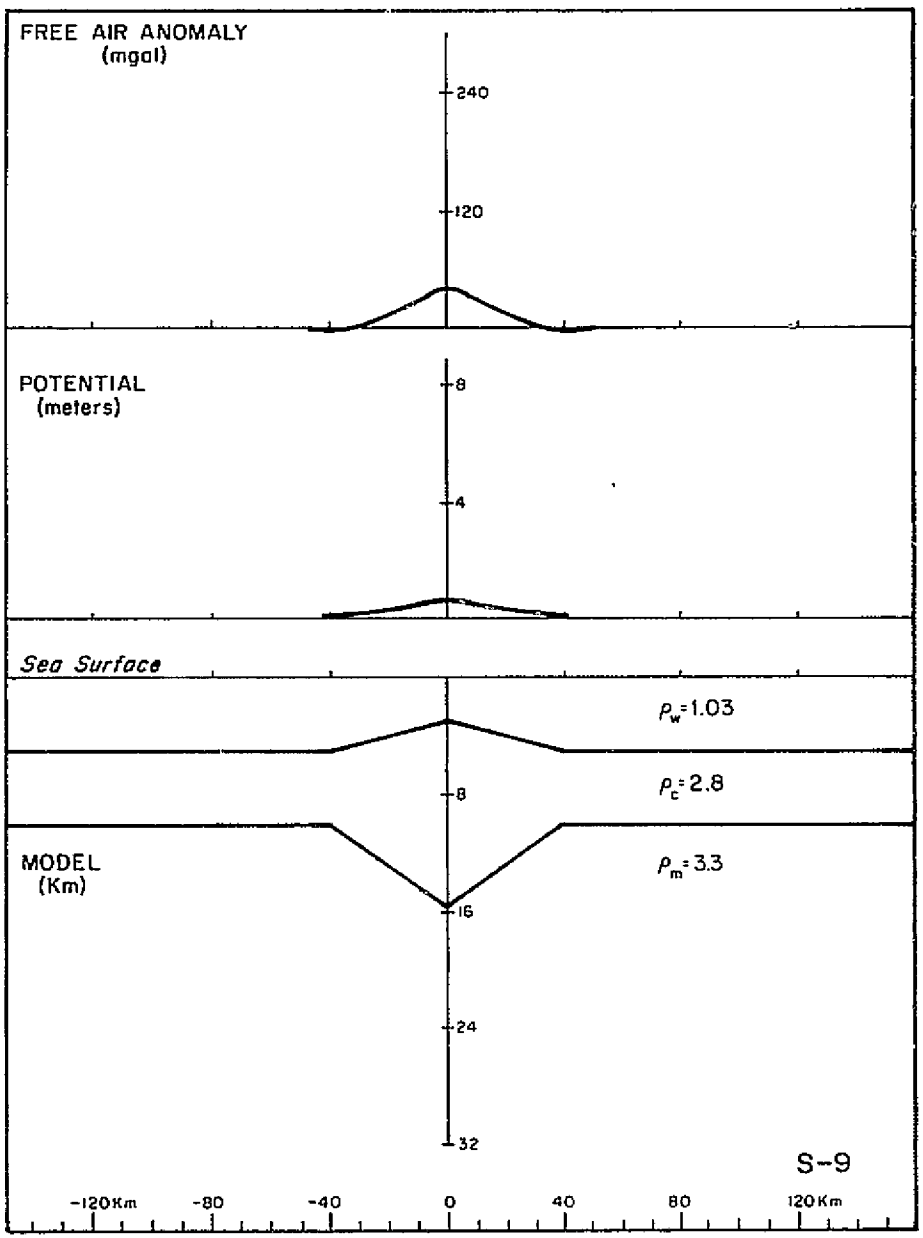
FREE AIR ANOMALY
(mgal)
240
120
POTENTIAL
(meters)
8
4
Sea Surface
ρ_w=1.03
ρ_c=2.8
8
MODEL
(Km)
ρ_m=3.3
16
24
32
S-9
-120Km
-80
-40
0
40
80
120Km

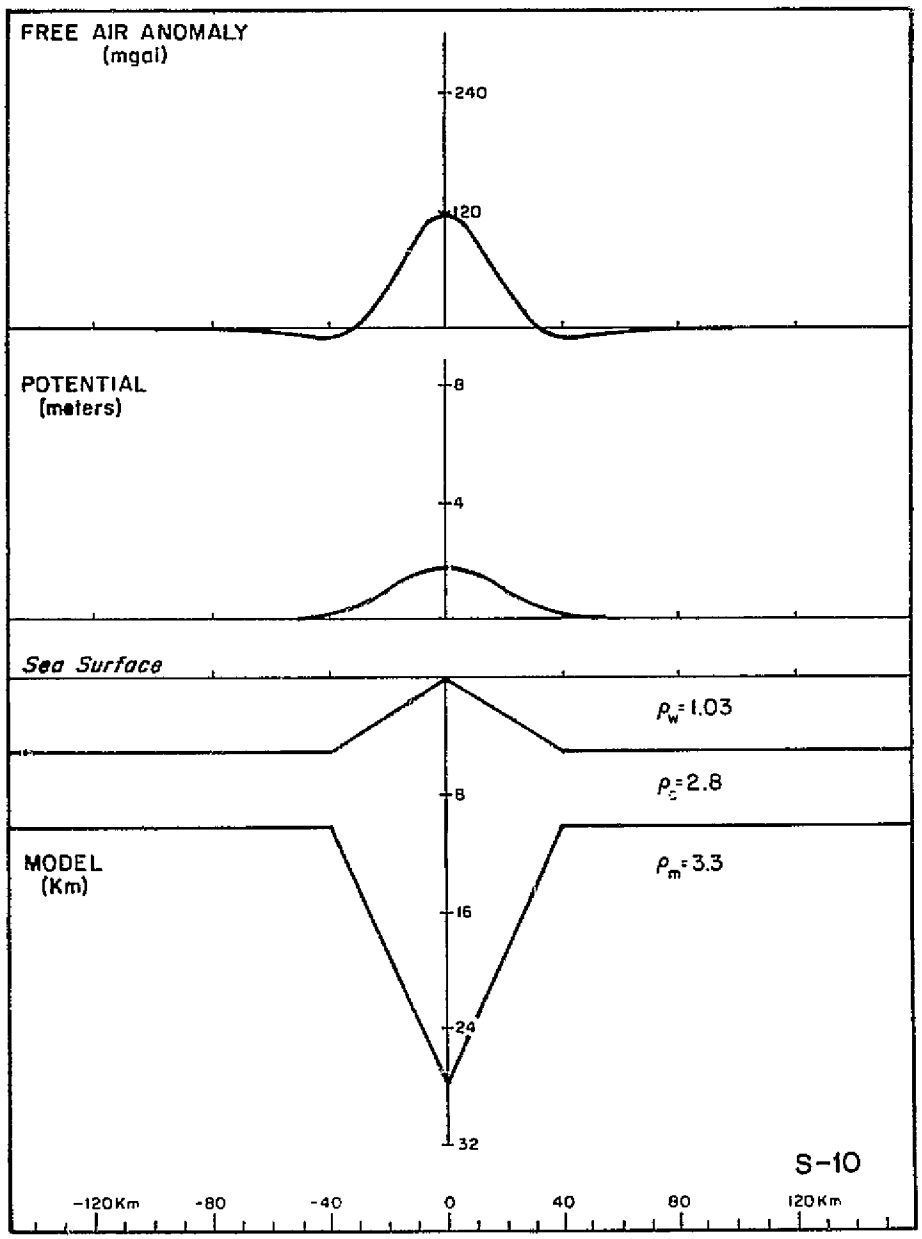
FREE AIR ANOMALY
(mgal)
240
120
POTENTIAL
(meters)
8
4
Sea Surface
ρ_w=1.03
ρ_c=2.8
8
MODEL
(Km)
ρ_m=3.3
16
24
32
S-10
-120Km
-80
-40
0
40
80
120Km

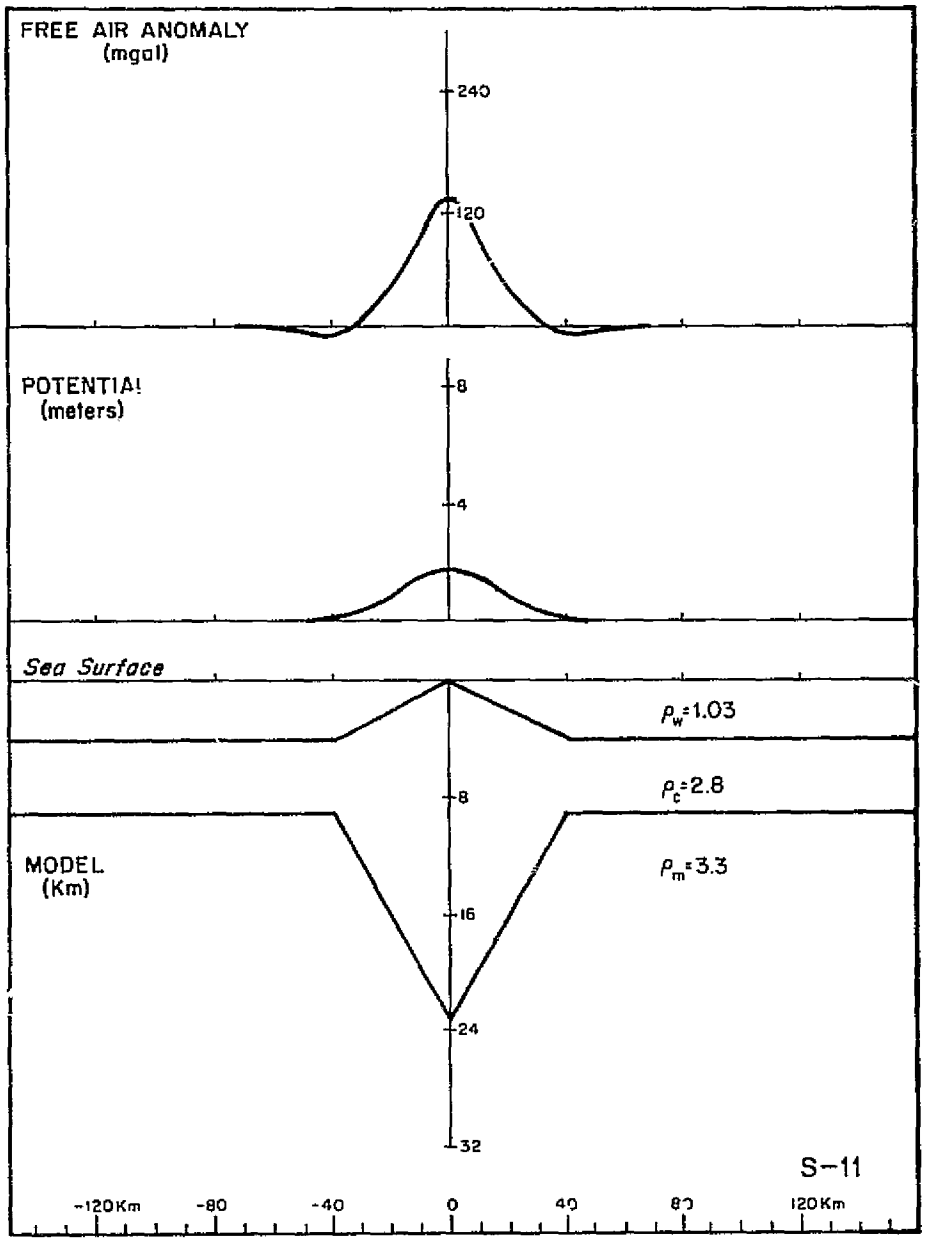
FREE AIR ANOMALY
(mgal)
240
120
POTENTIAL
(meters)
8
4
Sea Surface
ρ_w=1.03
ρ_c=2.8
8
MODEL
(Km)
ρ_m=3.3
16
24
32
S-11
-120Km
-80
-40
0
40
80
120Km

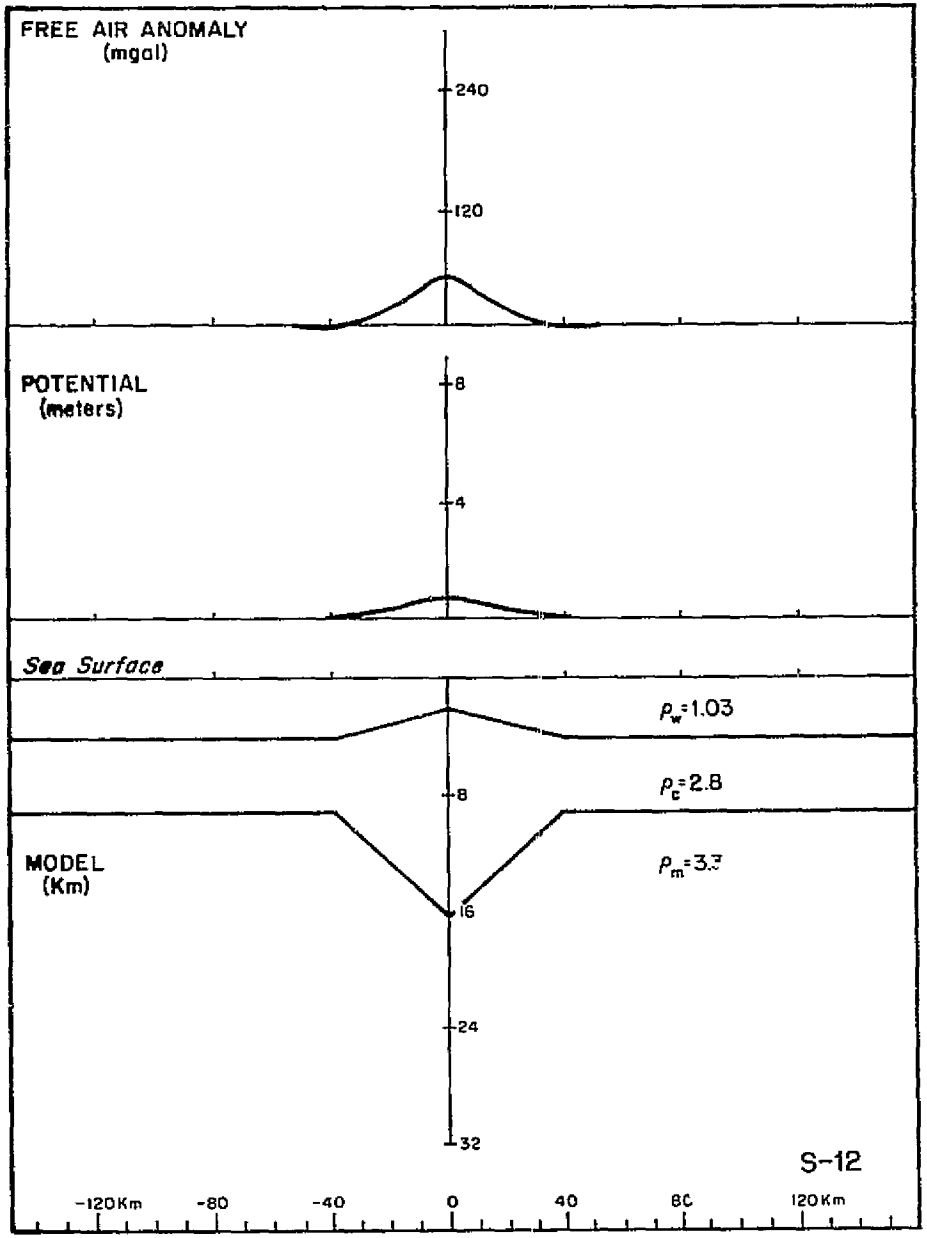
FREE AIR ANOMALY
(mgal)
240
120
POTENTIAL
(meters)
8
4
Sea Surface
ρ_w=1.03
ρ_c=2.8
8
MODEL
(Km)
ρ_m=3.3
16
24
32
S-12
-120Km
-80
-40
0
40
80
120Km

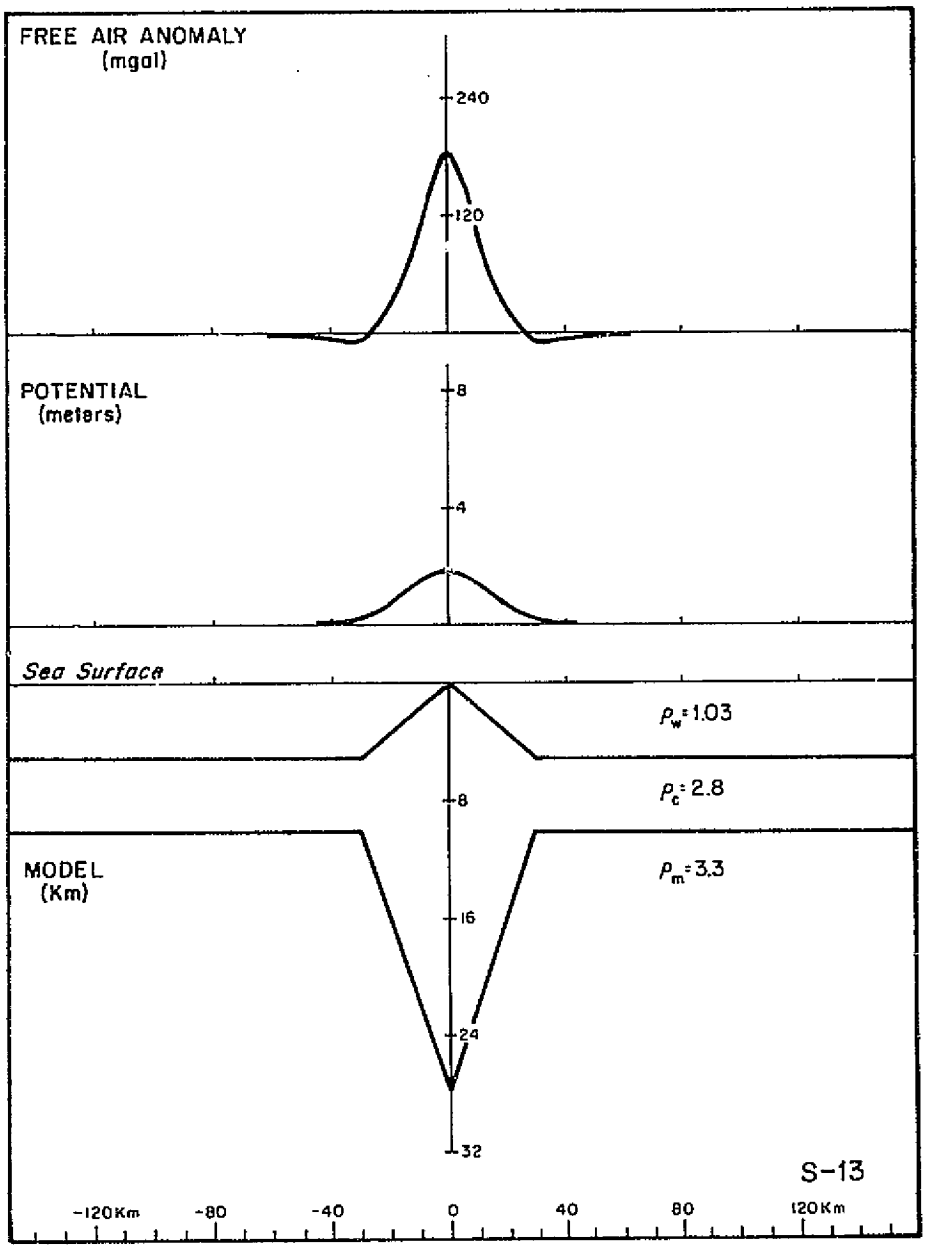
FREE AIR ANOMALY
(mgal)
240
120
POTENTIAL
(meters)
8
4
Sea Surface
ρ_w=1.03
ρ_c=2.8
8
MODEL
(Km)
ρ_m=3.3
16
24
32
S-13
-120Km
-80
-40
0
40
80
120Km

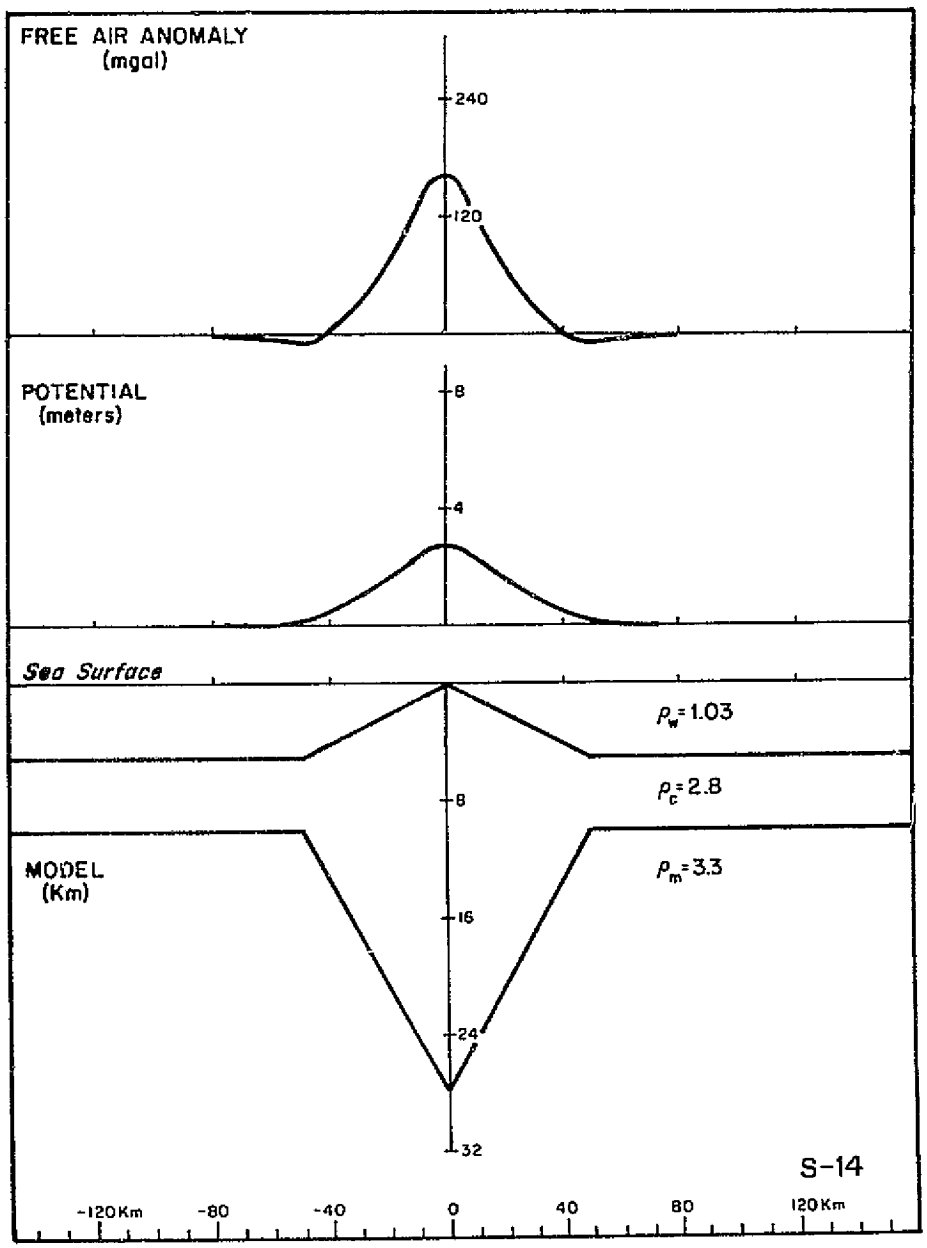
FREE AIR ANOMALY
(mgal)
240
120
POTENTIAL
(meters)
8
4
Sea Surface
ρ_w=1.03
ρ_c=2.8
8
MODEL
(Km)
ρ_m=3.3
16
24
32
S-14
-120Km
-80
-40
0
40
80
120Km

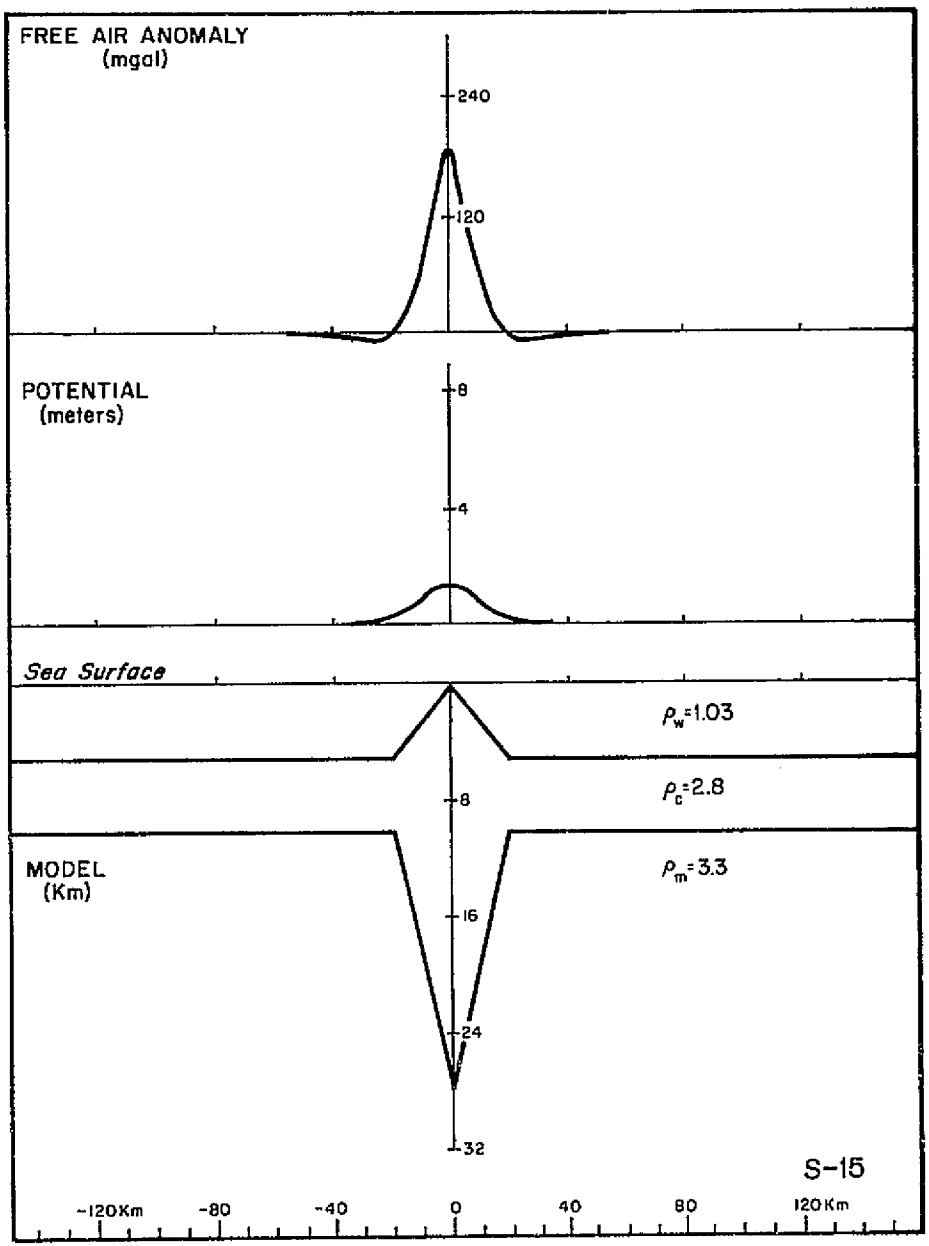
FREE AIR ANOMALY
(mgal)
240
120
POTENTIAL
(meters)
8
4
Sea Surface
ρ_w=1.03
ρ_c=2.8
8
MODEL
(Km)
ρ_m=3.3
16
24
32
S-15
-120Km
-80
-40
0
40
80
120Km

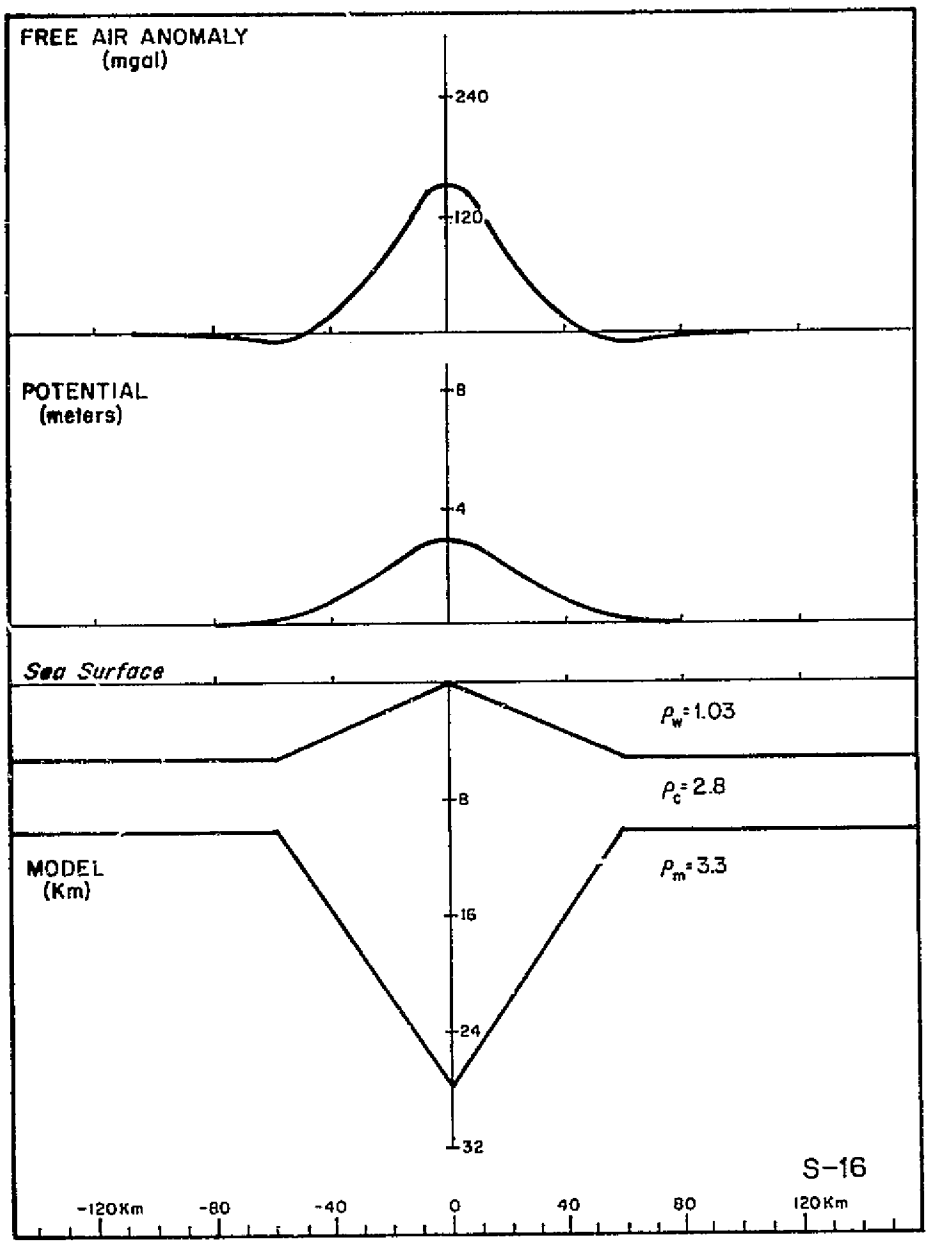
FREE AIR ANOMALY
(mgal)
240
120
POTENTIAL
(meters)
8
4
Sea Surface
ρ_w=1.03
ρ_c=2.8
8
MODEL
(Km)
ρ_m=3.3
16
24
32
S-16
-120Km
-80
-40
0
40
80
120Km

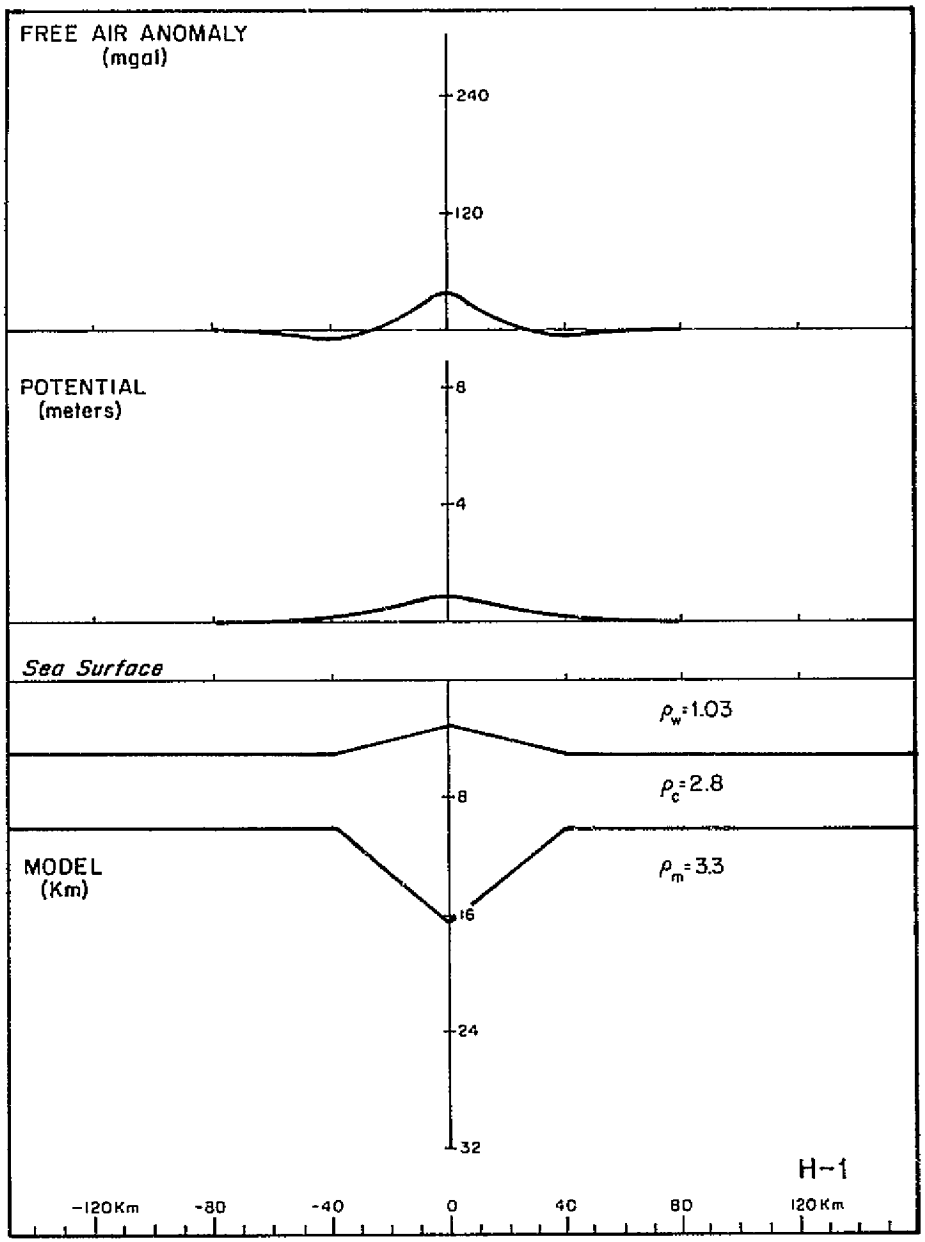
FREE AIR ANOMALY
(mgal)
240
120
POTENTIAL
(meters)
8
4
Sea Surface
ρ_w=1.03
ρ_c=2.8
8
MODEL
(Km)
ρ_m=3.3
16
24
32
H-1
-120Km
-80
-40
0
40
80
120Km

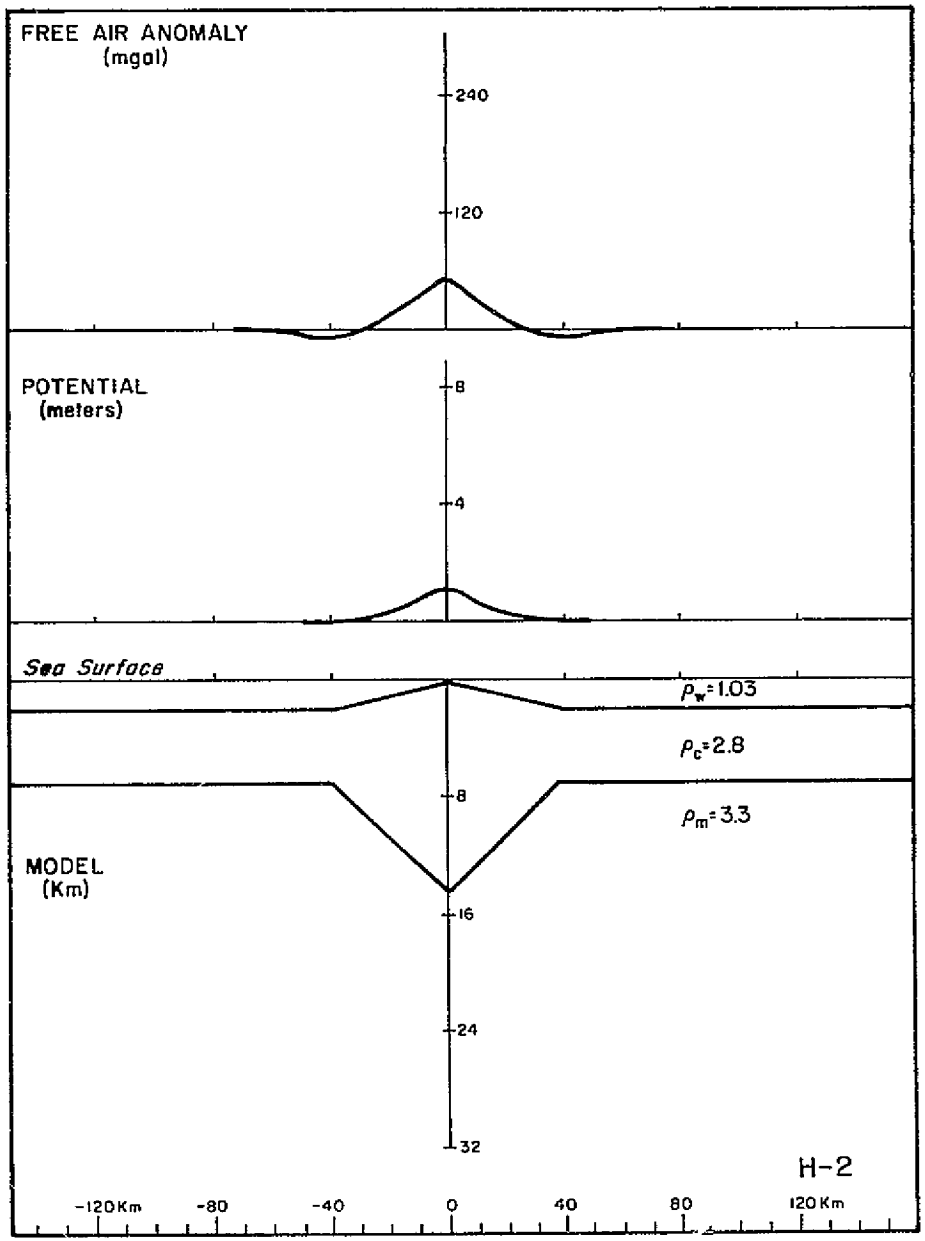
FREE AIR ANOMALY
(mgal)
240
120
POTENTIAL
(meters)
8
4
Sea Surface
ρ_w=1.03
ρ_c=2.8
8
MODEL
(Km)
ρ_m=3.3
16
24
32
H-2
-120Km
-80
-40
0
40
80
120Km

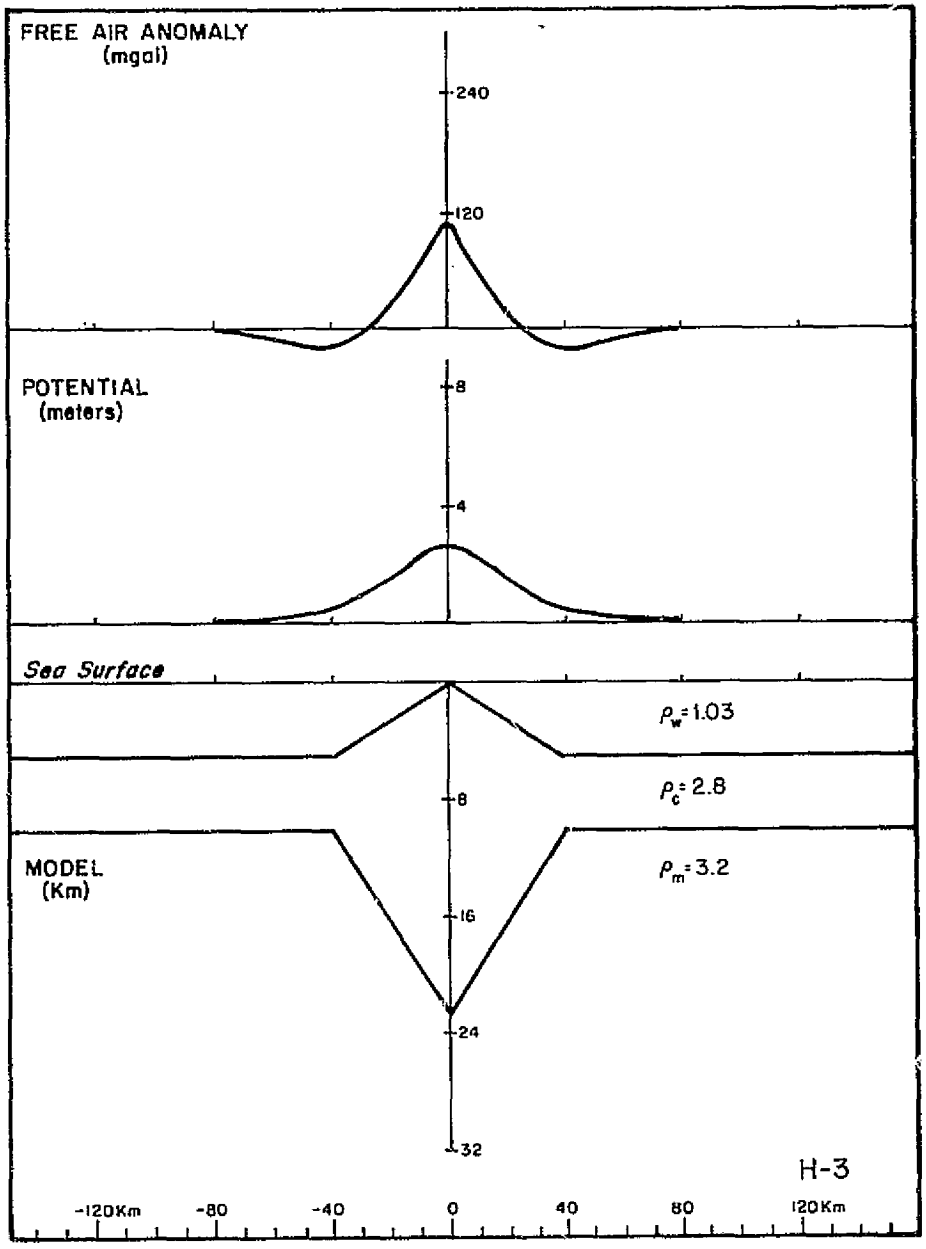
FREE AIR ANOMALY
(mgal)
240
120
POTENTIAL
(meters)
8
4
Sea Surface
ρ_w = 1.03
ρ_c = 2.8
8
MODEL
(Km)
ρ_m = 3.2
16
24
32
H-3
-120Km
-80
-40
0
40
80
120Km

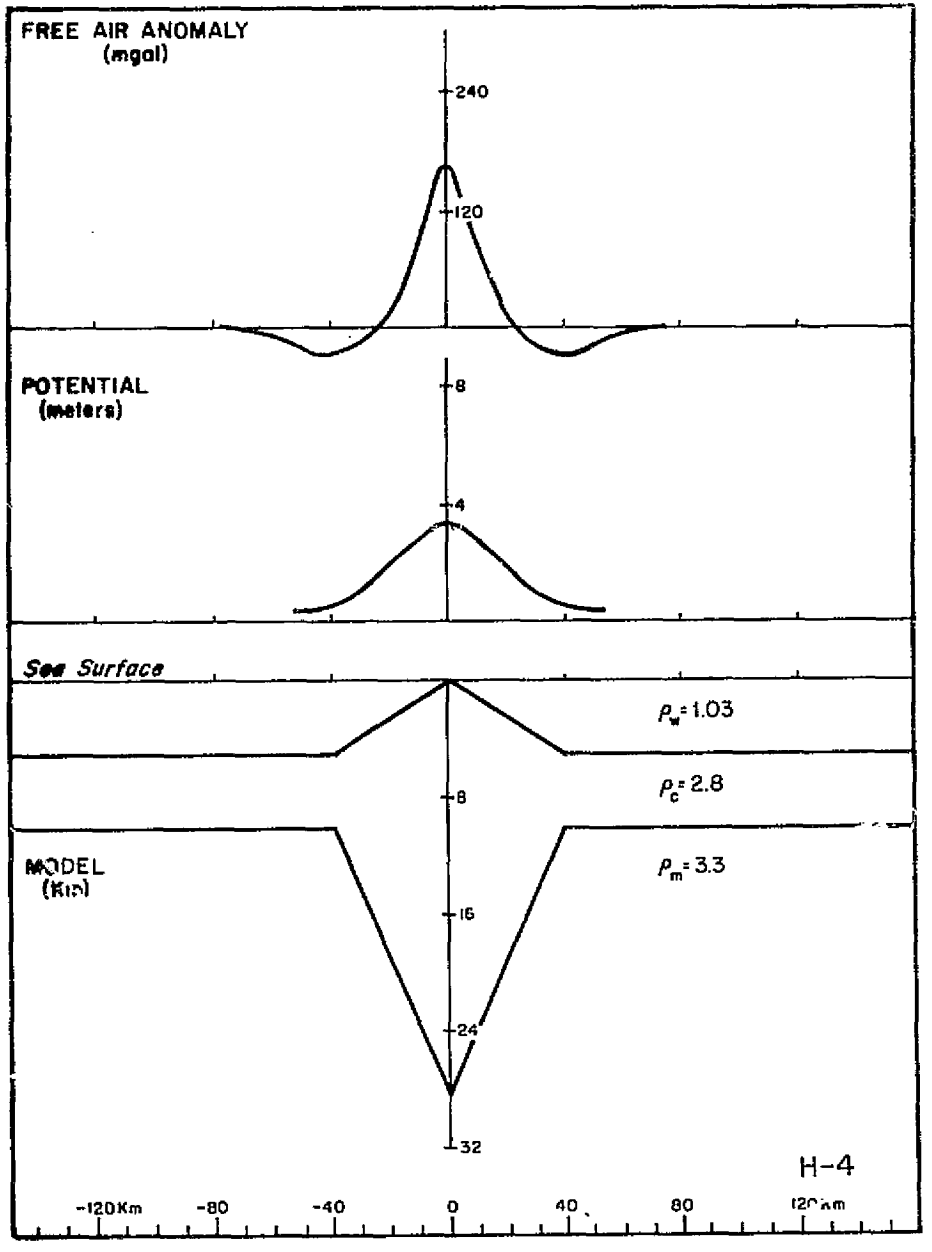
FREE AIR ANOMALY
(mgal)
240
120
POTENTIAL
(meters)
8
4
Sea Surface
ρ_w = 1.03
ρ_c = 2.8
8
MODEL
(Km)
ρ_m = 3.3
16
24
32
H-4
-120Km
-80
-40
0
40
80
120Km

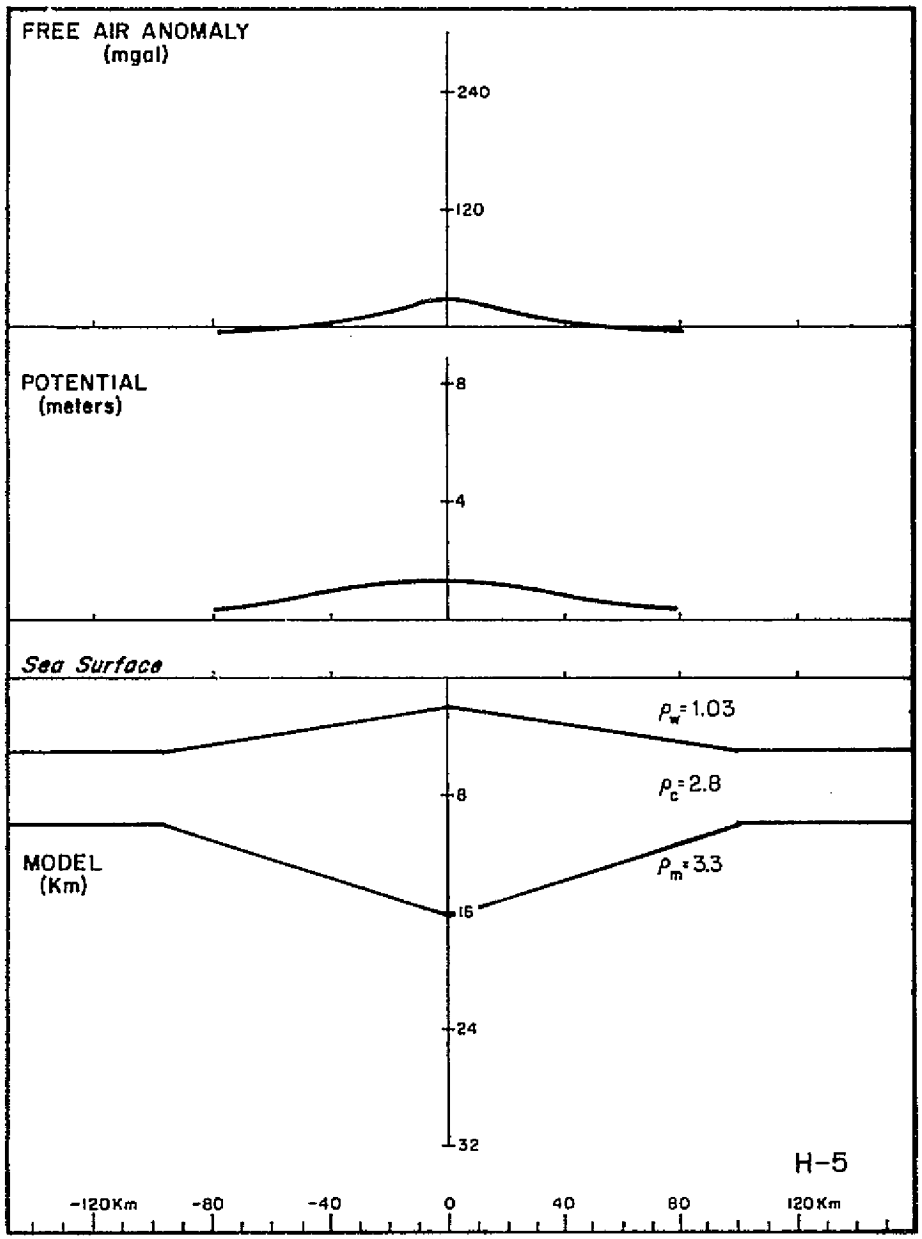
FREE AIR ANOMALY
(mgal)
240
120
POTENTIAL
(meters)
8
4
Sea Surface
ρ_w=1.03
ρ_c=2.8
8
MODEL
(Km)
ρ_m=3.3
16
24
32
H-5
-120Km
-80
-40
0
40
80
120Km

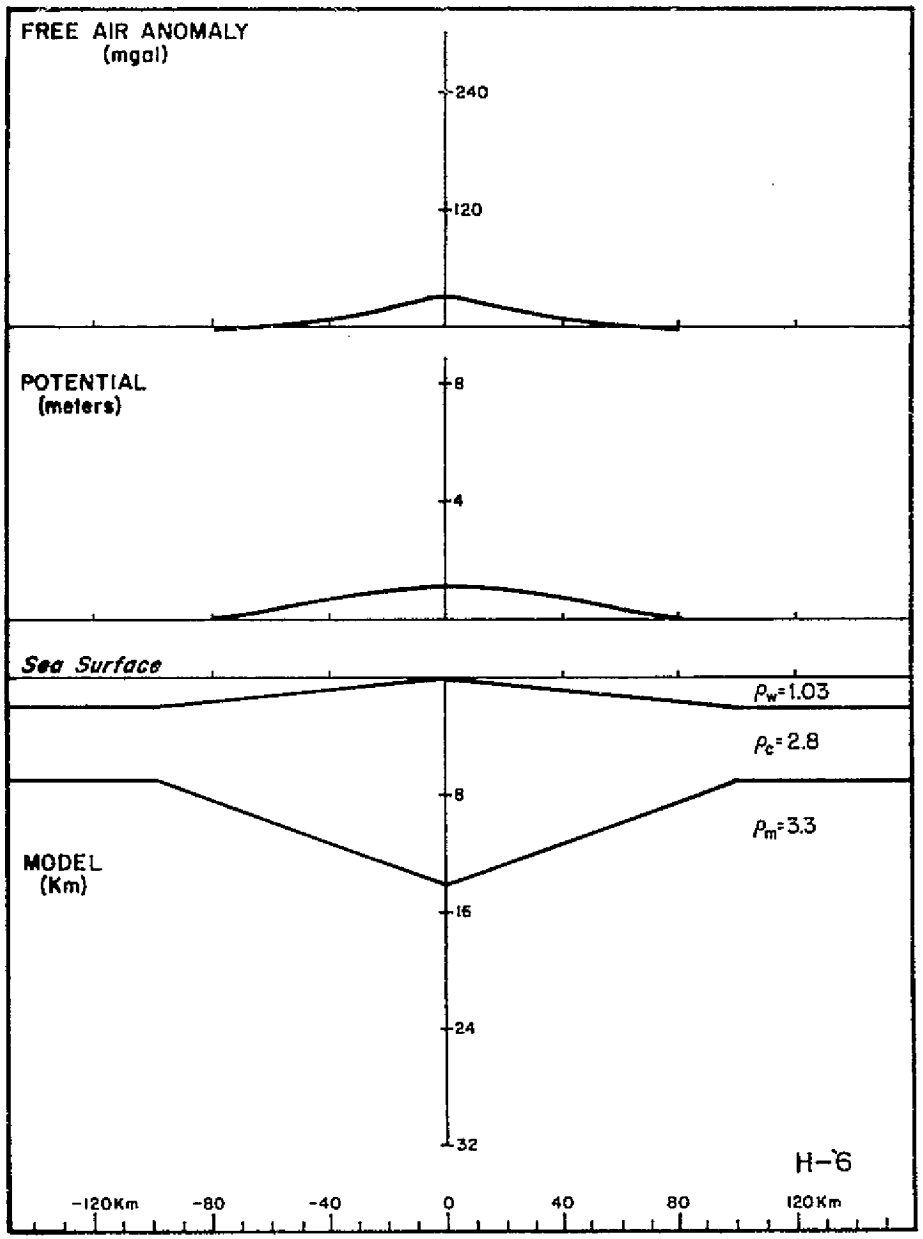
FREE AIR ANOMALY
(mgal)
240
120
POTENTIAL
(meters)
8
4
Sea Surface
ρ_w=1.03
ρ_c=2.8
8
MODEL
(Km)
ρ_m=3.3
16
24
32
H-6
-120Km
-80
-40
0
40
80
120Km

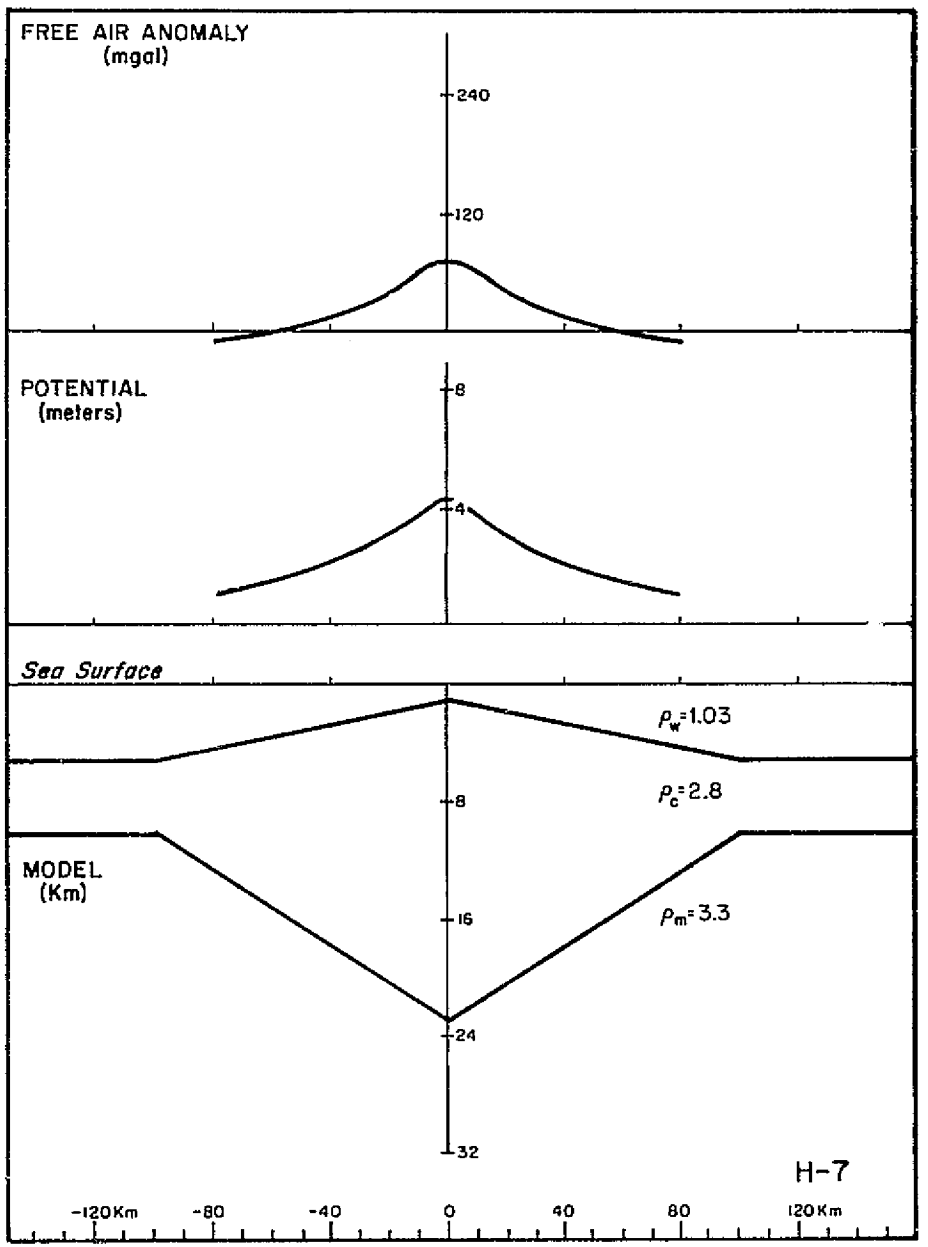
FREE AIR ANOMALY
(mgal)
240
120
POTENTIAL
(meters)
8
4
Sea Surface
ρ_w=1.03
ρ_c=2.8
MODEL
(Km)
8
16
ρ_m=3.3
24
32
H-7
-120Km
-80
-40
0
40
80
120Km

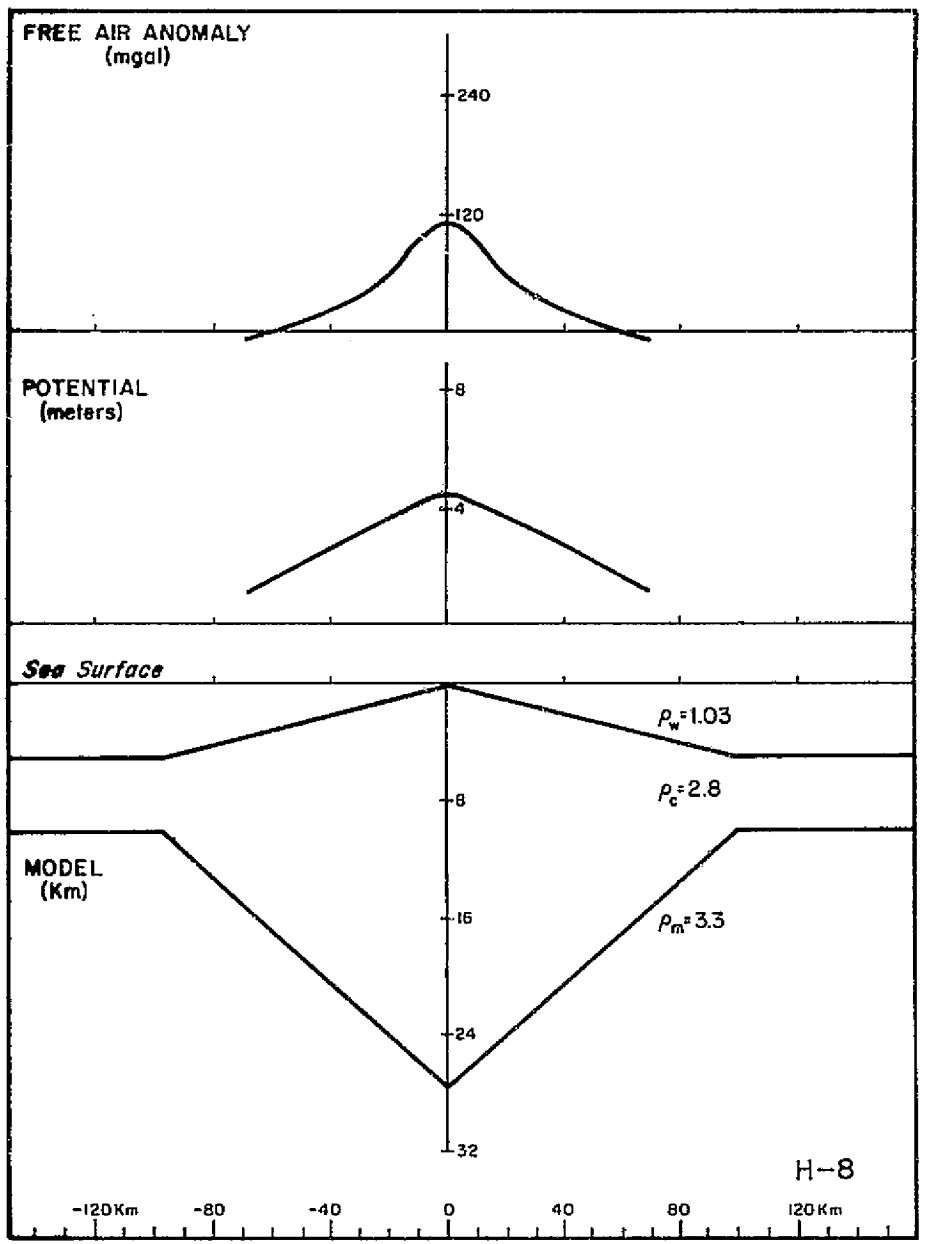
FREE AIR ANOMALY
(mgal)
240
120
POTENTIAL
(meters)
8
4
Sea Surface
ρ_w=1.03
ρ_c=2.8
MODEL
(Km)
8
16
ρ_m=3.3
24
32
H-8
-120Km
-80
-40
0
40
80
120Km

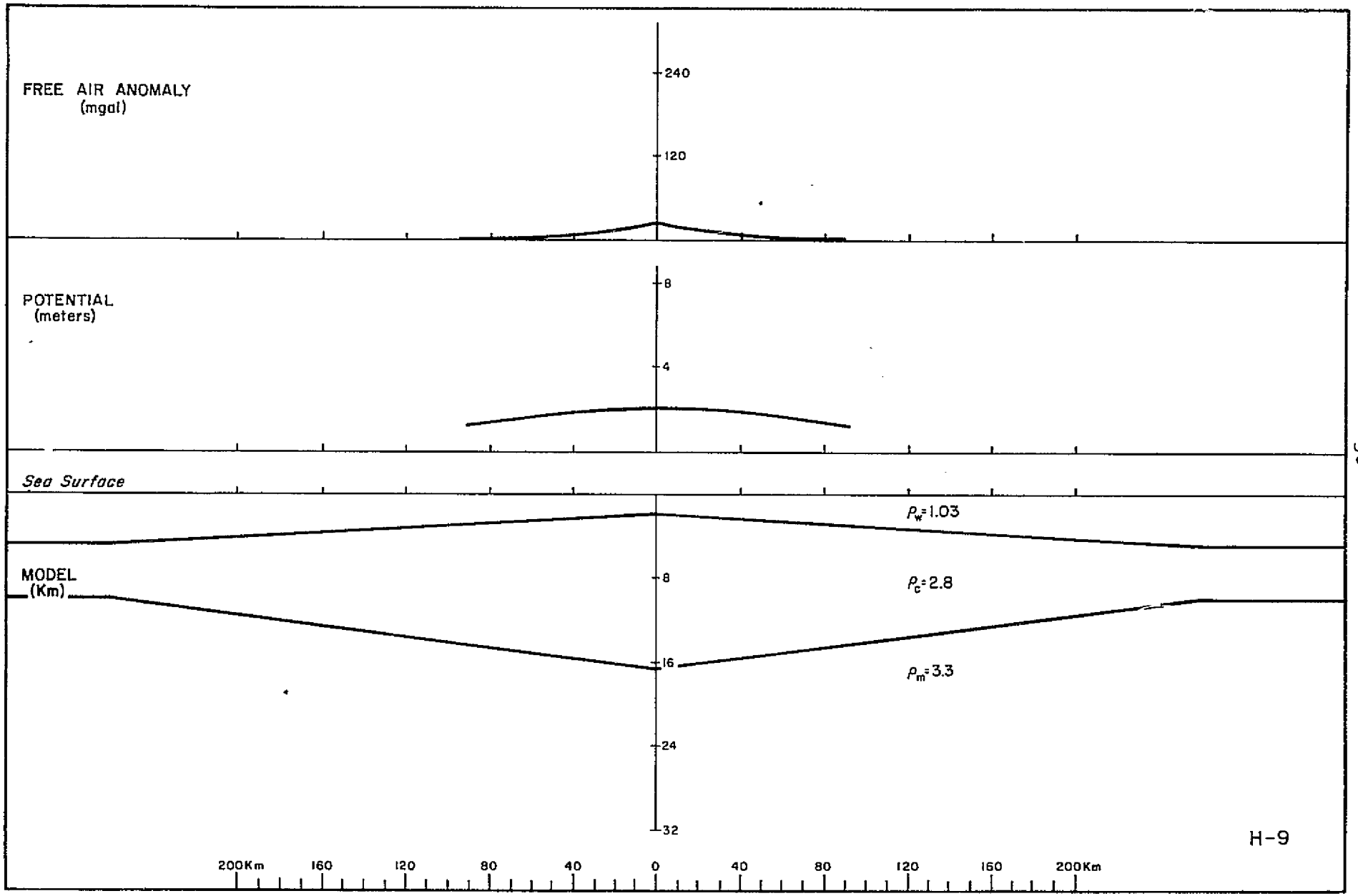
FREE AIR ANOMALY
(mgal)
240
120
POTENTIAL
(meters)
8
4
Sea Surface
ρ_w=1.03
MODEL
(Km)
8
ρ_c=2.8
16
ρ_m=3.3
24
32
H-9
200Km
160
120
80
40
0
40
80
120
160
200Km

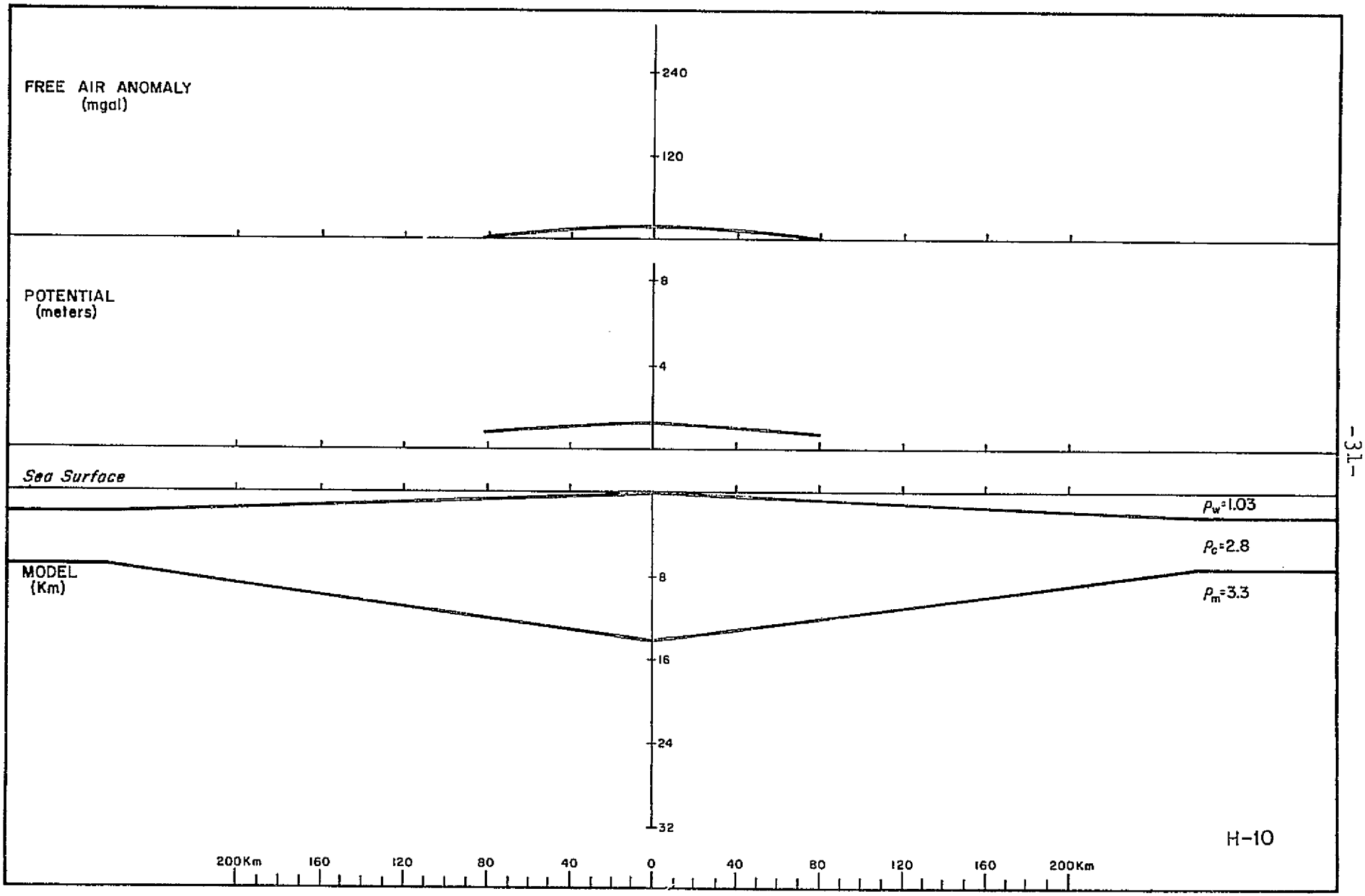
FREE AIR ANOMALY
(mgal)
240
120
POTENTIAL
(meters)
8
4
Sea Surface
ρ_w=1.03
ρ_c=2.8
MODEL
(Km)
8
ρ_m=3.3
16
24
32
H-10
200Km
160
120
80
40
0
40
80
120
160
200Km

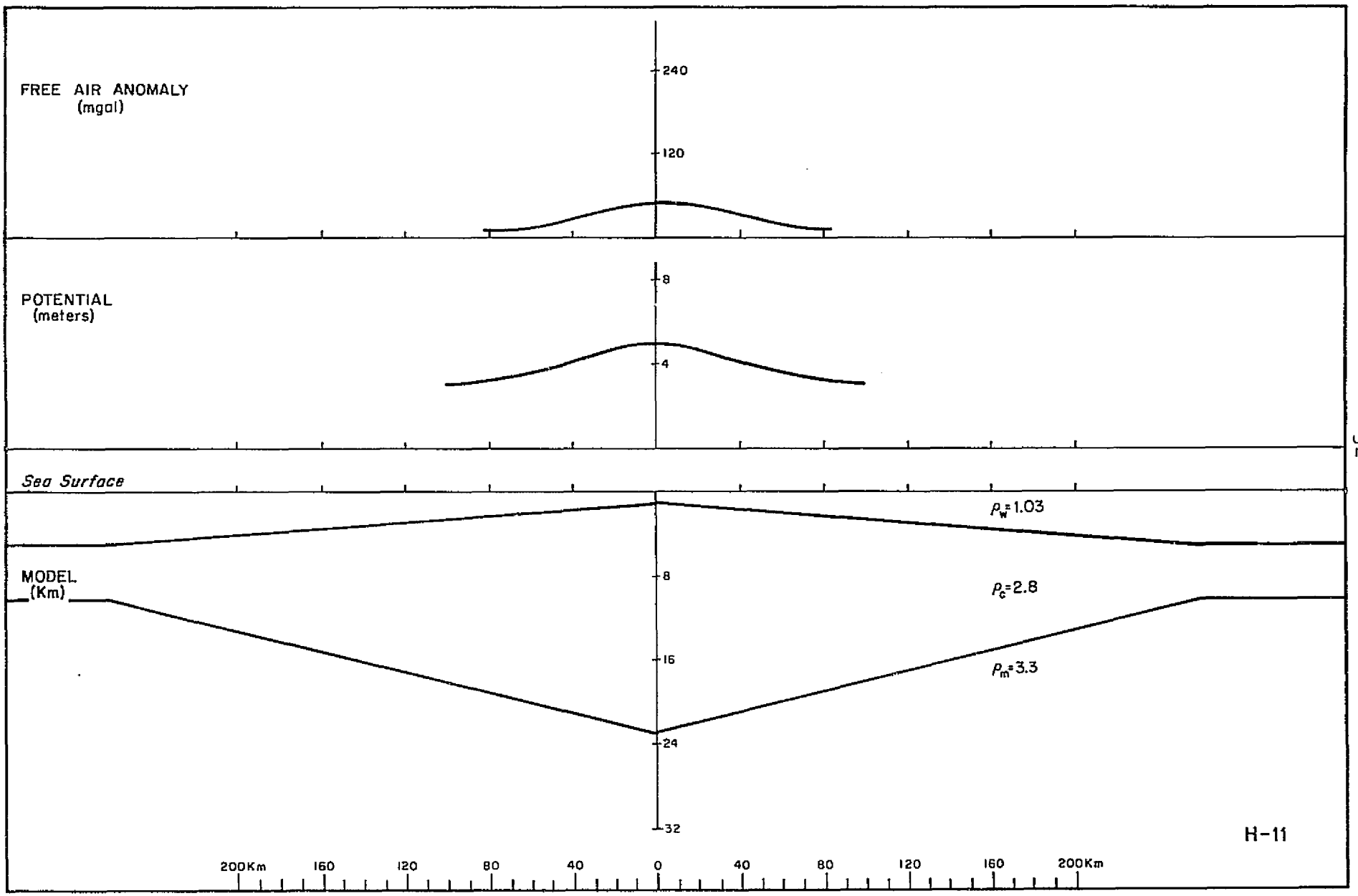
FREE AIR ANOMALY
(mgal)
240
120
POTENTIAL
(meters)
8
4
Sea Surface
ρ_w=1.03
MODEL
(Km)
8
16
24
32
ρ_c=2.8
ρ_m=3.3
H-11
200Km
160
120
80
40
0
40
80
120
160
200Km

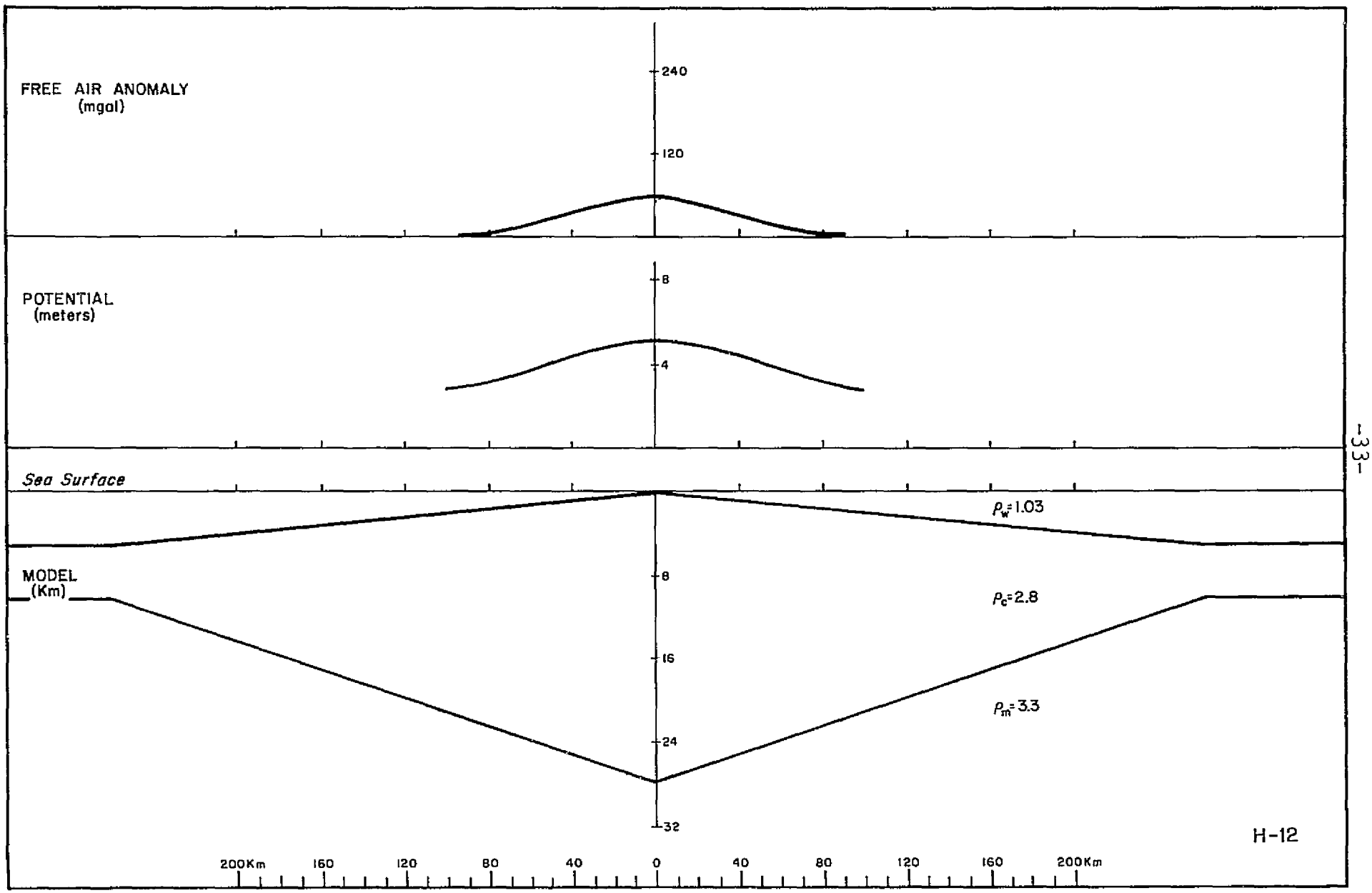
FREE AIR ANOMALY
(mgal)
240
120
POTENTIAL
(meters)
8
4
Sea Surface
ρ_w=1.03
MODEL
(Km)
8
ρ_c=2.8
16
ρ_m=3.3
24
32
H-12
200Km
160
120
80
40
0
40
80
120
160
200Km

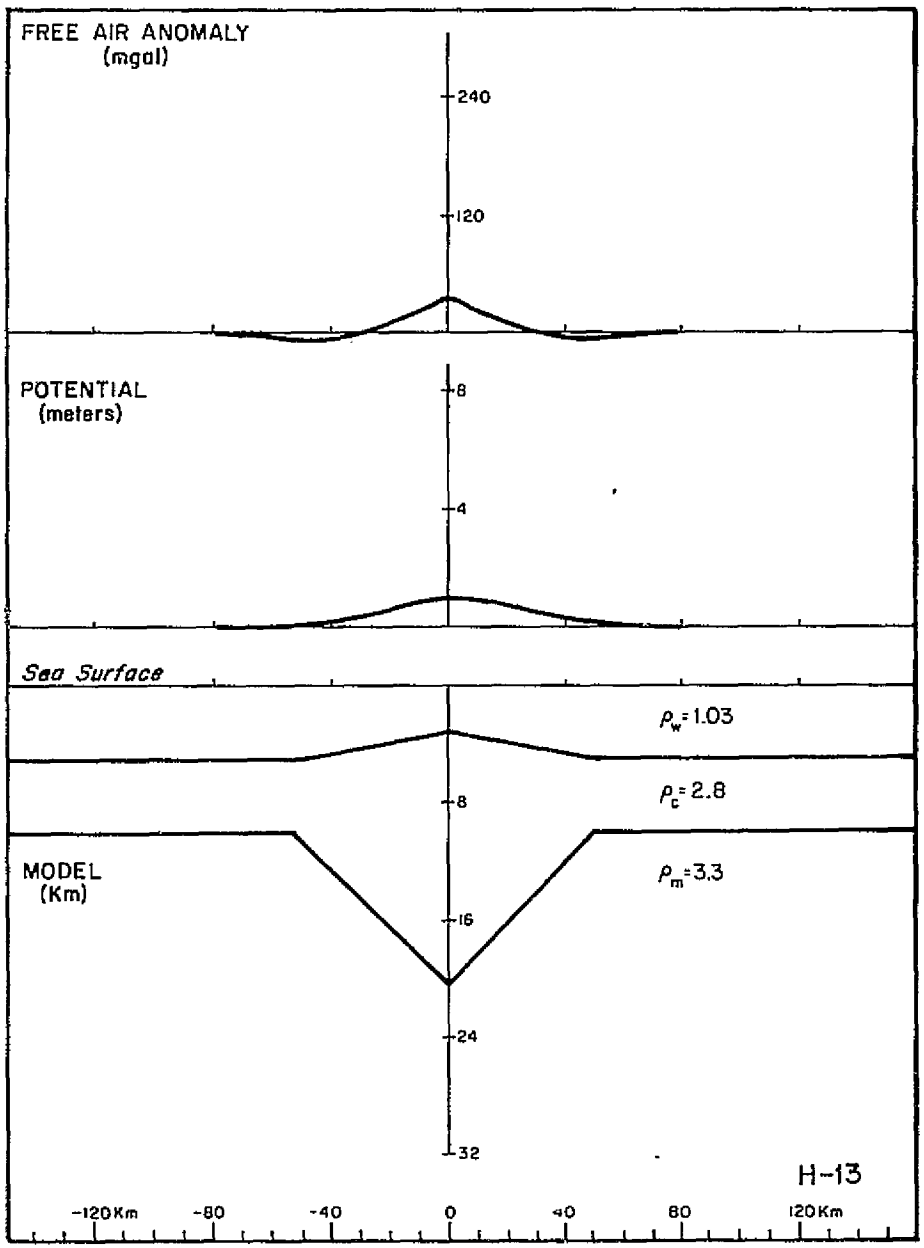
FREE AIR ANOMALY
(mgal)
240
120
POTENTIAL
(meters)
8
4
Sea Surface
ρ_w=1.03
ρ_c=2.8
8
ρ_m=3.3
MODEL
(Km)
16
24
32
H-13
-120Km
-80
-40
0
40
80
120Km

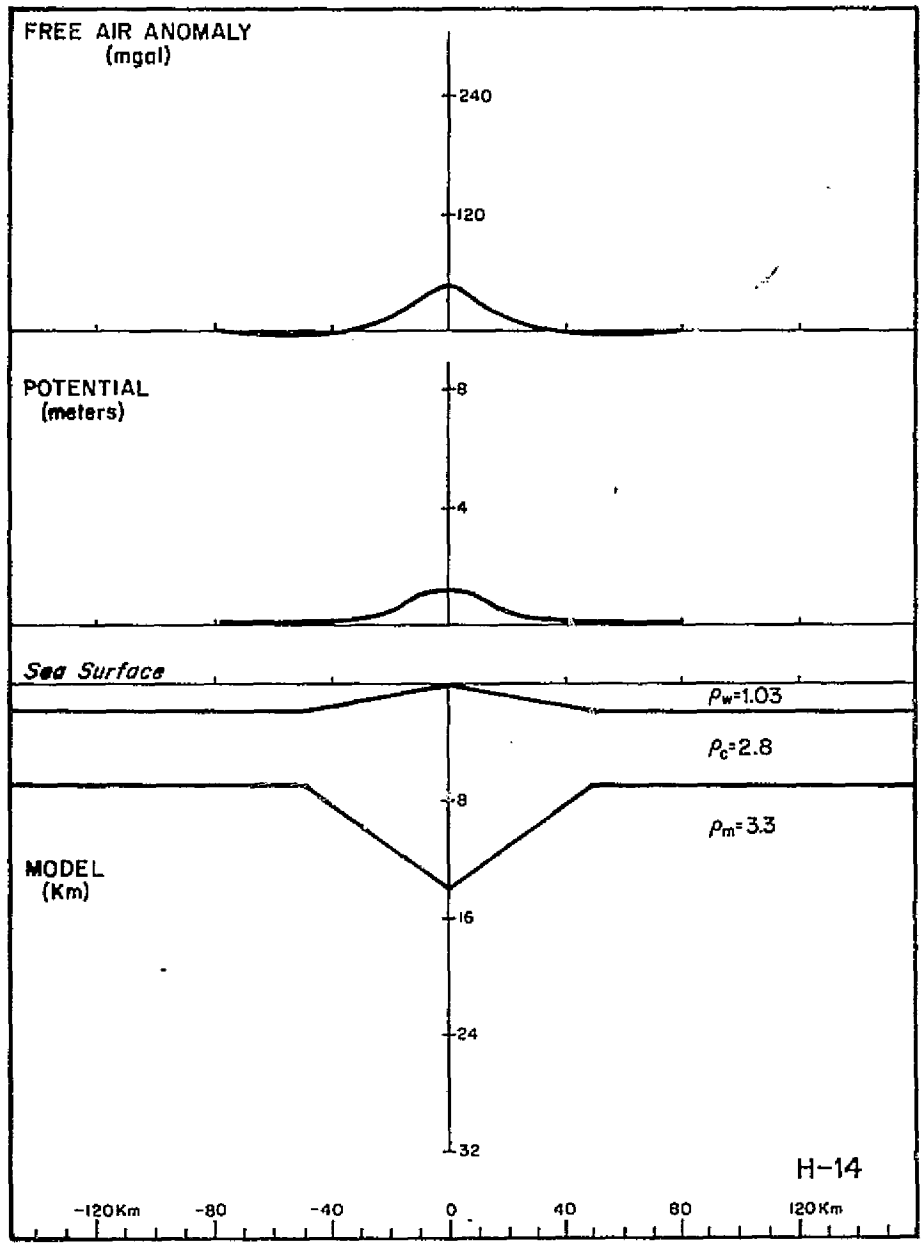
FREE AIR ANOMALY
(mgal)
240
120
POTENTIAL
(meters)
8
4
Sea Surface
ρ_w=1.03
ρ_c=2.8
8
ρ_m=3.3
MODEL
(Km)
16
24
32
H-14
-120Km
-80
-40
0
40
80
120Km

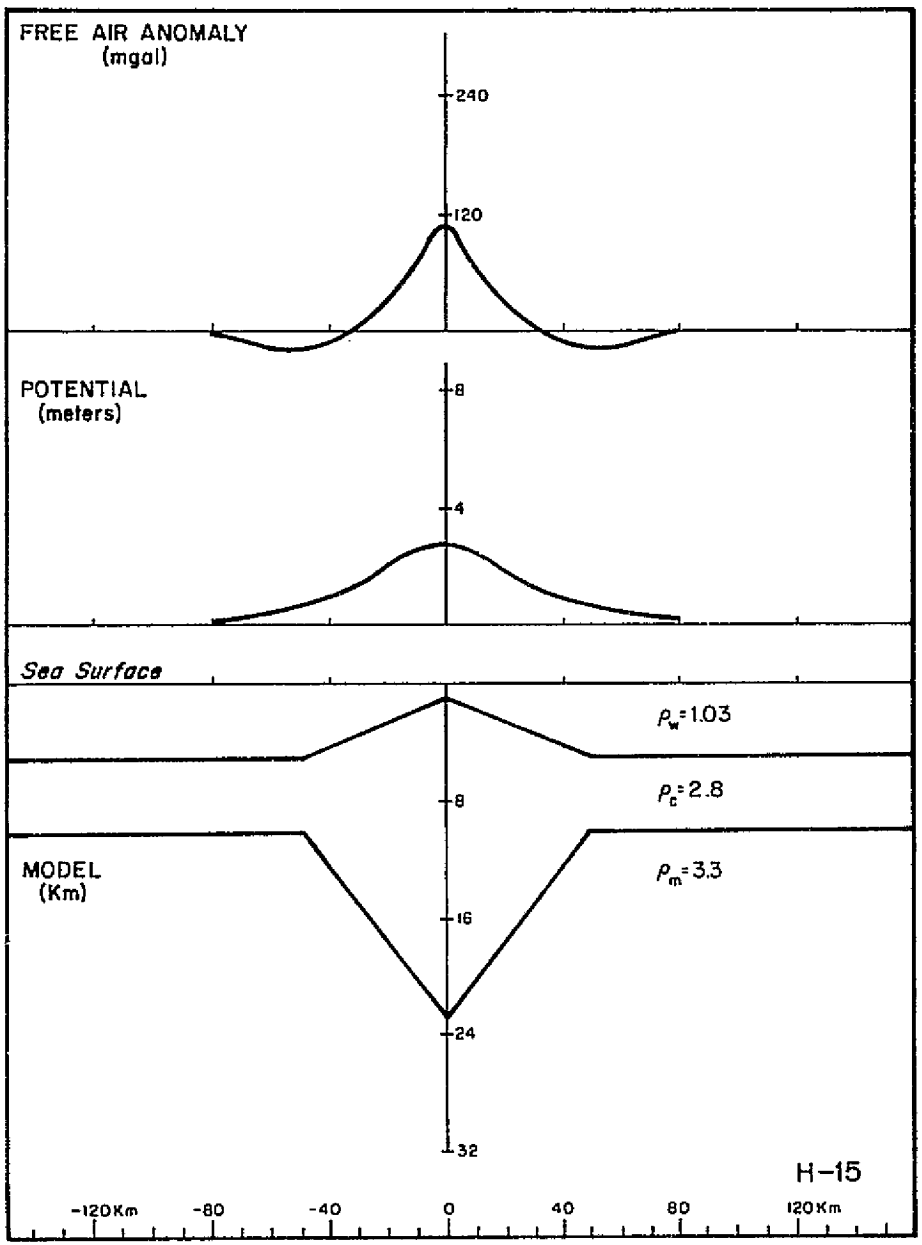
FREE AIR ANOMALY
(mgal)
240
120
POTENTIAL
(meters)
8
4
Sea Surface
ρ_w=1.03
ρ_c=2.8
ρ_m=3.3
MODEL
(Km)
8
16
24
32
H-15
-120Km
-80
-40
0
40
80
120Km

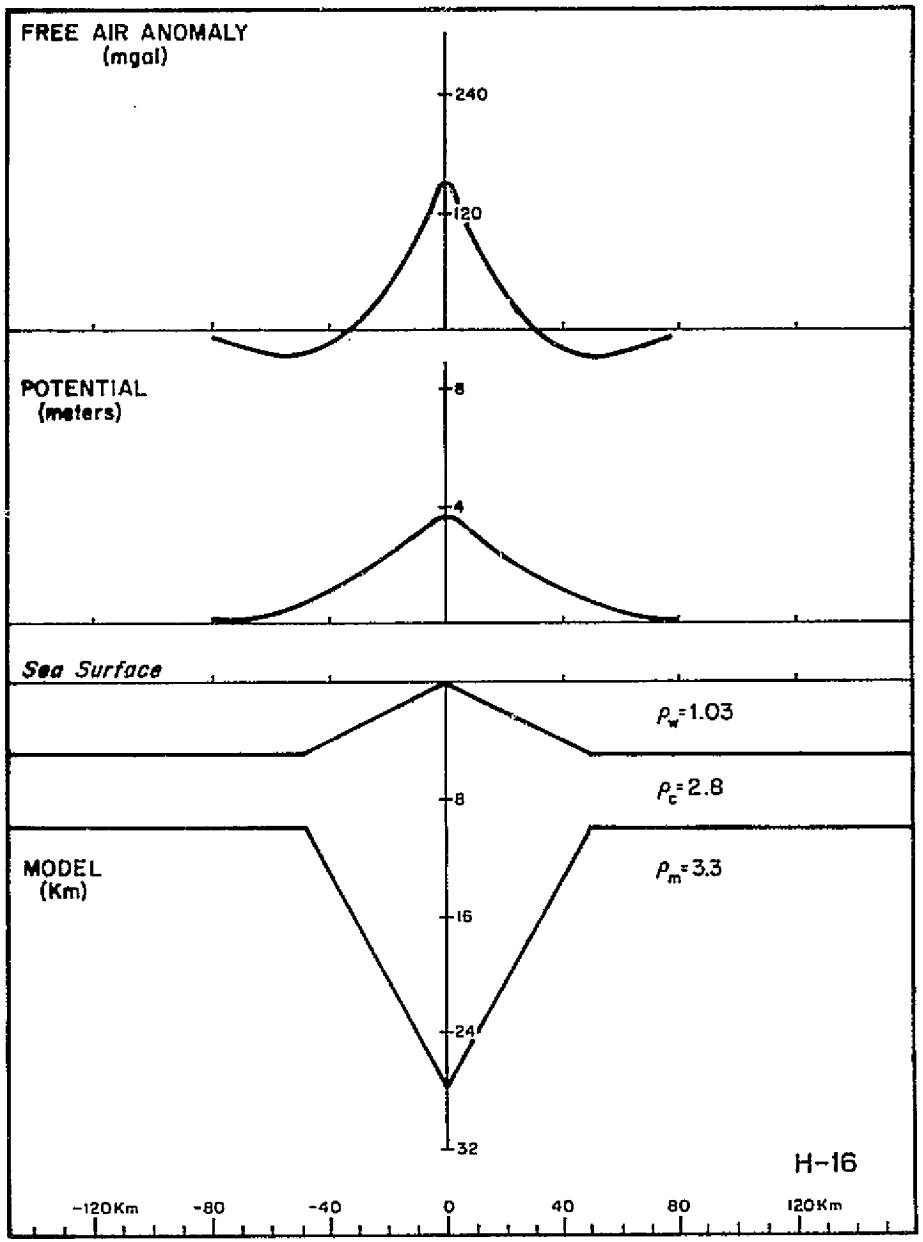
FREE AIR ANOMALY
(mgal)
240
120
POTENTIAL
(meters)
8
4
Sea Surface
ρ_w=1.03
ρ_c=2.8
ρ_m=3.3
MODEL
(Km)
8
16
24
32
H-16
-120Km
-80
-40
0
40
80
120Km

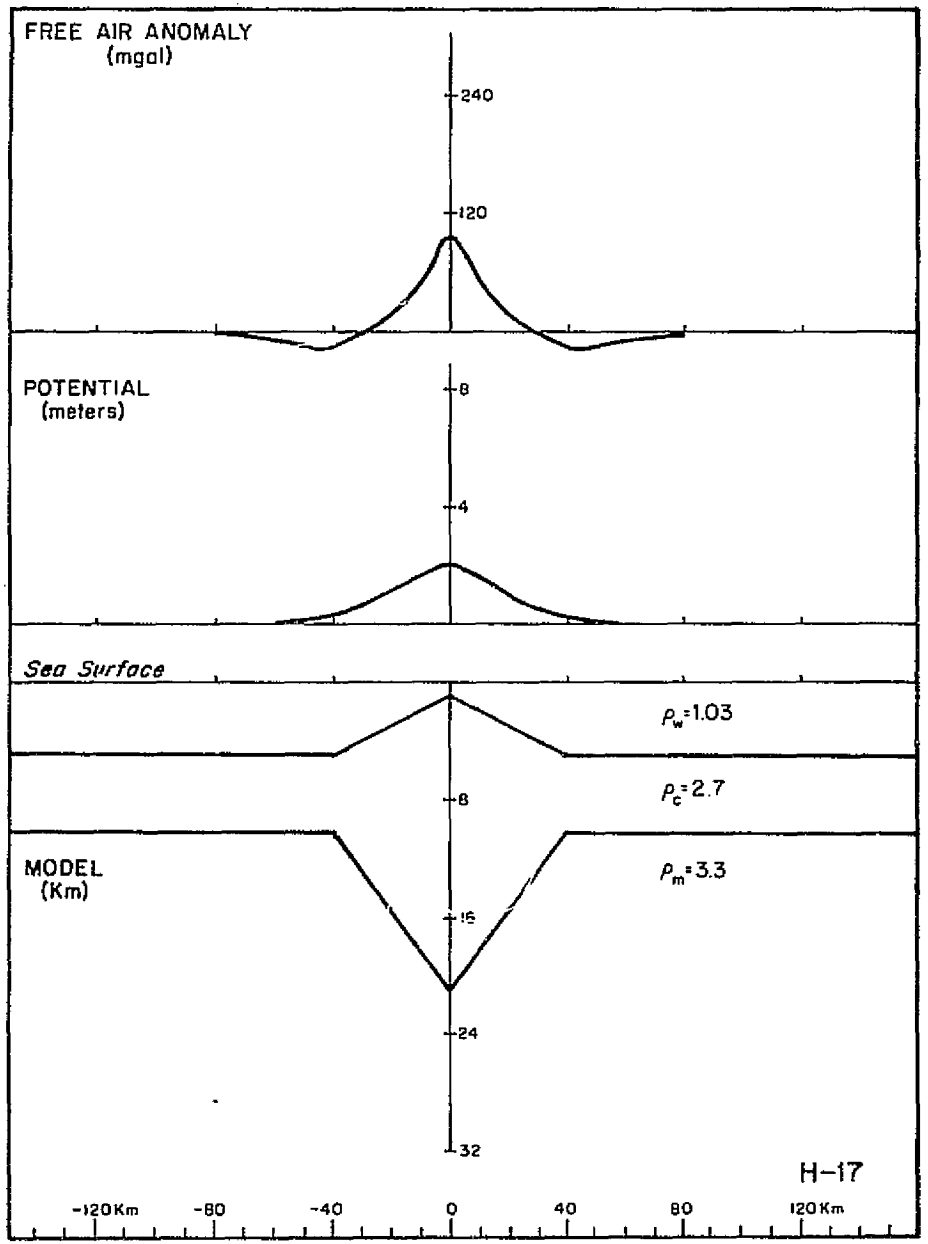
FREE AIR ANOMALY
(mgal)
240
120
POTENTIAL
(meters)
8
4
Sea Surface
ρ_w=1.03
ρ_c=2.7
ρ_m=3.3
MODEL
(Km)
8
16
24
32
H-17
-120Km
-80
-40
0
40
80
120Km

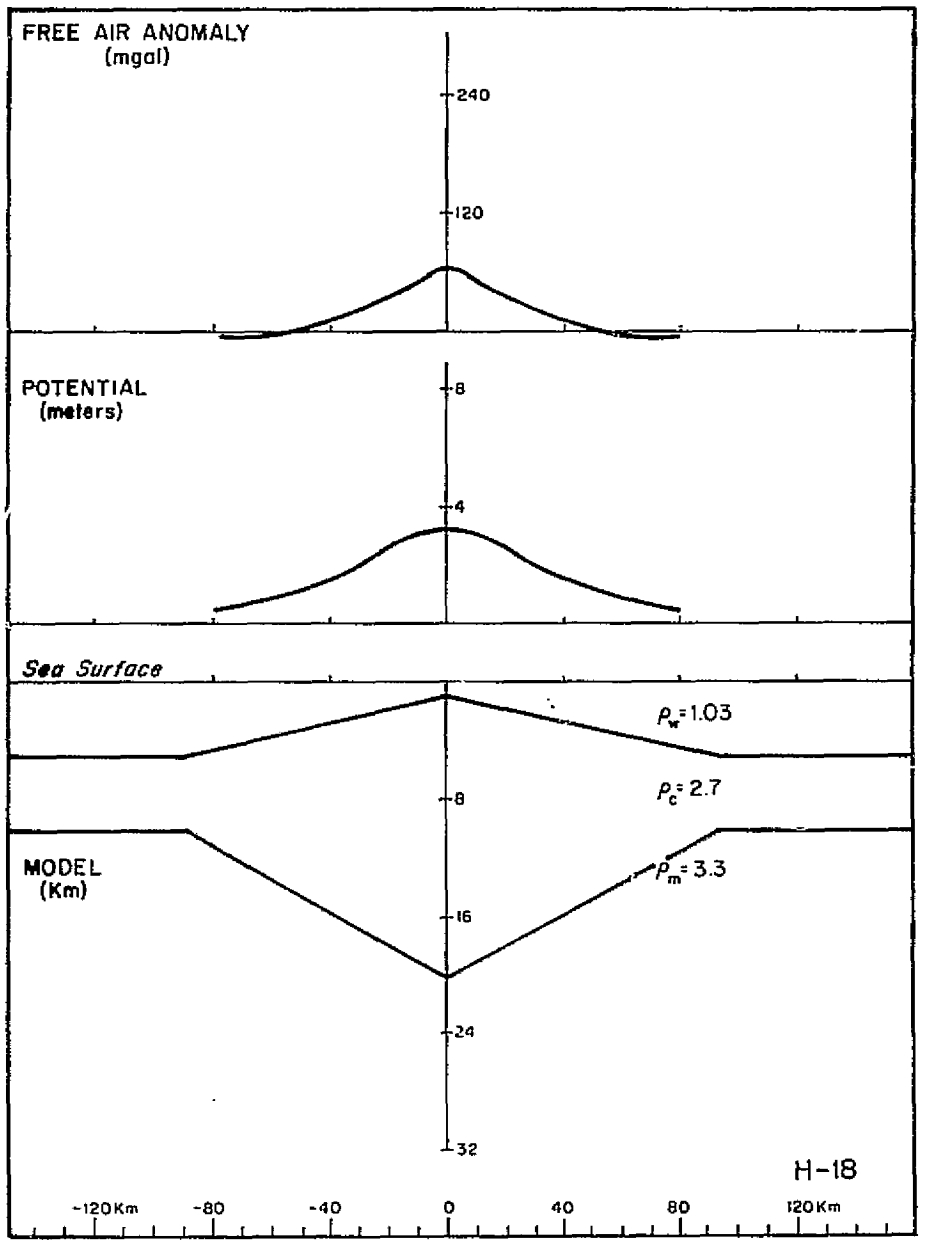
FREE AIR ANOMALY
(mgal)
240
120
POTENTIAL
(meters)
8
4
Sea Surface
ρ_w=1.03
ρ_c=2.7
ρ_m=3.3
MODEL
(Km)
8
16
24
32
H-18
-120Km
-80
-40
0
40
80
120Km

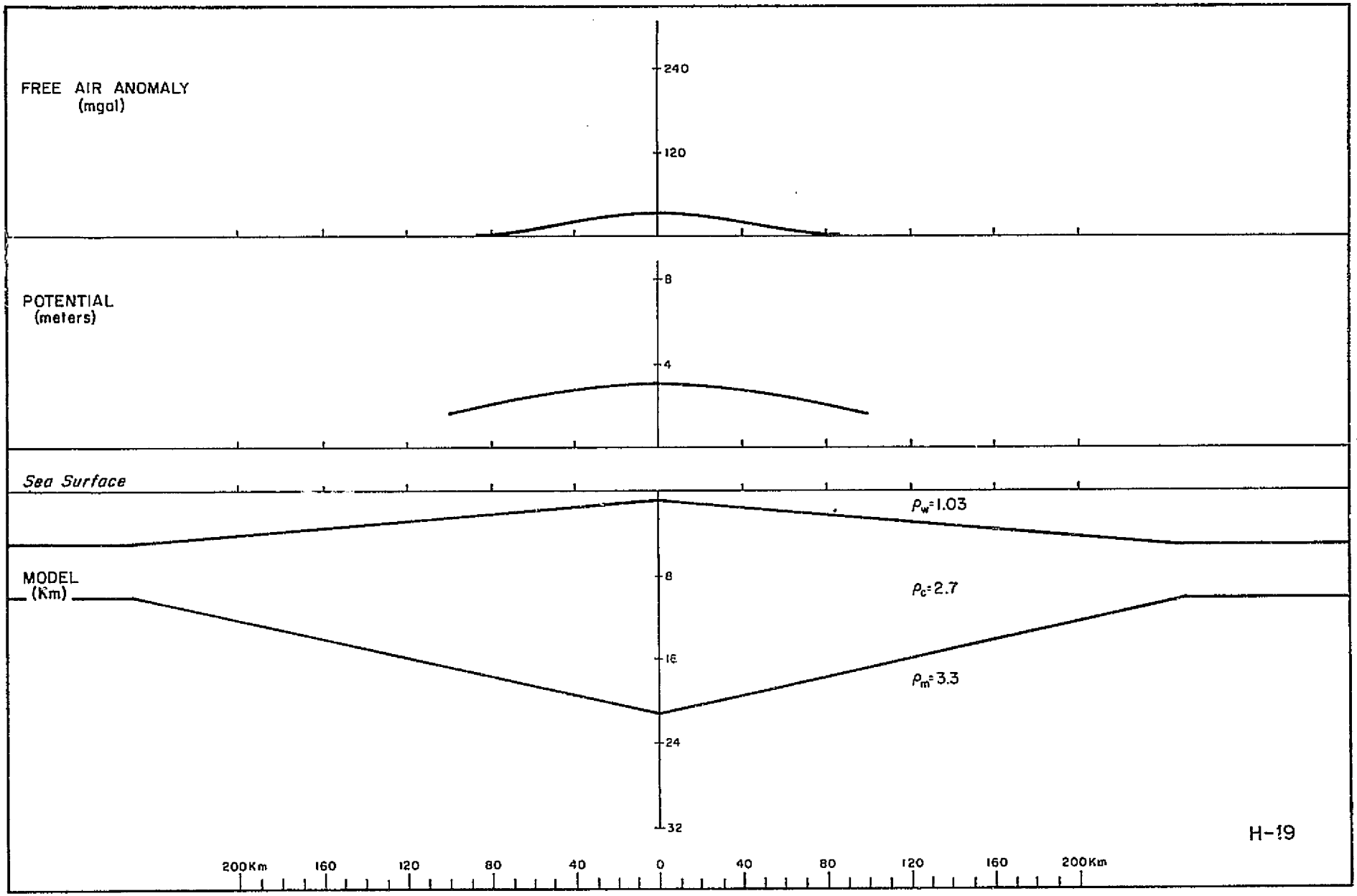
FREE AIR ANOMALY
(mgal)
240
120
POTENTIAL
(meters)
8
4
Sea Surface
ρ_w=1.03
MODEL
(Km)
8
ρ_c=2.7
16
ρ_m=3.3
24
32
H-19
200Km
160
120
80
40
0
40
80
120
160
200Km

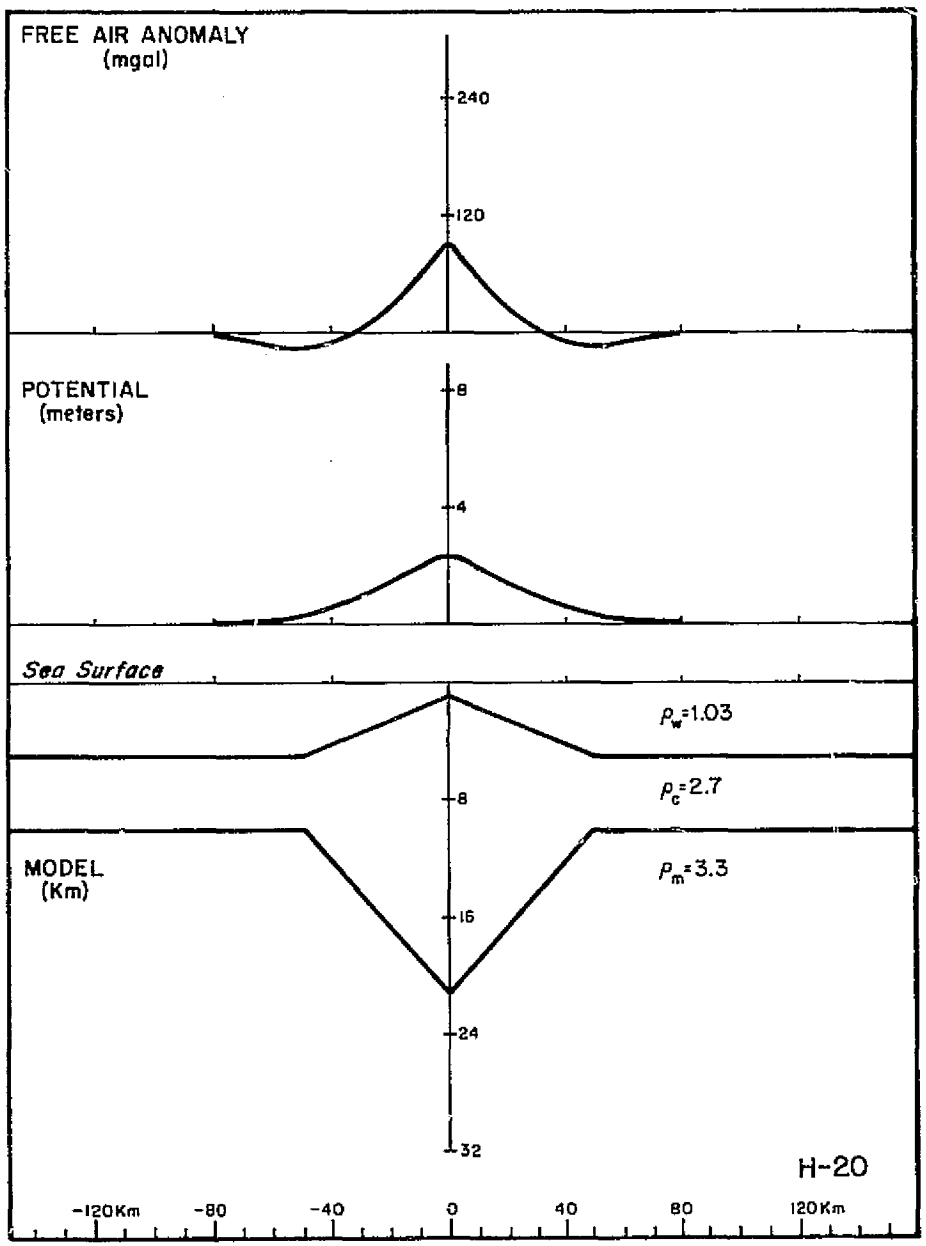
FREE AIR ANOMALY
(mgal)
240
120
POTENTIAL
(meters)
8
4
Sea Surface
ρ_w=1.03
ρ_c=2.7
8
MODEL
(Km)
ρ_m=3.3
16
24
32
H-20
-120Km
-80
-40
0
40
80
120Km

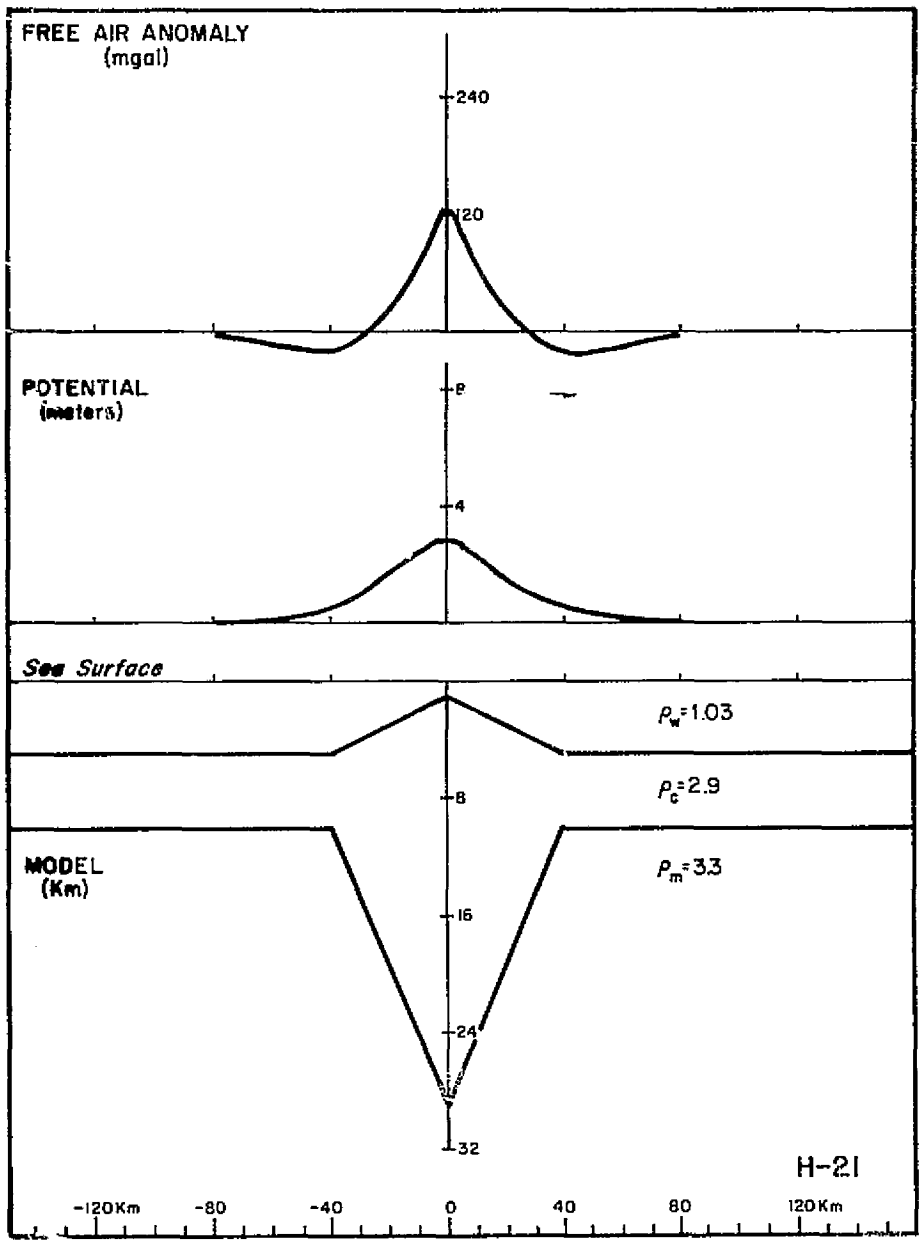
FREE AIR ANOMALY
(mgal)
240
120
POTENTIAL
(meters)
8
4
Sea Surface
ρ_w=1.03
ρ_c=2.9
8
MODEL
(Km)
ρ_m=3.3
16
24
32
H-21
-120Km
-80
-40
0
40
80
120Km

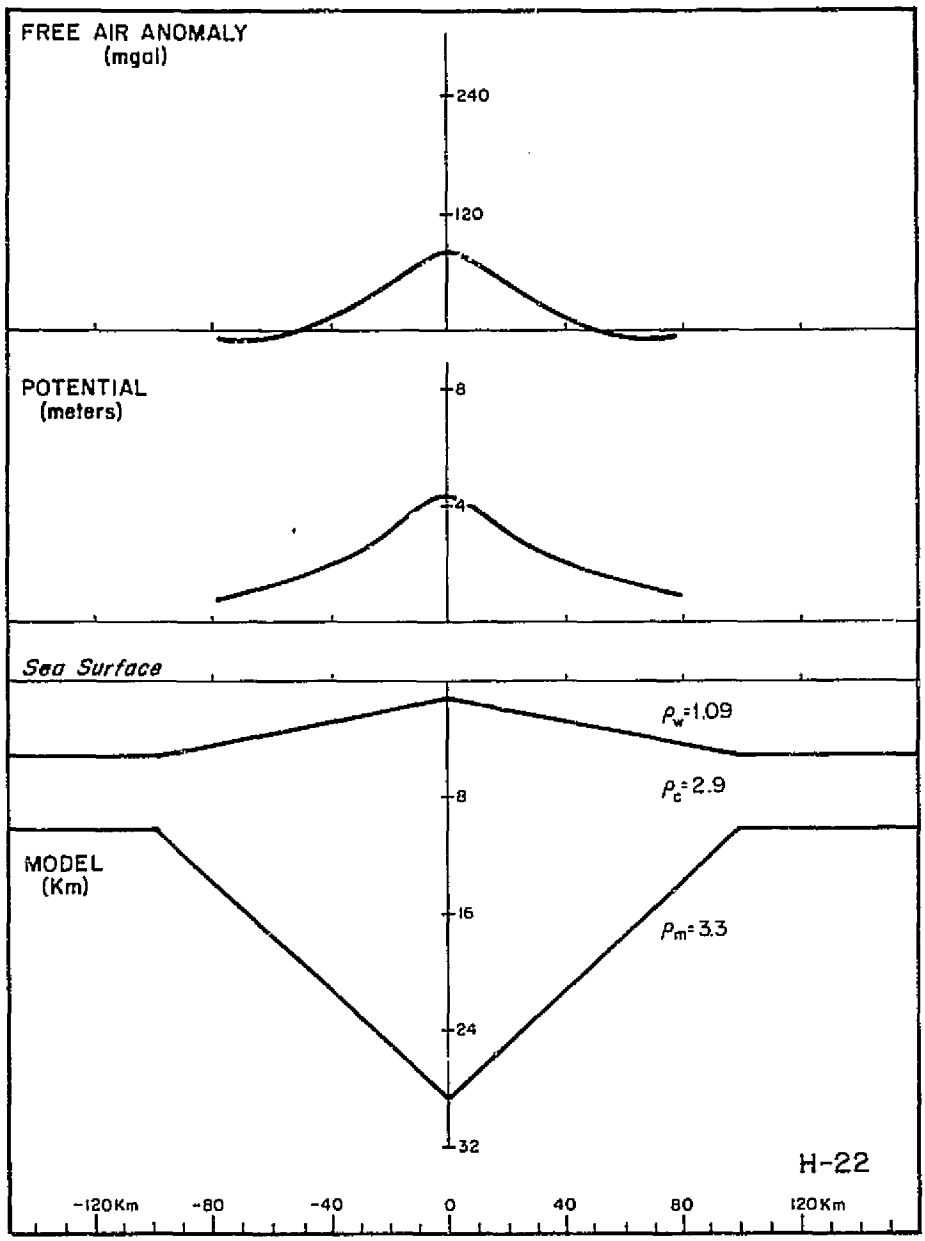
FREE AIR ANOMALY
(mgal)
240
120
POTENTIAL
(meters)
8
4
Sea Surface
ρ_w=1.09
ρ_c=2.9
8
MODEL
(Km)
16
ρ_m=3.3
24
32
H-22
-120Km
-80
-40
0
40
80
120Km

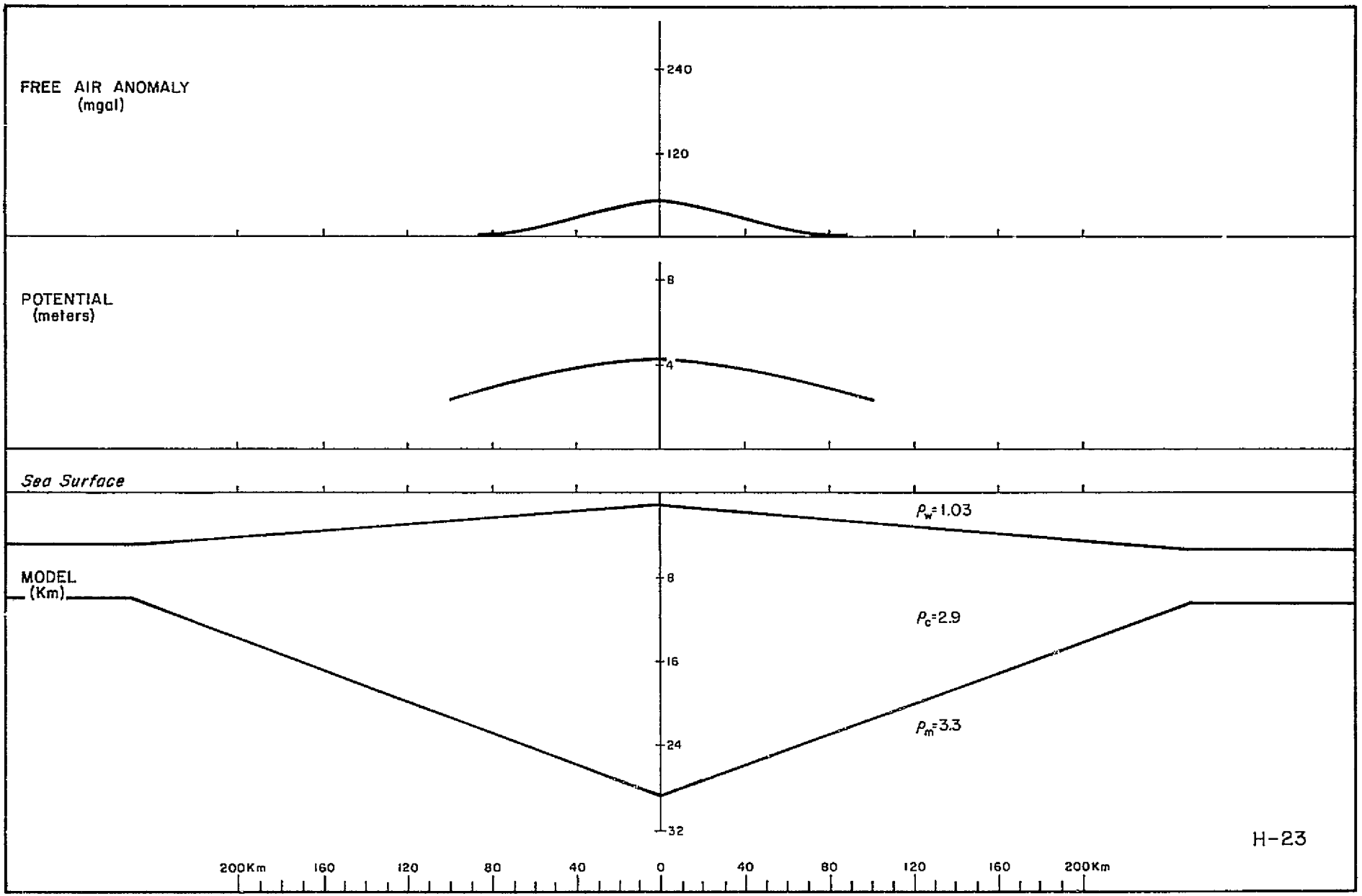
FREE AIR ANOMALY
(mgal)
240
120
POTENTIAL
(meters)
8
4
Sea Surface
ρ_w=1.03
MODEL
(Km)
8
16
24
32
ρ_c=2.9
ρ_m=3.3
H-23
200Km
160
120
80
40
0
40
80
120
160
200Km

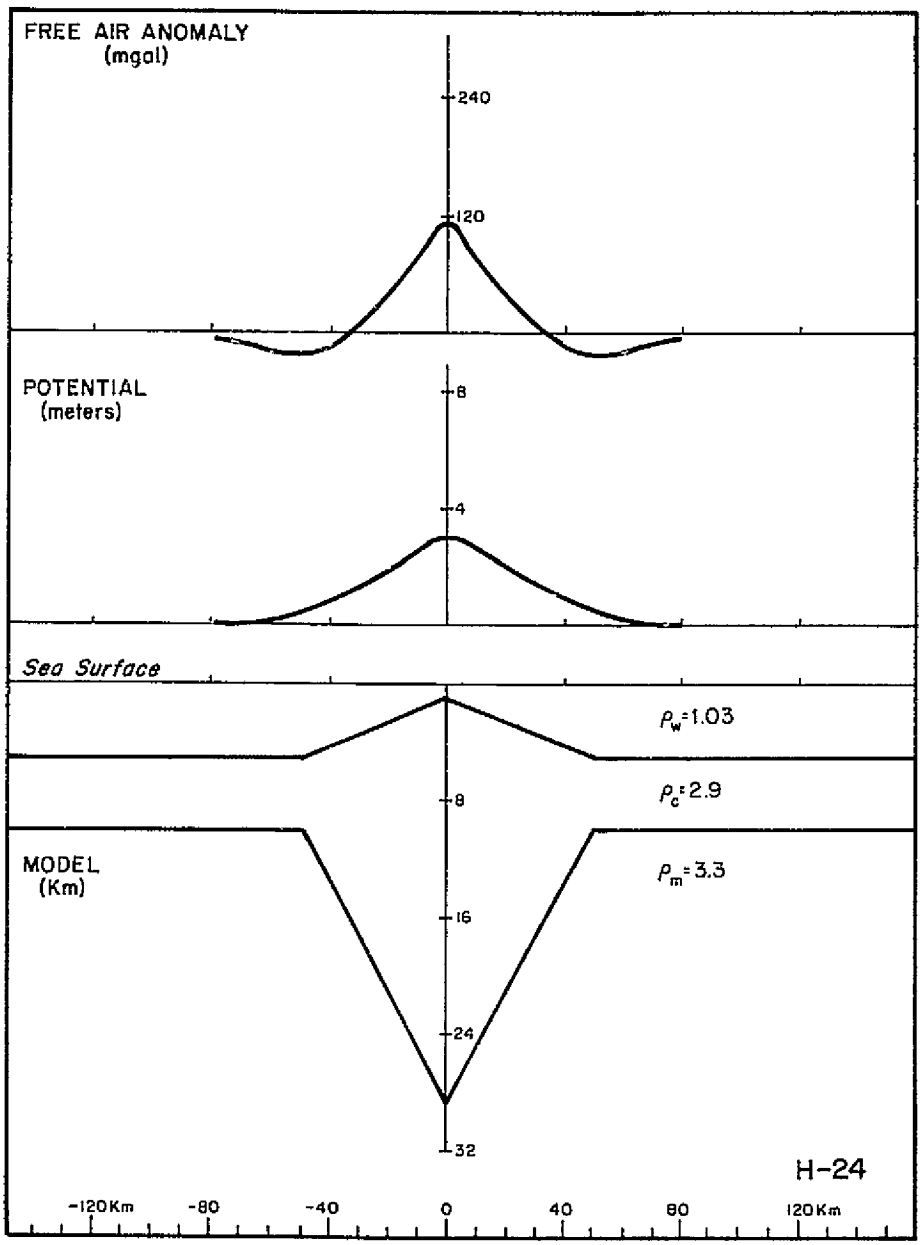
FREE AIR ANOMALY
(mgal)
240
120
POTENTIAL
(meters)
8
4
Sea Surface
ρ_w=1.03
ρ_c=2.9
ρ_m=3.3
MODEL
(Km)
8
16
24
32
H-24
-120Km
-80
-40
0
40
80
120Km

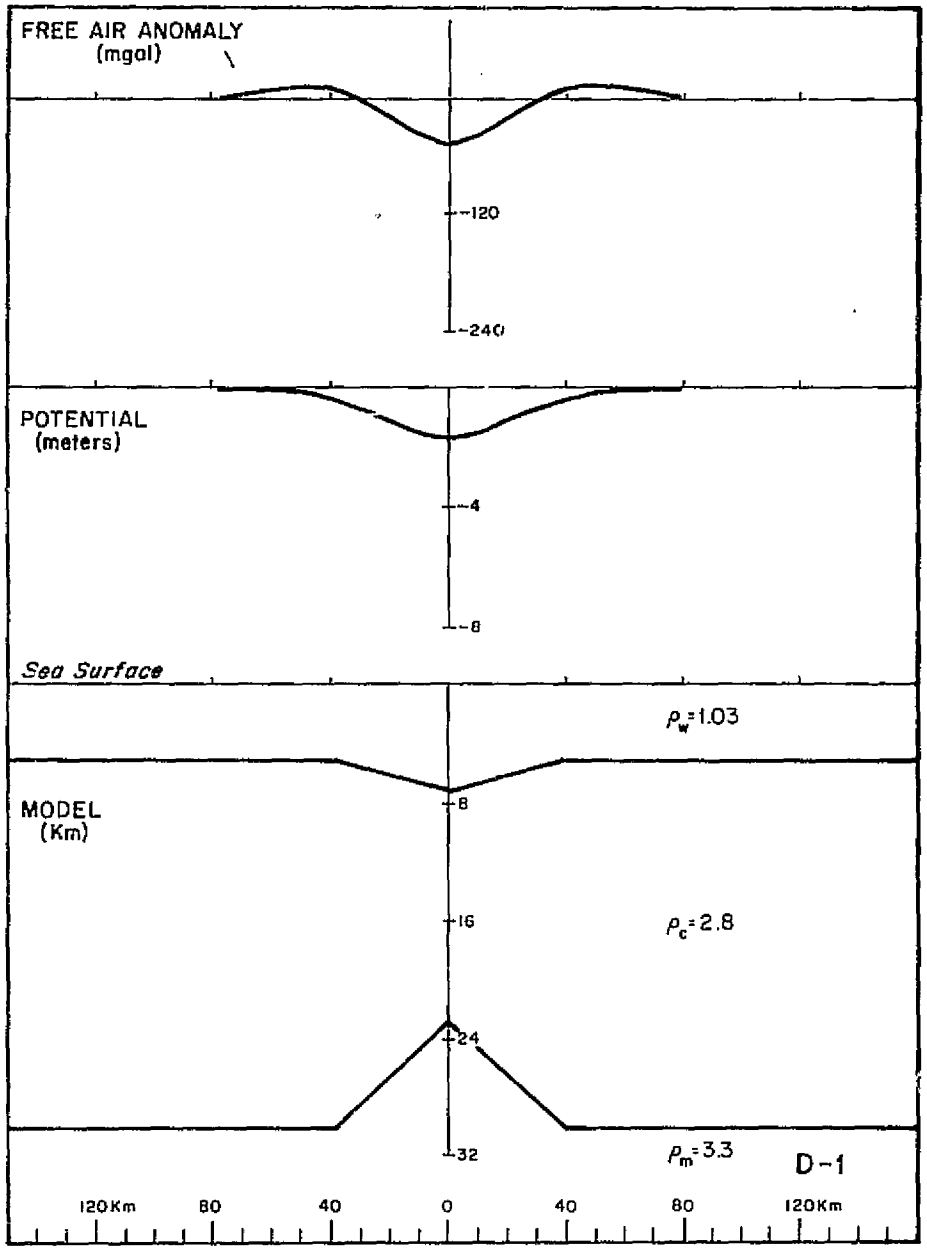
FREE AIR ANOMALY
(mgal)
-120
-240
POTENTIAL
(meters)
-4
-8
Sea Surface
ρ_w=1.03
MODEL
(Km)
8
16
ρ_c=2.8
24
32
ρ_m=3.3
D-1
120Km
80
40
0
40
80
120Km

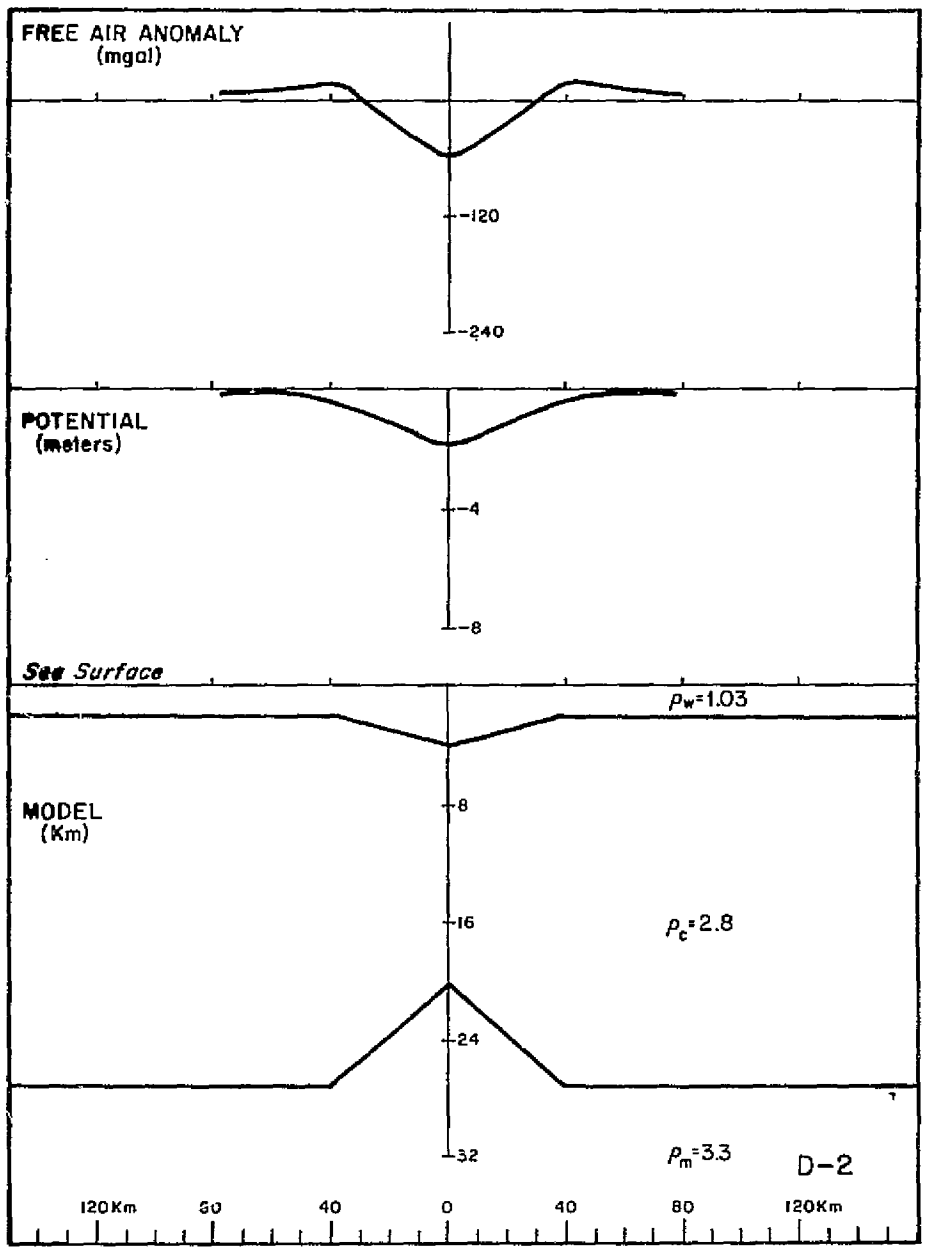
FREE AIR ANOMALY
(mgal)
-120
-240
POTENTIAL
(meters)
-4
-8
Sea Surface
ρ_w=1.03
MODEL
(Km)
8
16
ρ_c=2.8
24
32
ρ_m=3.3
D-2
120Km
80
40
0
40
80
120Km

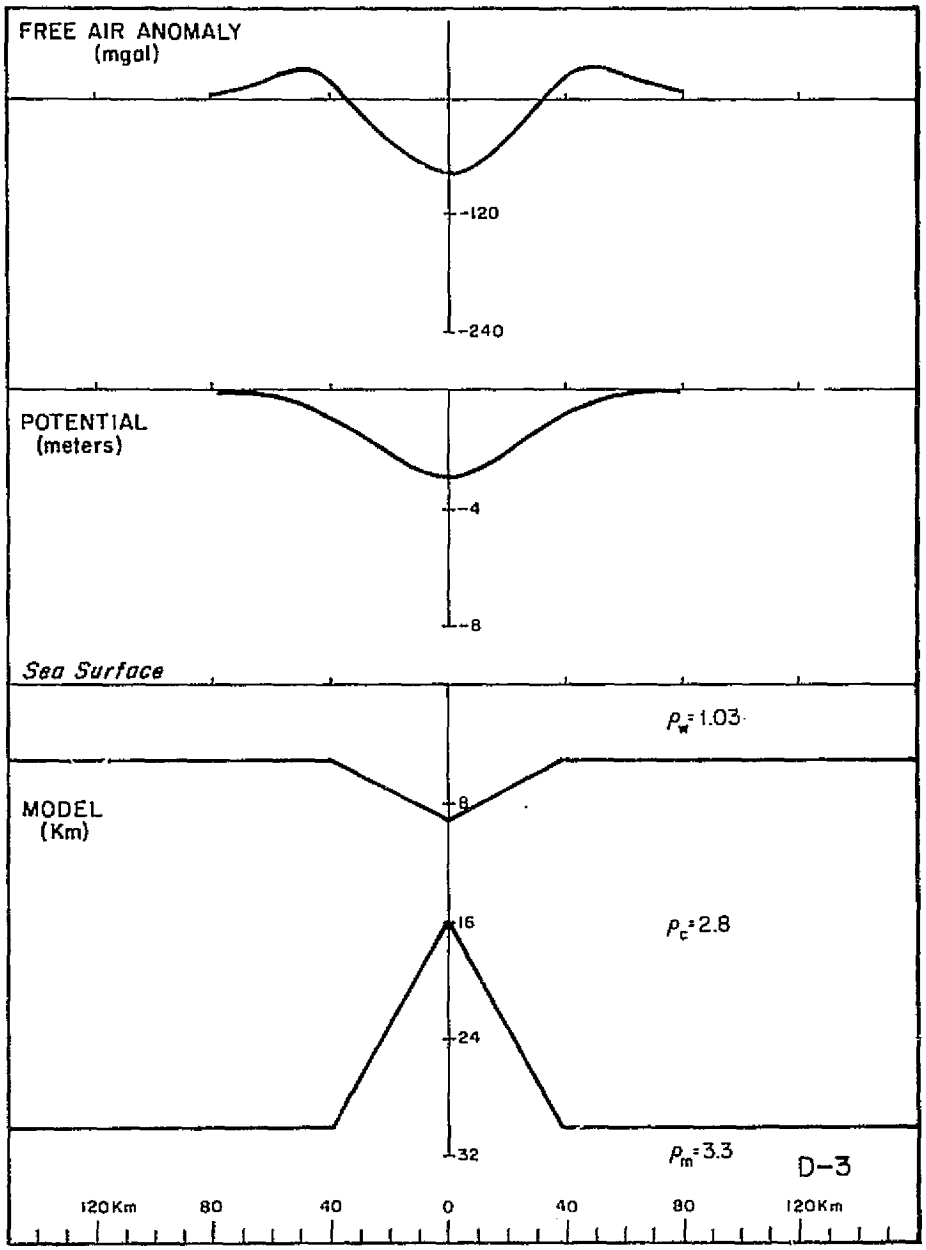
FREE AIR ANOMALY
(mgal)
-120
-240
POTENTIAL
(meters)
-4
-8
Sea Surface
ρ_w=1.03
MODEL
(Km)
8
16
24
32
ρ_c=2.8
ρ_m=3.3
D-3
120Km
80
40
0
40
80
120Km

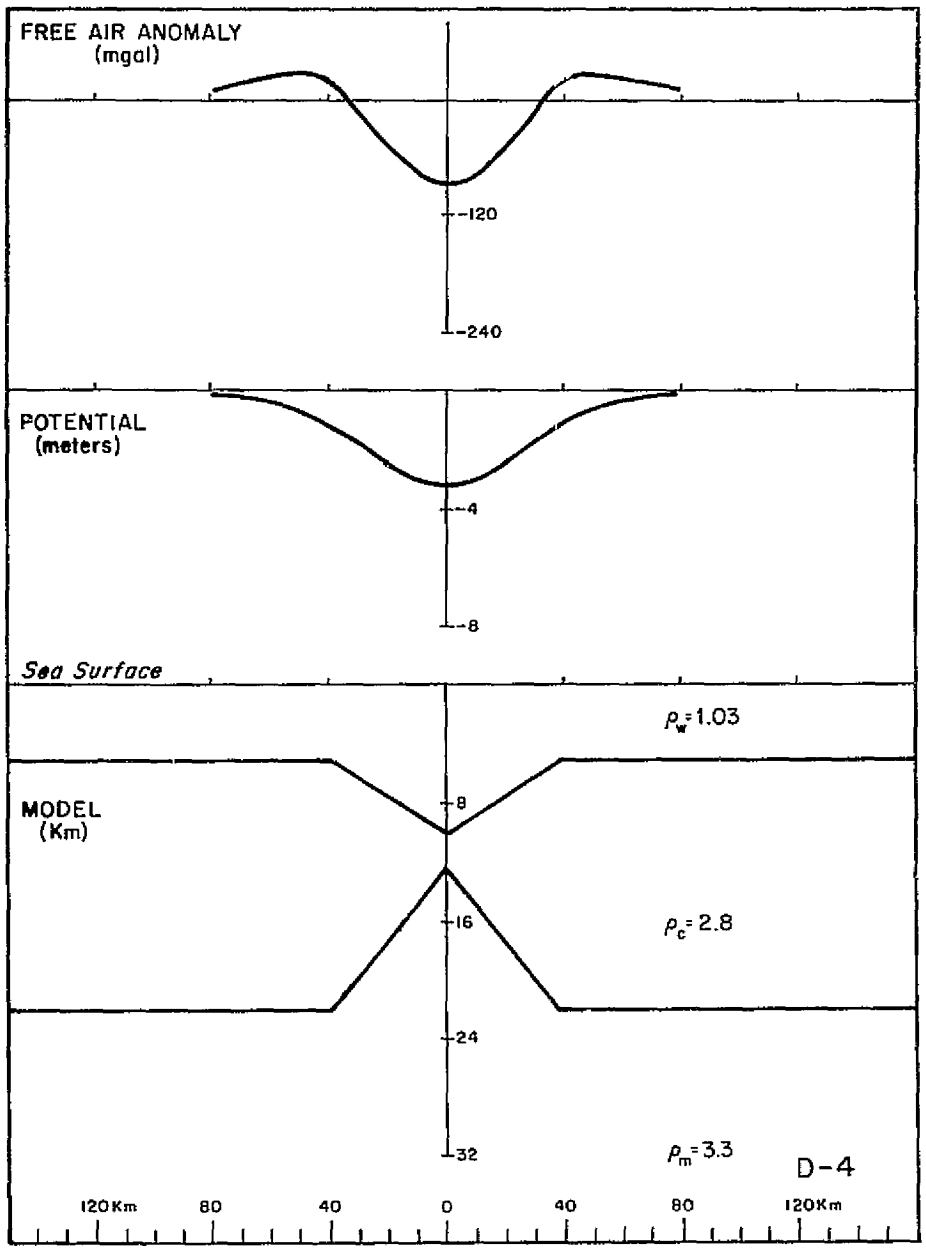
FREE AIR ANOMALY
(mgal)
-120
-240
POTENTIAL
(meters)
-4
-8
Sea Surface
ρ_w=1.03
MODEL
(Km)
8
16
24
32
ρ_c=2.8
ρ_m=3.3
D-4
120Km
80
40
0
40
80
120Km

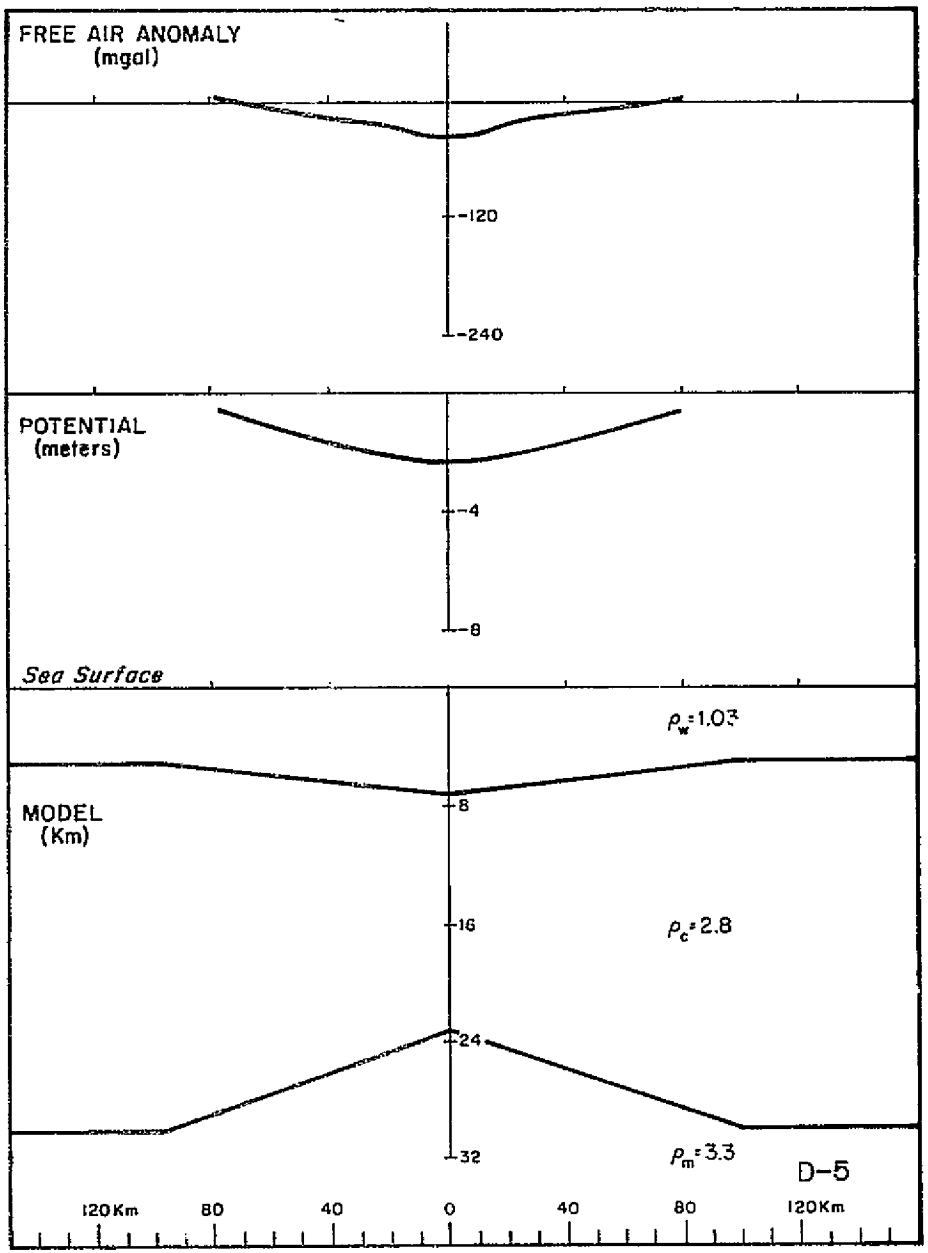
FREE AIR ANOMALY
(mgal)
-120
-240
POTENTIAL
(meters)
-4
-8
Sea Surface
ρ_w=1.03
MODEL
(Km)
8
16
ρ_c=2.8
24
32
ρ_m=3.3
D-5
120Km
80
40
0
40
80
120Km

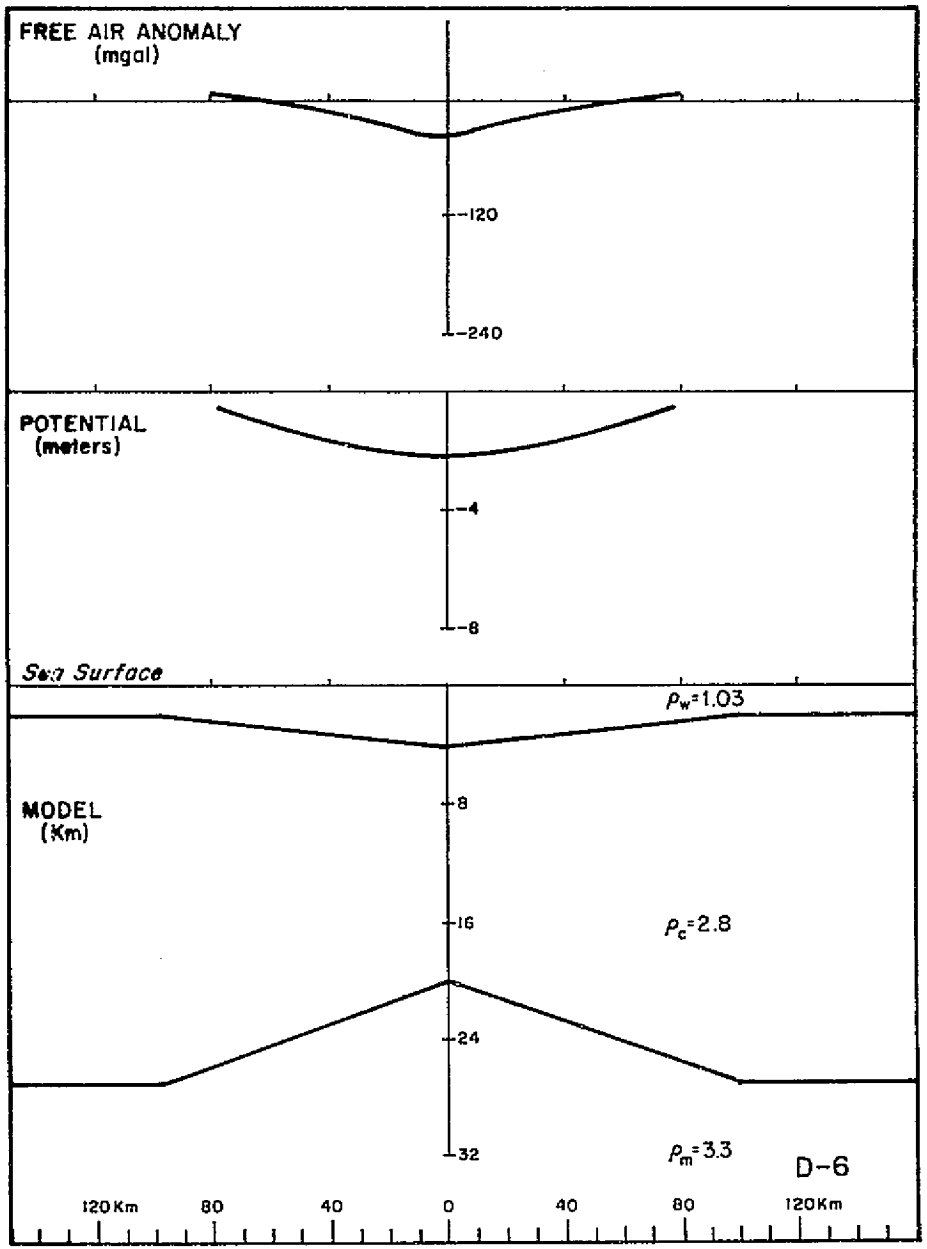
FREE AIR ANOMALY
(mgal)
-120
-240
POTENTIAL
(meters)
-4
-8
Sea Surface
ρ_w=1.03
MODEL
(Km)
8
16
ρ_c=2.8
24
32
ρ_m=3.3
D-6
120Km
80
40
0
40
80
120Km

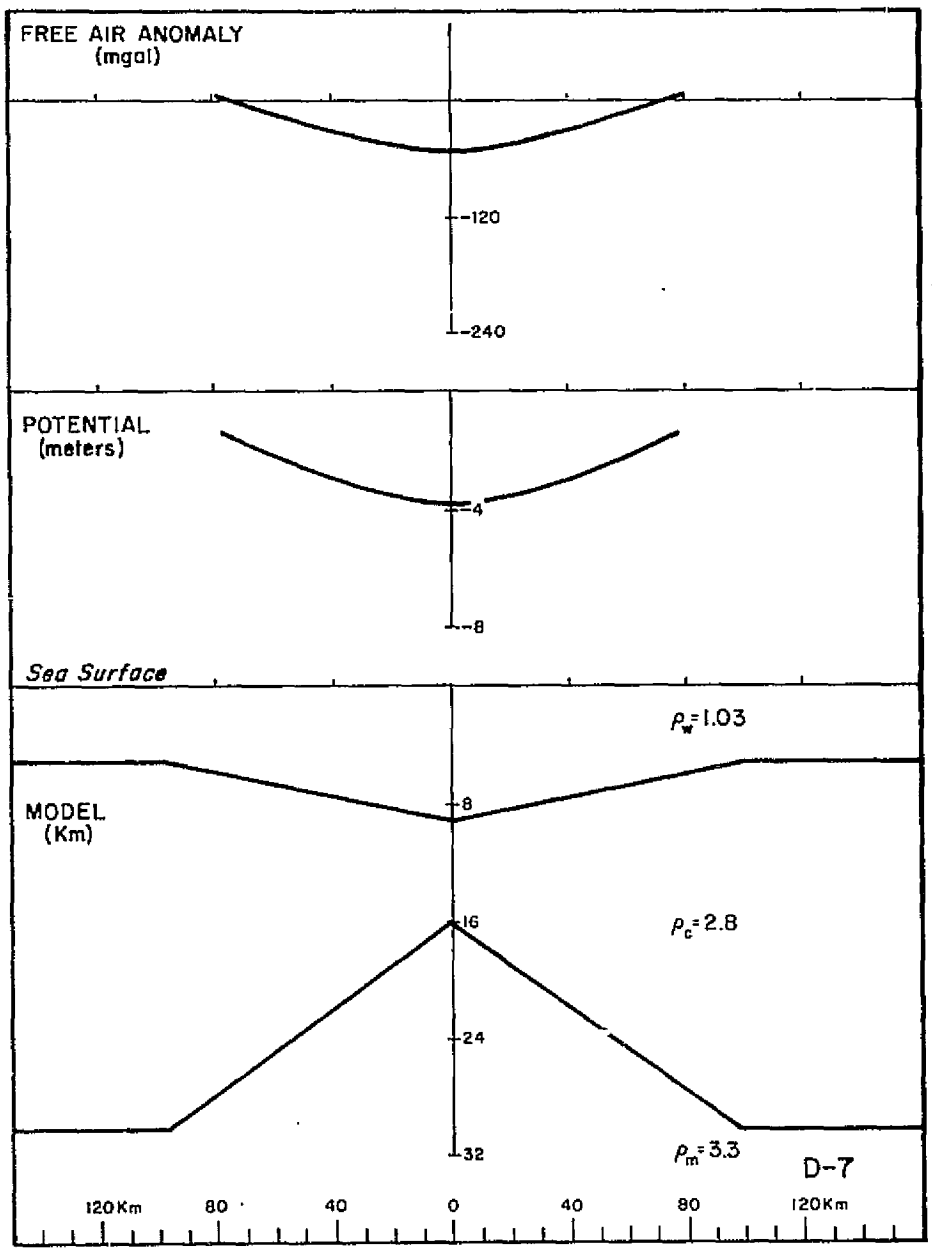
FREE AIR ANOMALY
(mgal)
-120
-240
POTENTIAL
(meters)
-4
-8
Sea Surface
ρ_w=1.03
MODEL
(Km)
8
16
ρ_c=2.8
24
32
ρ_m=3.3
D-7
120Km
80
40
0
40
80
120Km

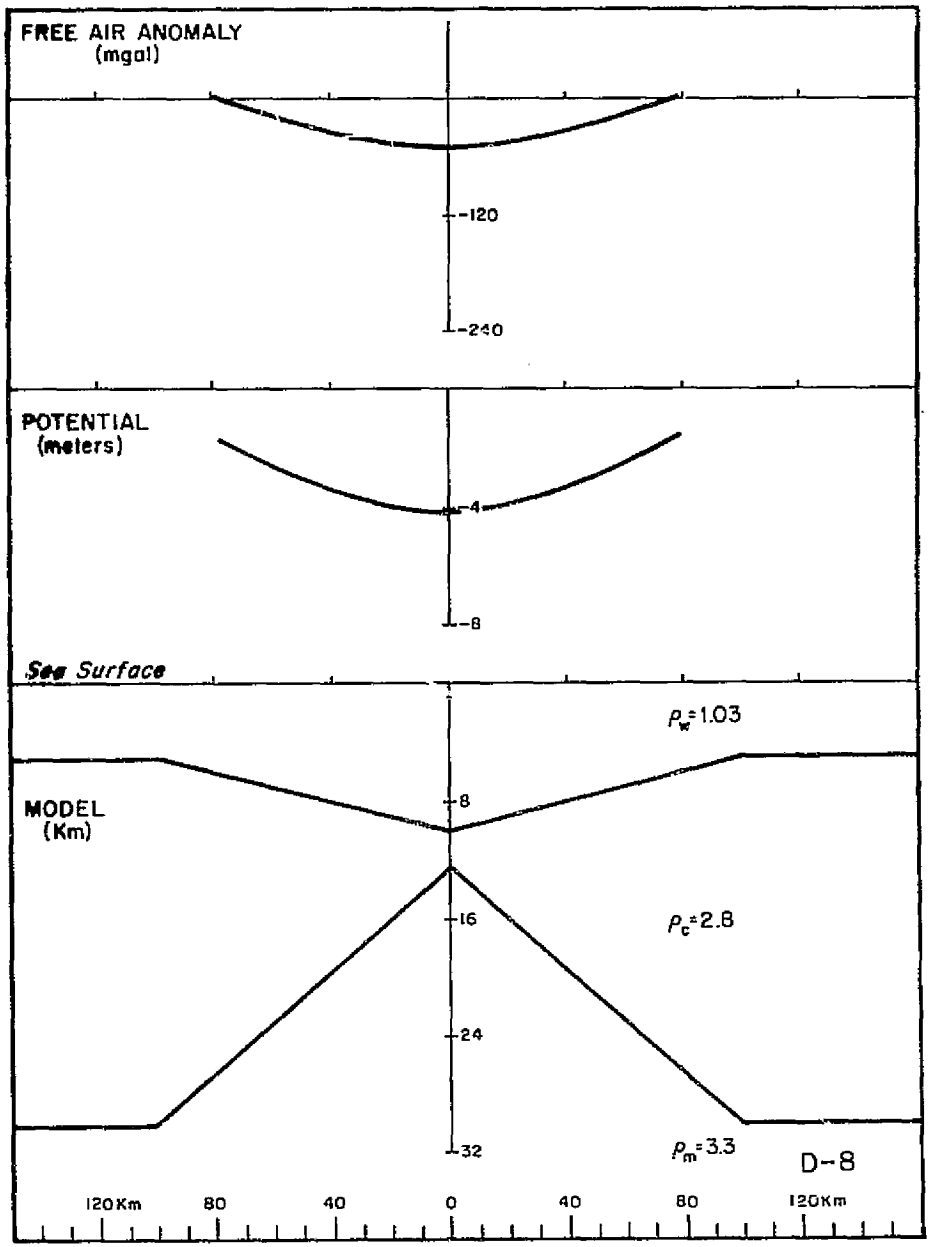
FREE AIR ANOMALY
(mgal)
-120
-240
POTENTIAL
(meters)
-4
-8
Sea Surface
ρ_w=1.03
MODEL
(Km)
8
16
ρ_c=2.8
24
32
ρ_m=3.3
D-8
120Km
80
40
0
40
80
120Km

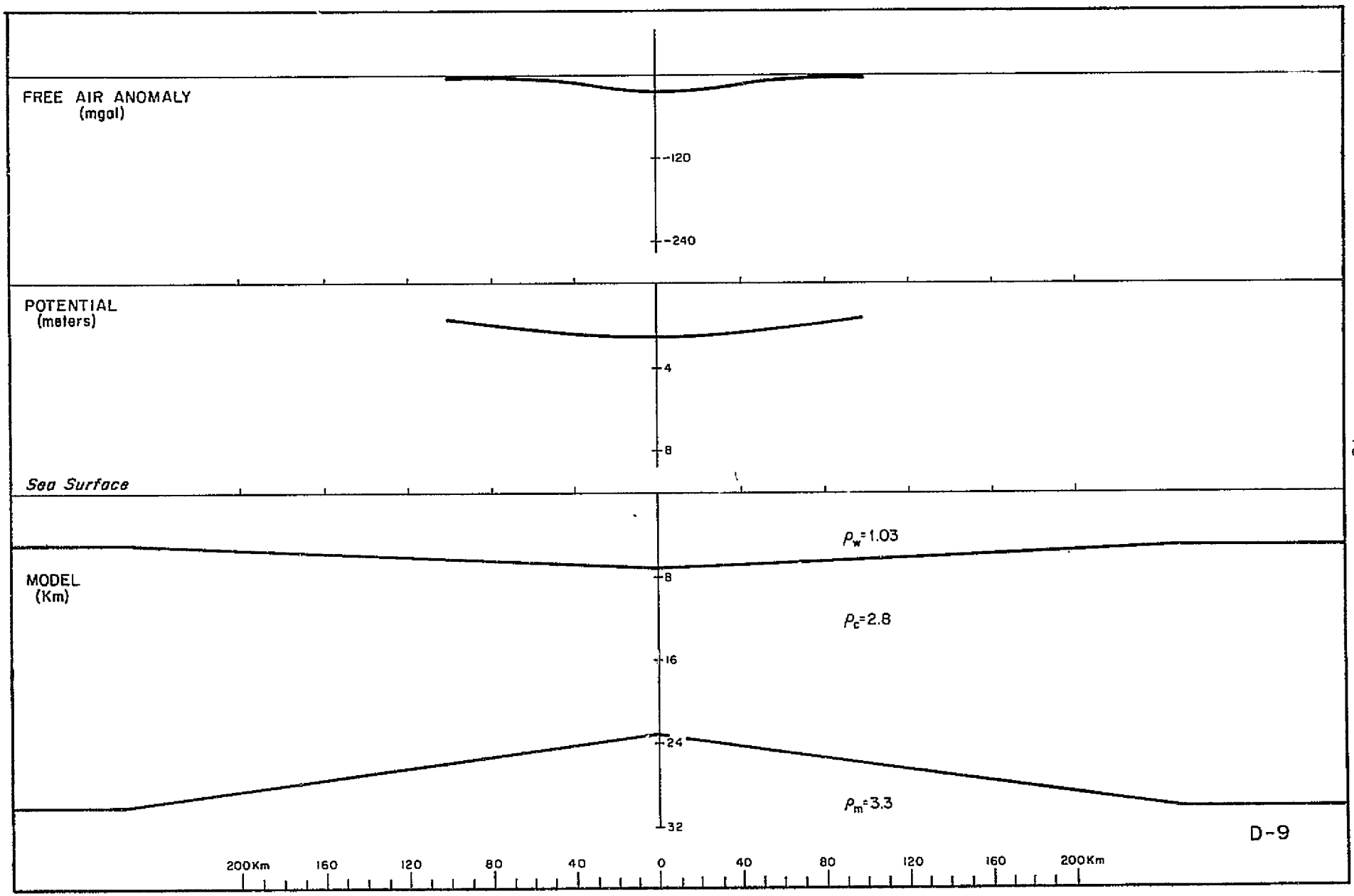
FREE AIR ANOMALY
(mgal)
-120
-240
POTENTIAL
(meters)
4
8
Sea Surface
ρ_w=1.03
MODEL
(Km)
8
ρ_c=2.8
16
24
ρ_m=3.3
32
D-9
200Km
160
120
80
40
0
40
80
120
160
200Km

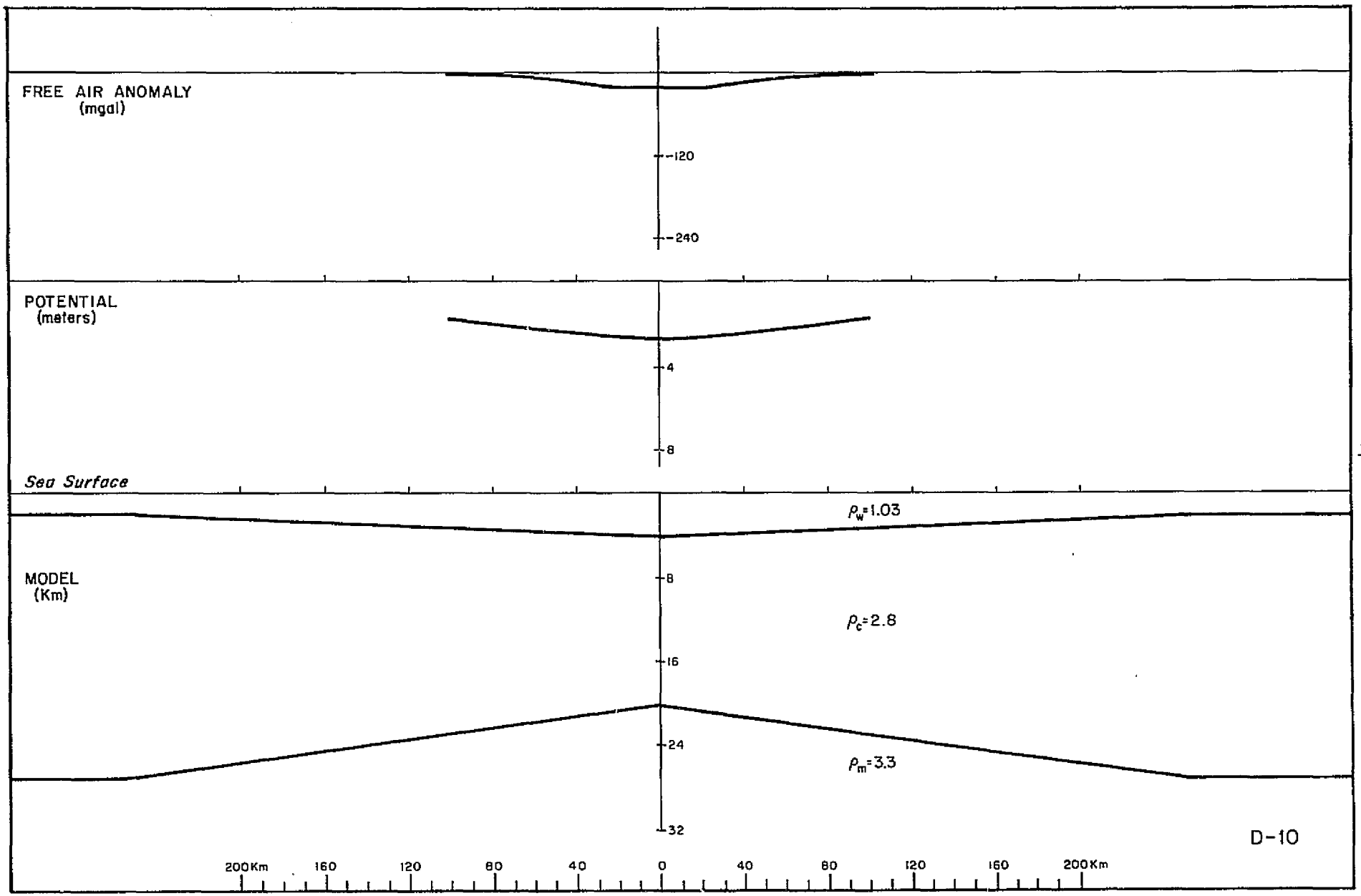
FREE AIR ANOMALY
(mgal)
-120
-240
POTENTIAL
(meters)
4
8
Sea Surface
ρ_w=1.03
MODEL
(Km)
8
ρ_c=2.8
16
24
ρ_m=3.3
32
D-10
200Km
160
120
80
40
0
40
80
120
160
200Km

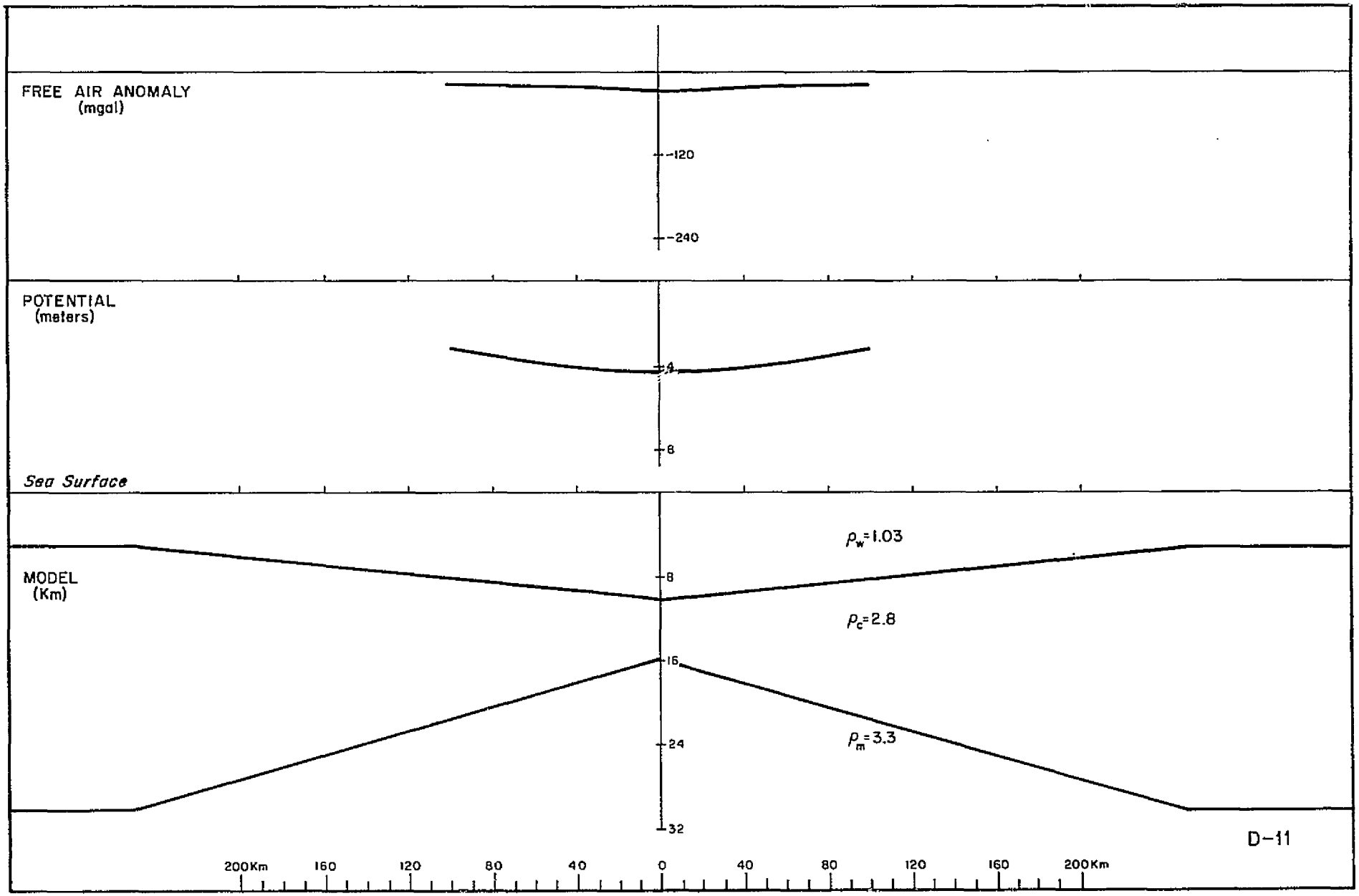
FREE AIR ANOMALY
(mgal)
-120
-240
POTENTIAL
(meters)
4
8
Sea Surface
ρ_w=1.03
MODEL
(Km)
8
ρ_c=2.8
16
24
ρ_m=3.3
32
D-11
200Km
160
120
80
40
0
40
80
120
160
200Km

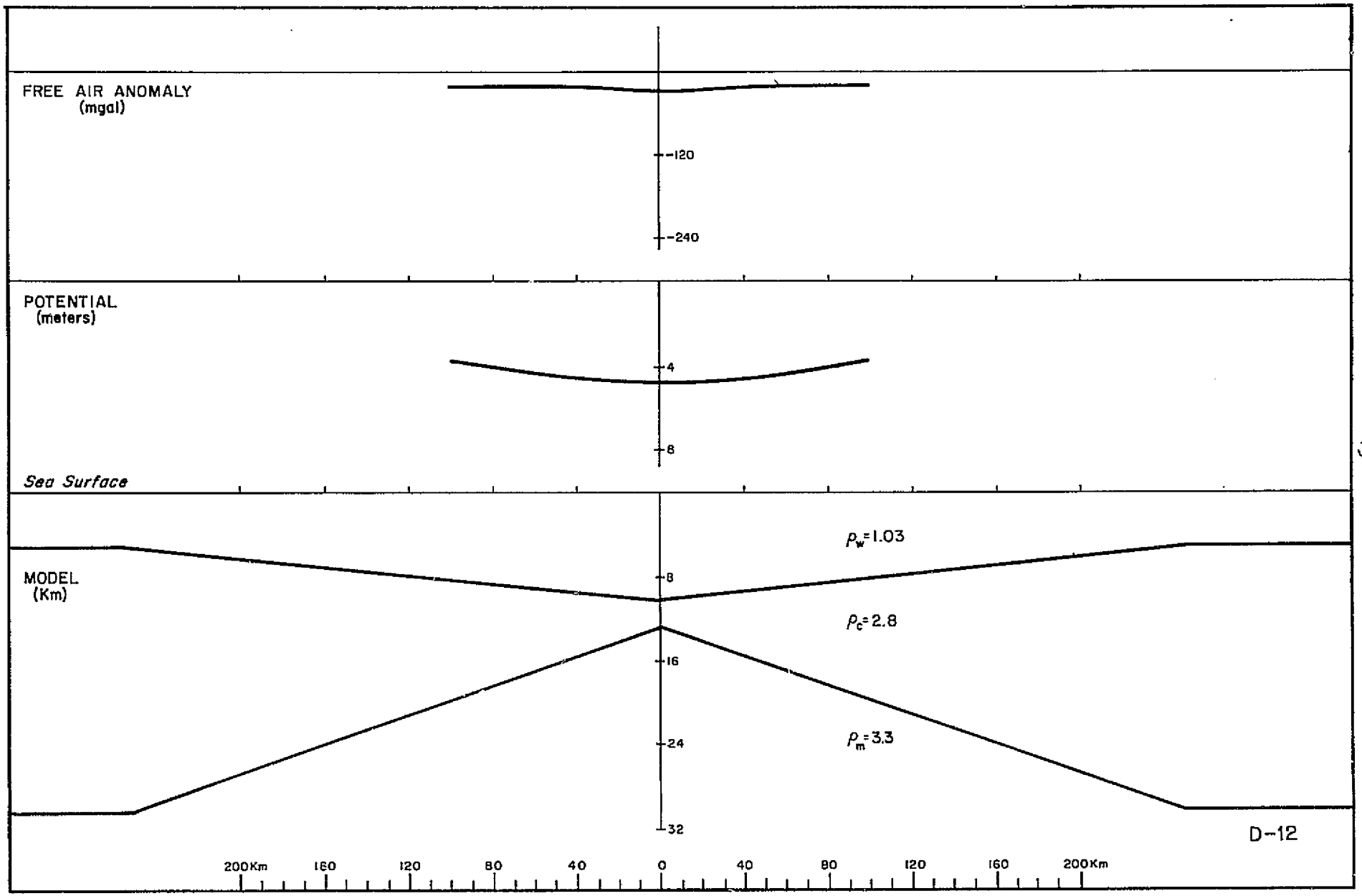
FREE AIR ANOMALY
(mgal)
-120
-240
POTENTIAL
(meters)
4
8
Sea Surface
ρ_w=1.03
MODEL
(Km)
8
ρ_c=2.8
16
24
ρ_m=3.3
32
D-12
200Km
160
120
80
40
0
40
80
120
160
200Km

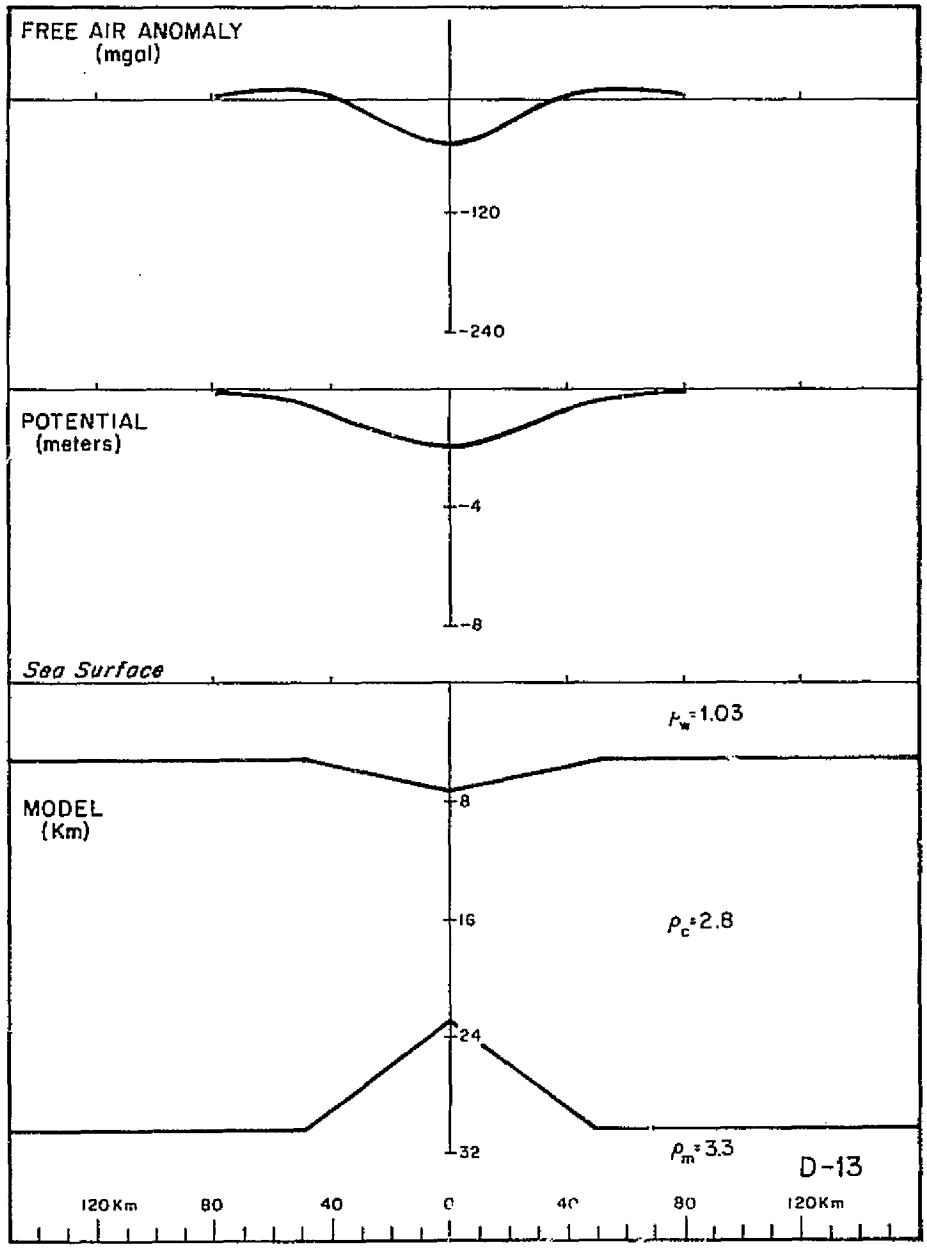
FREE AIR ANOMALY
(mgal)
-120
-240
POTENTIAL
(meters)
-4
-8
Sea Surface
ρ_w=1.03
MODEL
(Km)
8
16
ρ_c=2.8
24
32
ρ_m=3.3
D-13
120Km
80
40
0
40
80
120Km

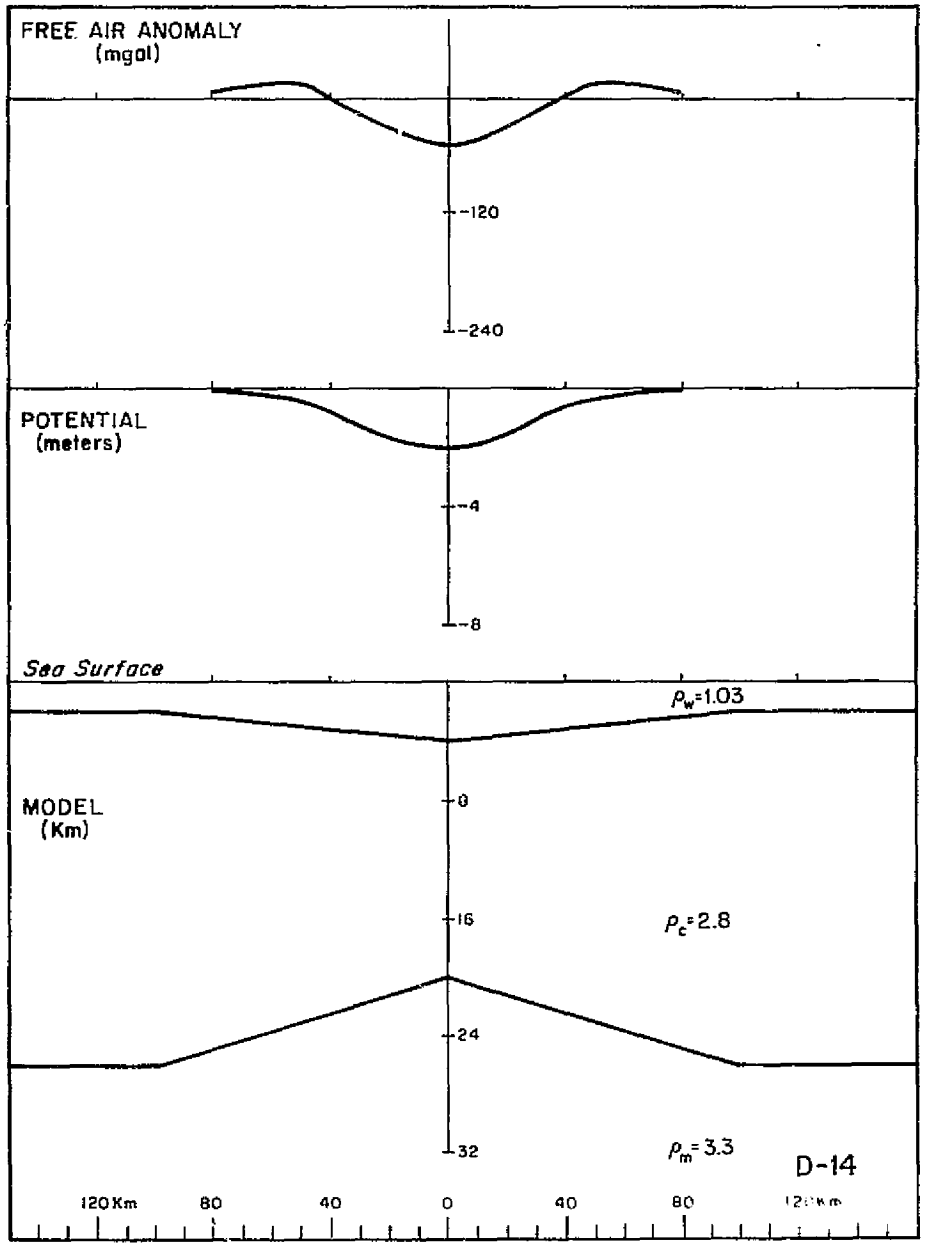
FREE AIR ANOMALY
(mgal)
-120
-240
POTENTIAL
(meters)
-4
-8
Sea Surface
ρ_w=1.03
MODEL
(Km)
0
16
ρ_c=2.8
24
32
ρ_m=3.3
D-14
120Km
80
40
0
40
80

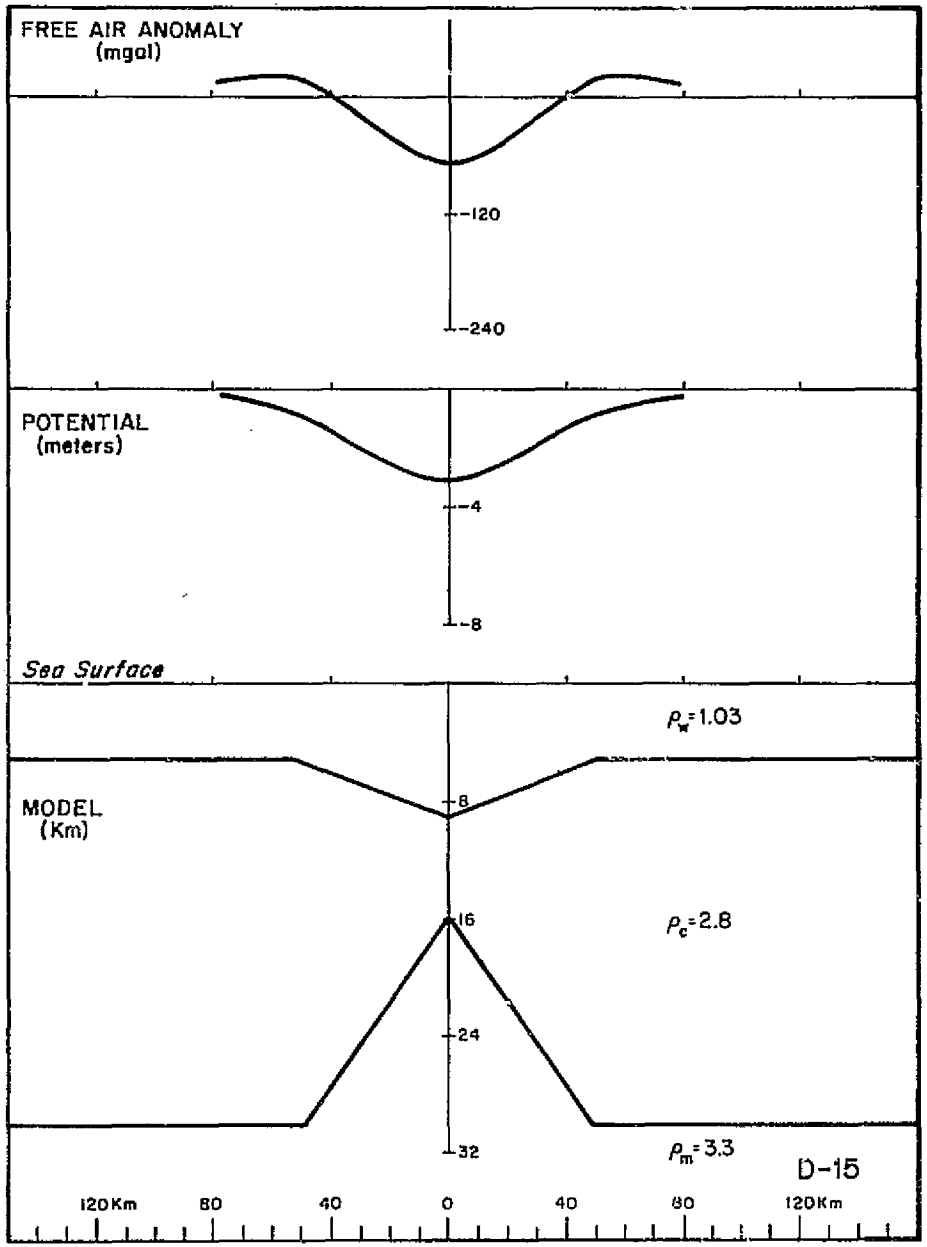
FREE AIR ANOMALY
(mgal)
-120
-240
POTENTIAL
(meters)
-4
-8
Sea Surface
ρ_w=1.03
MODEL
(Km)
8
16
ρ_c=2.8
24
32
ρ_m=3.3
D-15
120Km
80
40
0
40
80
120Km

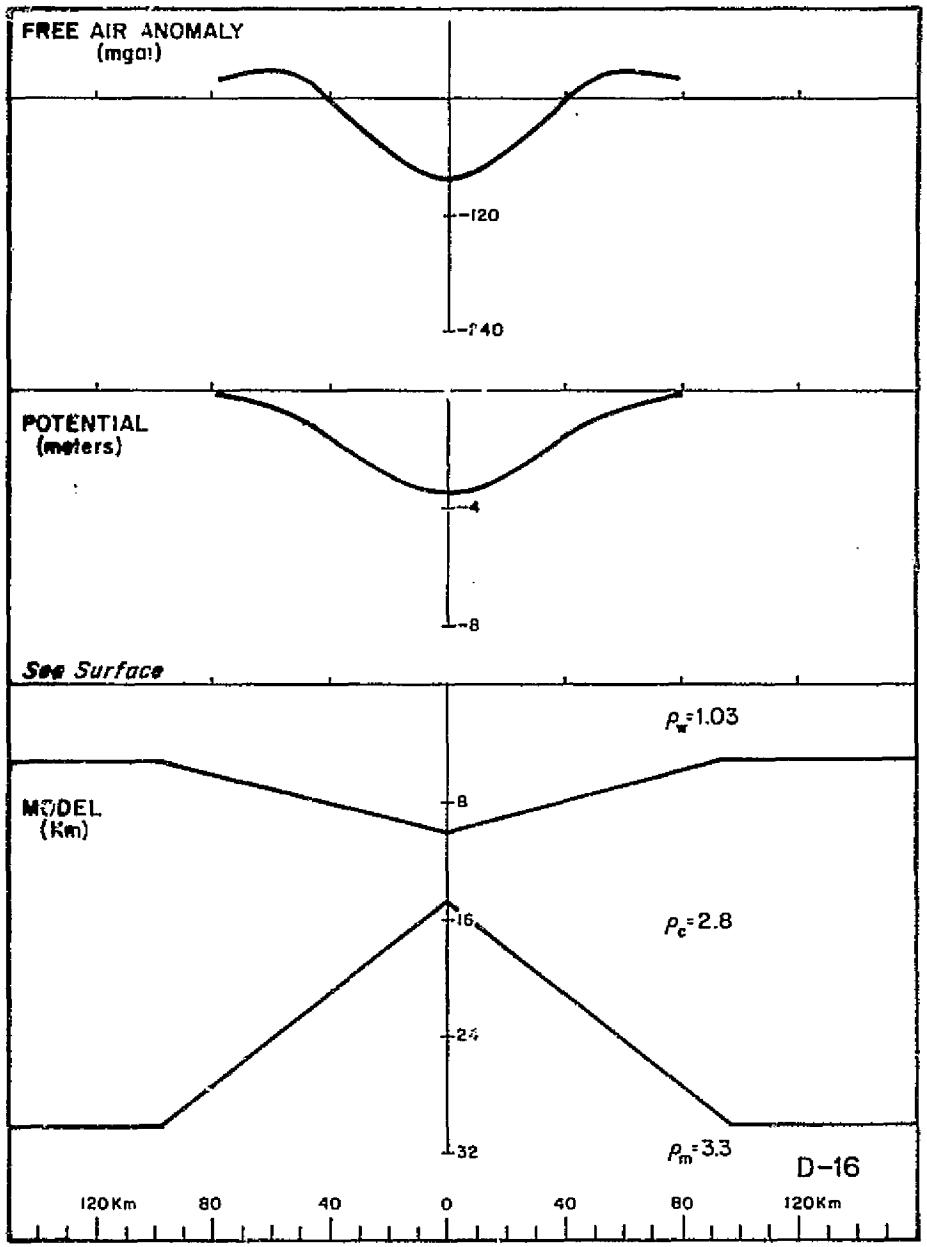
FREE AIR ANOMALY
(mgal)
-120
-240
POTENTIAL
(meters)
-4
-8
Sea Surface
ρ_w=1.03
MODEL
(Km)
8
16
ρ_c=2.8
24
32
ρ_m=3.3
D-16
120Km
80
40
0
40
80
120Km

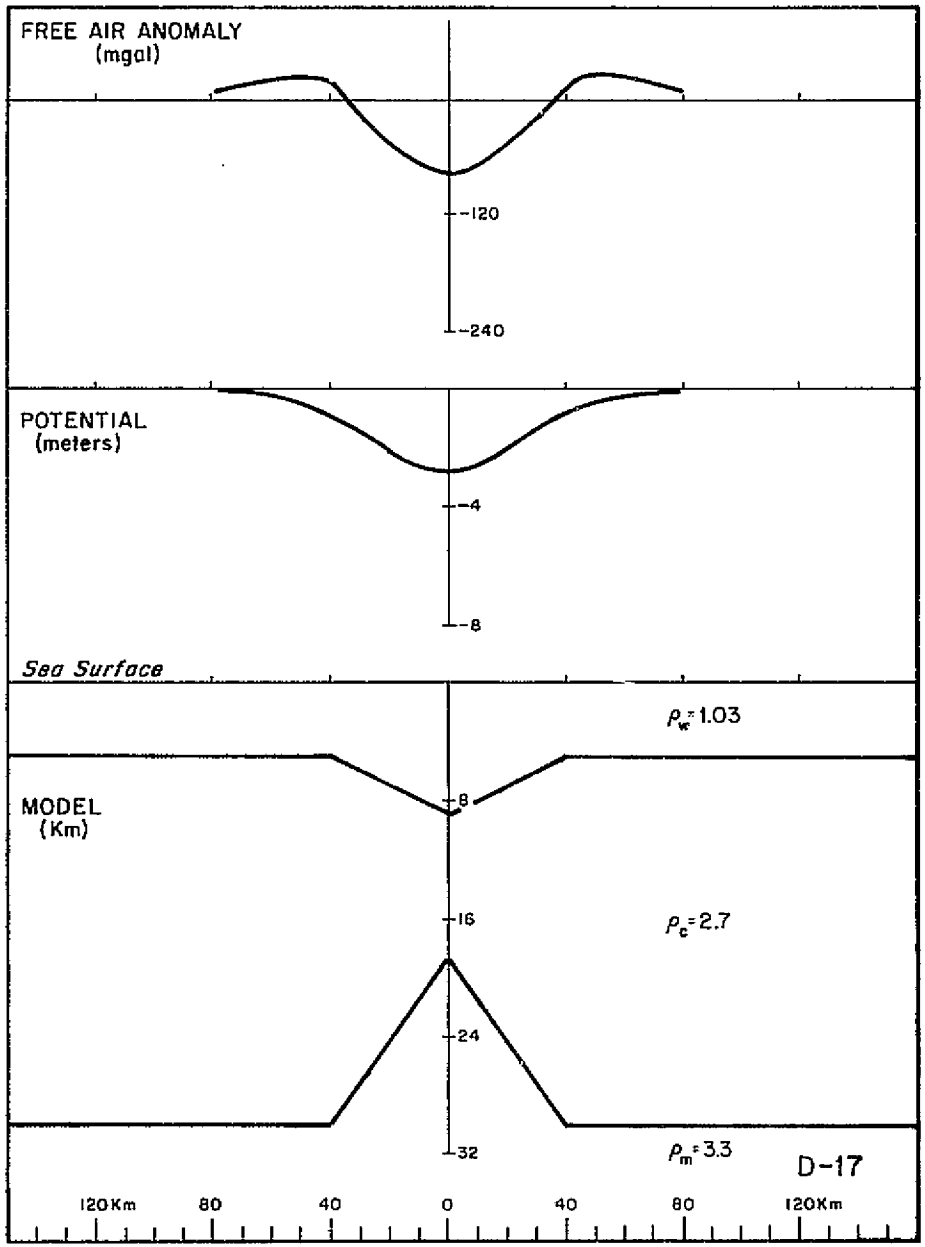
FREE AIR ANOMALY
(mgal)
-120
-240
POTENTIAL
(meters)
-4
-8
Sea Surface
ρ_w=1.03
MODEL
(Km)
8
16
ρ_c=2.7
24
32
ρ_m=3.3
D-17
120Km
80
40
0
40
80
120Km

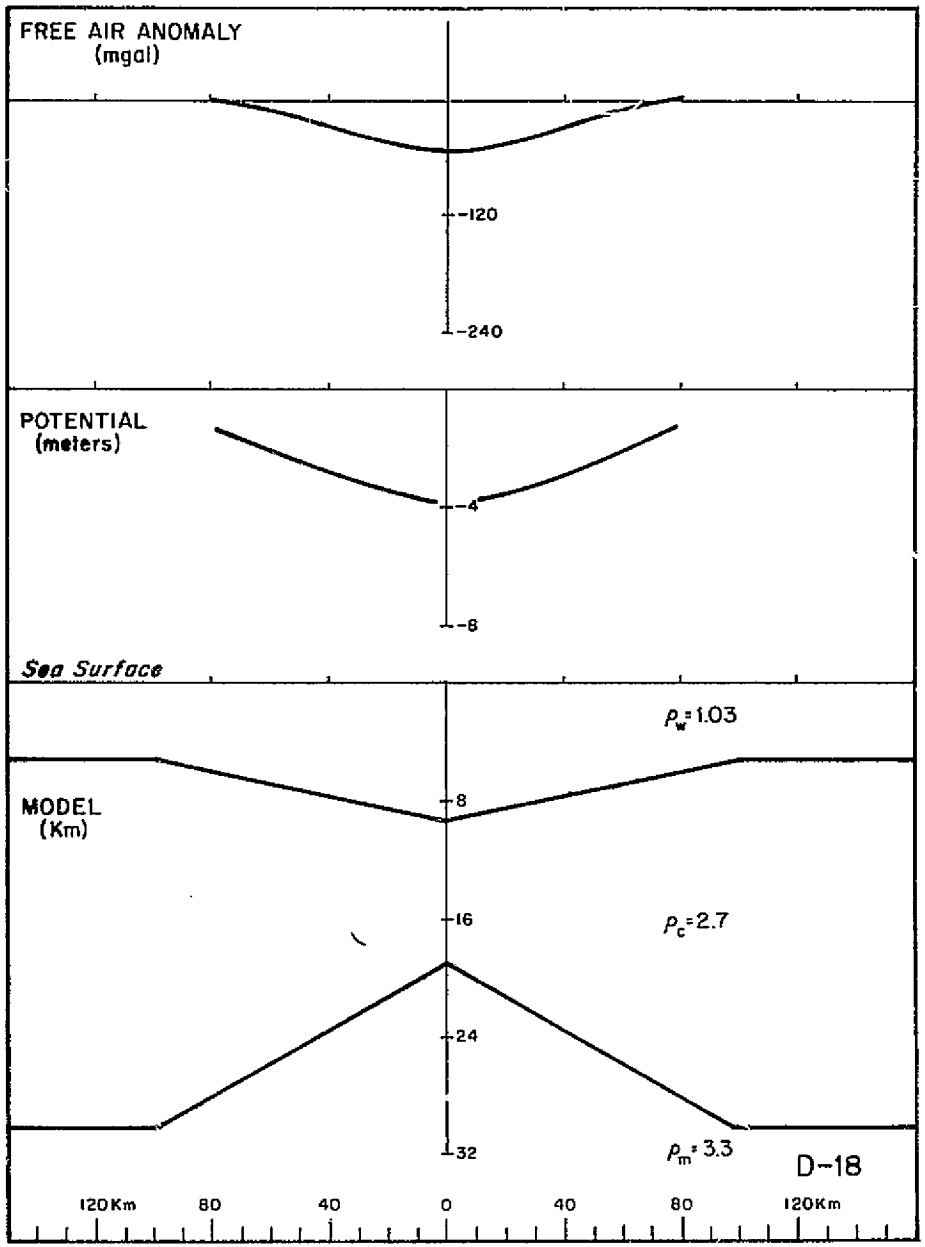
FREE AIR ANOMALY
(mgal)
-120
-240
POTENTIAL
(meters)
-4
-8
Sea Surface
ρ_w=1.03
MODEL
(Km)
8
16
ρ_c=2.7
24
32
ρ_m=3.3
D-18
120Km
80
40
0
40
80
120Km

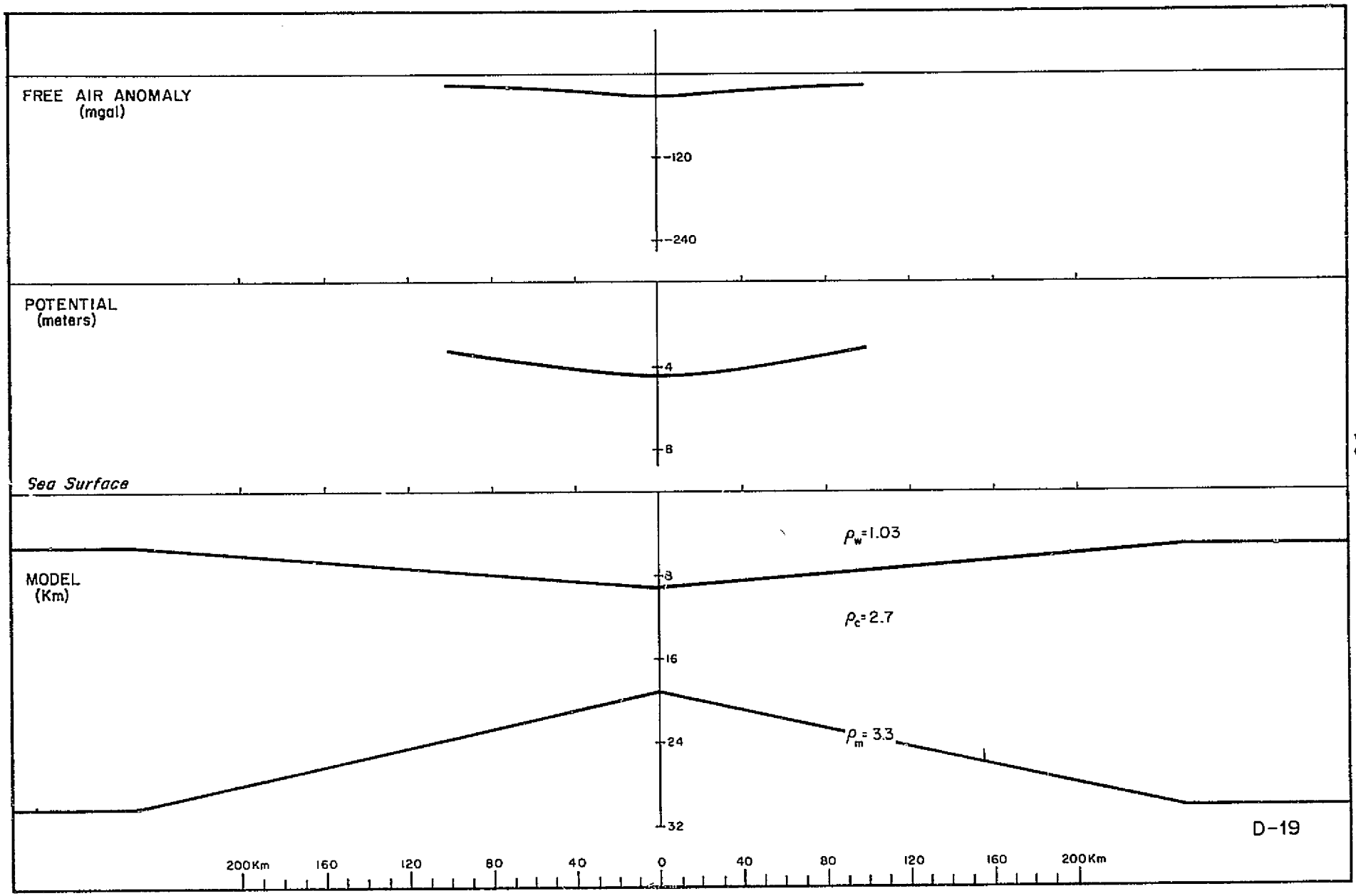
FREE AIR ANOMALY
(mgal)
-120
-240
POTENTIAL
(meters)
4
8
Sea Surface
ρ_w=1.03
MODEL
(Km)
8
ρ_c=2.7
16
24
ρ_m=3.3
32
D-19
200Km
160
120
80
40
0
40
80
120
160
200Km

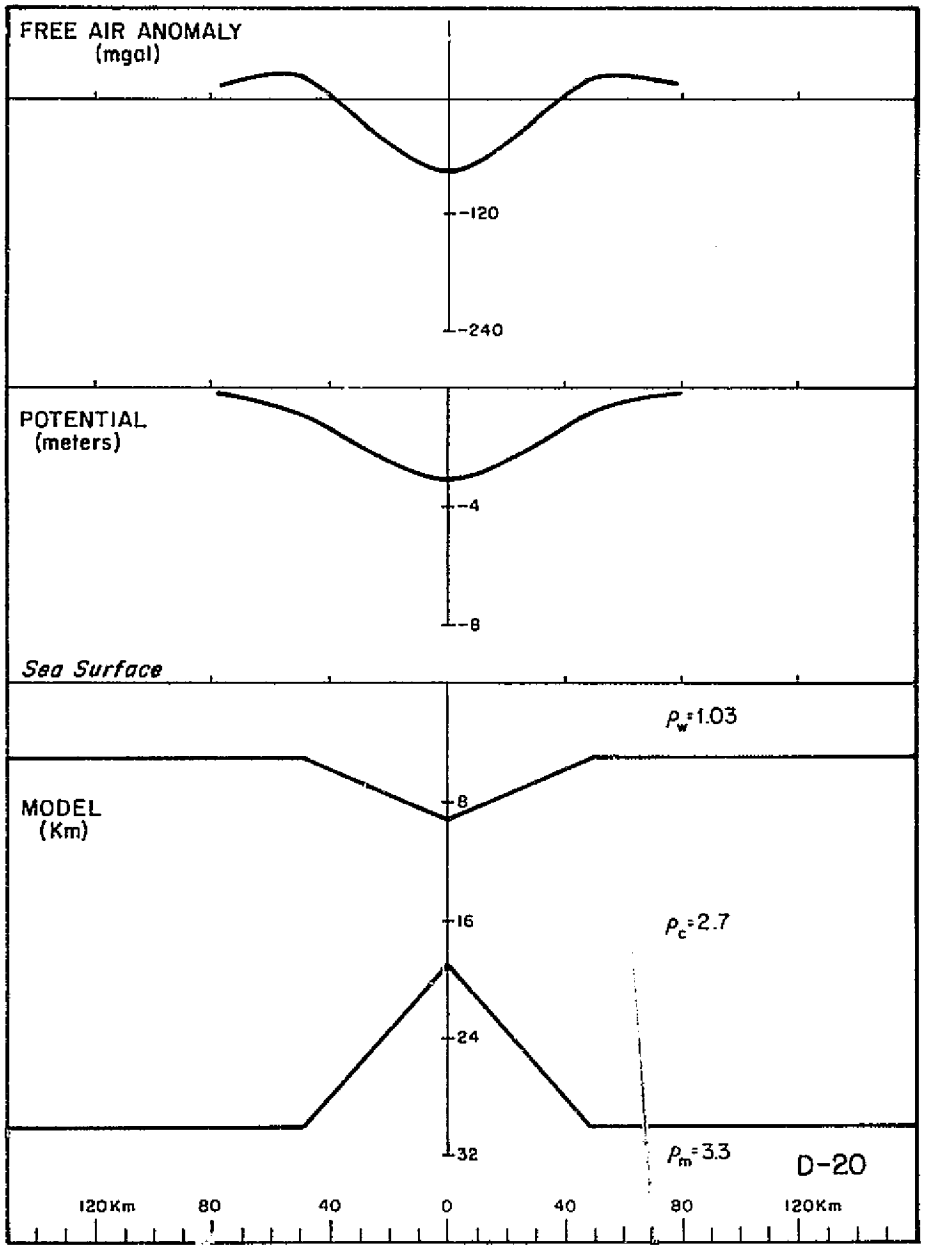
FREE AIR ANOMALY
(mgal)
-120
-240
POTENTIAL
(meters)
-4
-8
Sea Surface
ρ_w=1.03
MODEL
(Km)
8
16
ρ_c=2.7
24
32
ρ_m=3.3
D-20
120Km
80
40
0
40
80
120Km

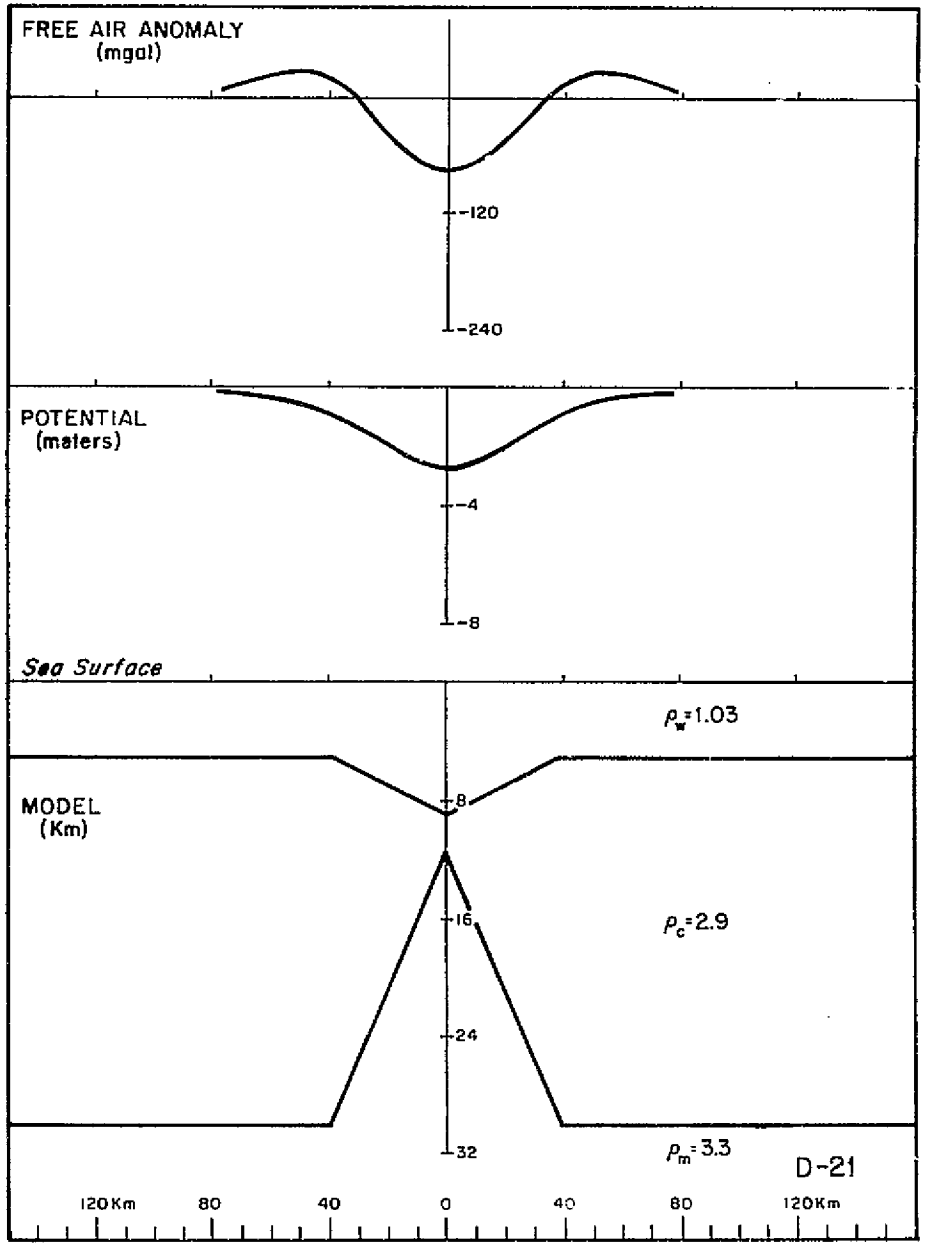
FREE AIR ANOMALY
(mgal)
-120
-240
POTENTIAL
(meters)
-4
-8
Sea Surface
ρ_w=1.03
MODEL
(Km)
8
16
ρ_c=2.9
24
32
ρ_m=3.3
D-21
120Km
80
40
0
40
80
120Km

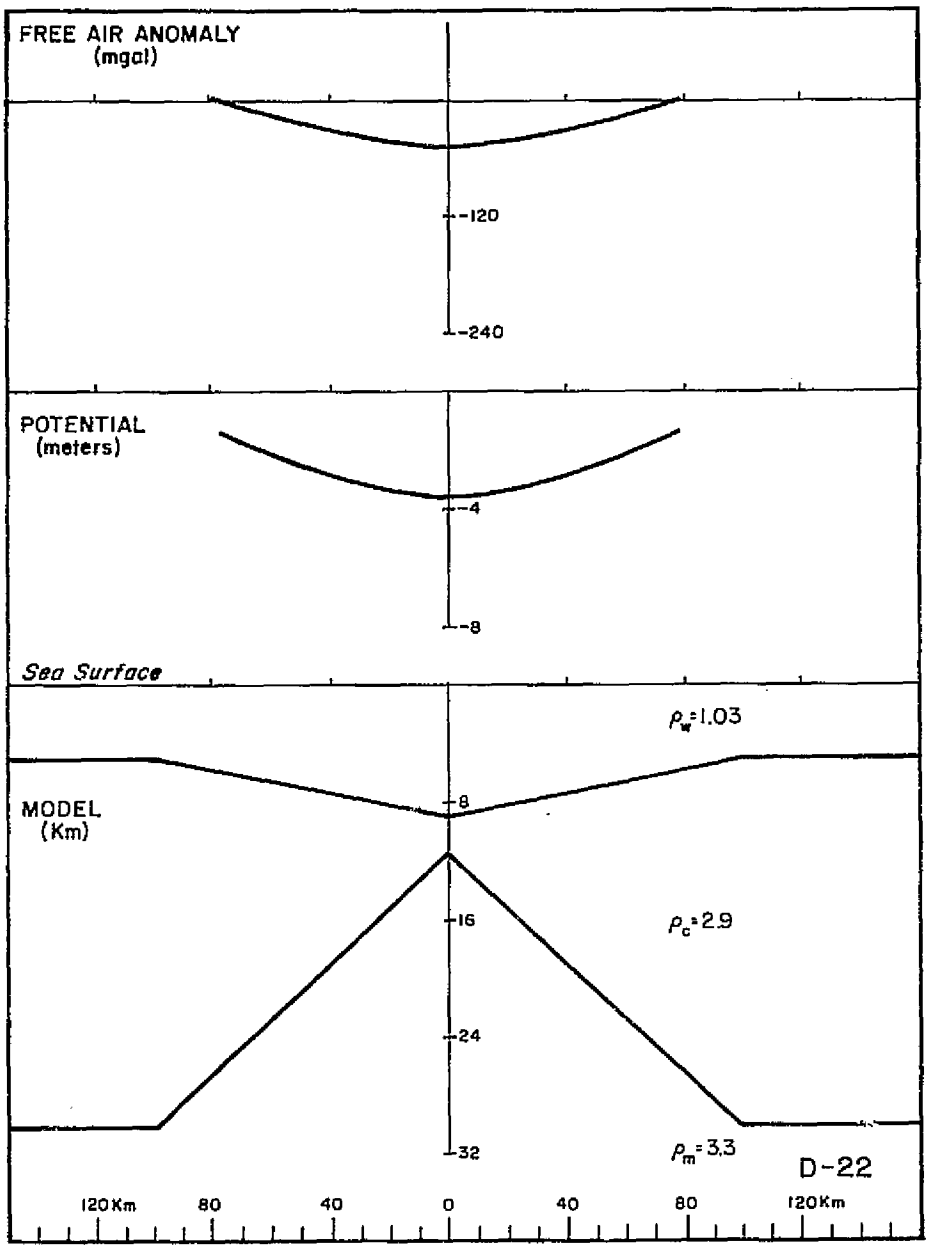
FREE AIR ANOMALY
(mgal)
-120
-240
POTENTIAL
(meters)
-4
-8
Sea Surface
ρ_w=1.03
MODEL
(Km)
-8
-16
ρ_c=2.9
-24
-32
ρ_m=3.3
D-22
120Km
80
40
0
40
80
120Km

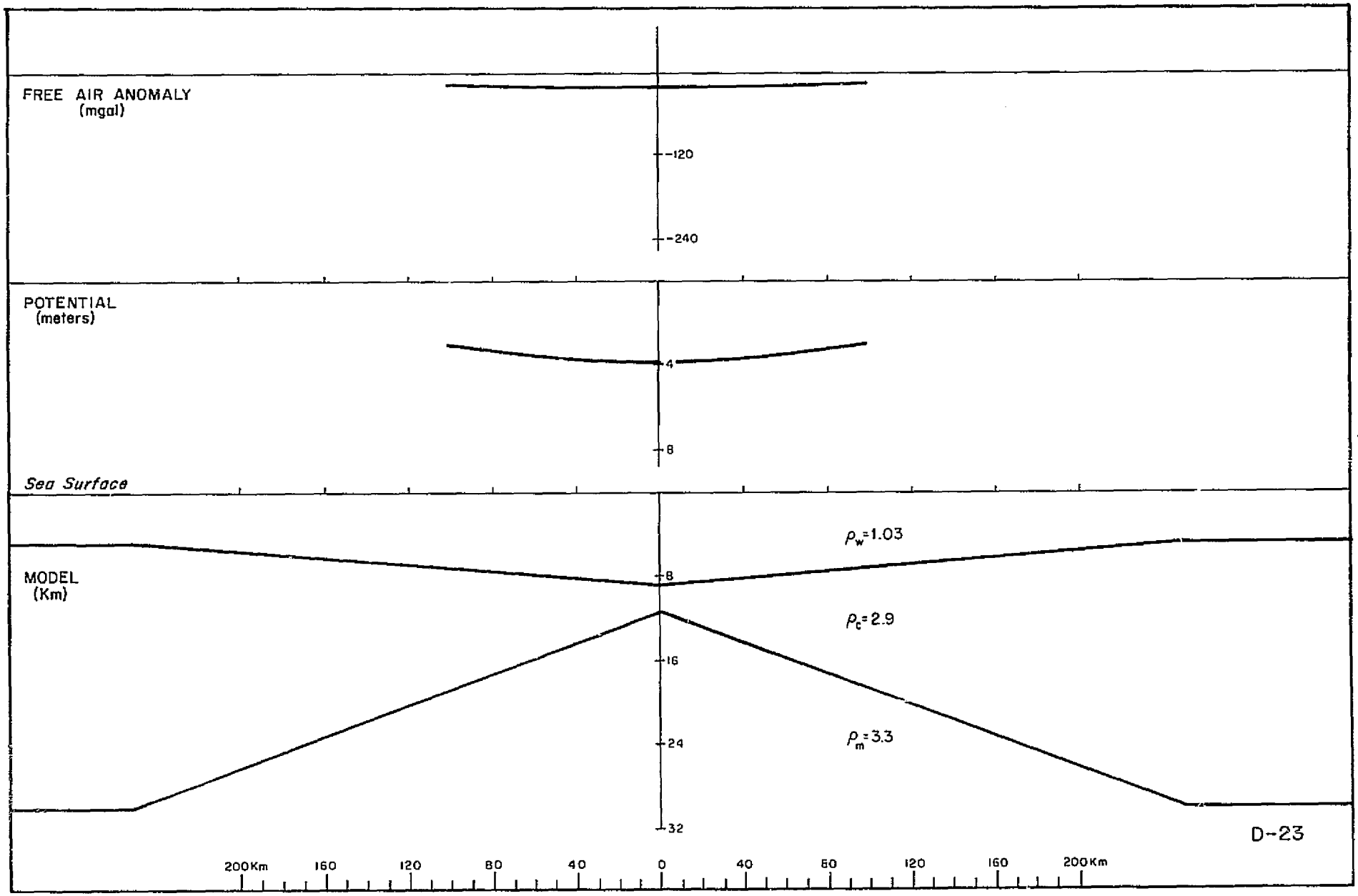
FREE AIR ANOMALY
(mgal)
-120
-240
POTENTIAL
(meters)
4
8
Sea Surface
ρ_w=1.03
MODEL
(Km)
8
ρ_c=2.9
16
24
ρ_m=3.3
32
D-23
200Km
160
120
80
40
0
40
80
120
160
200Km

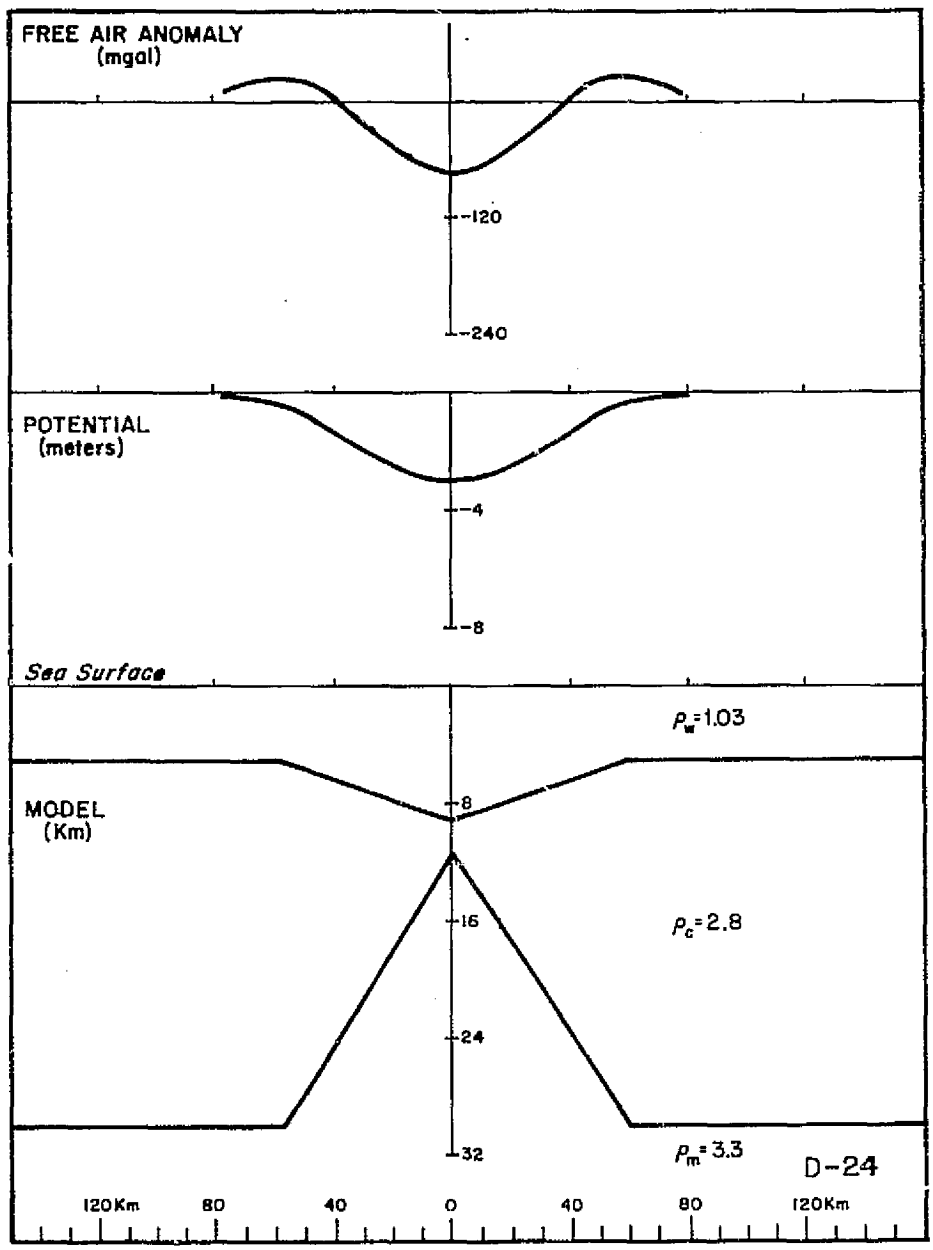
FREE AIR ANOMALY
(mgal)
-120
-240
POTENTIAL
(meters)
-4
-8
Sea Surface
ρ_w=1.03
MODEL
(Km)
8
16
ρ_c=2.8
24
32
ρ_m=3.3
D-24
120Km
80
40
0
40
80
120Km

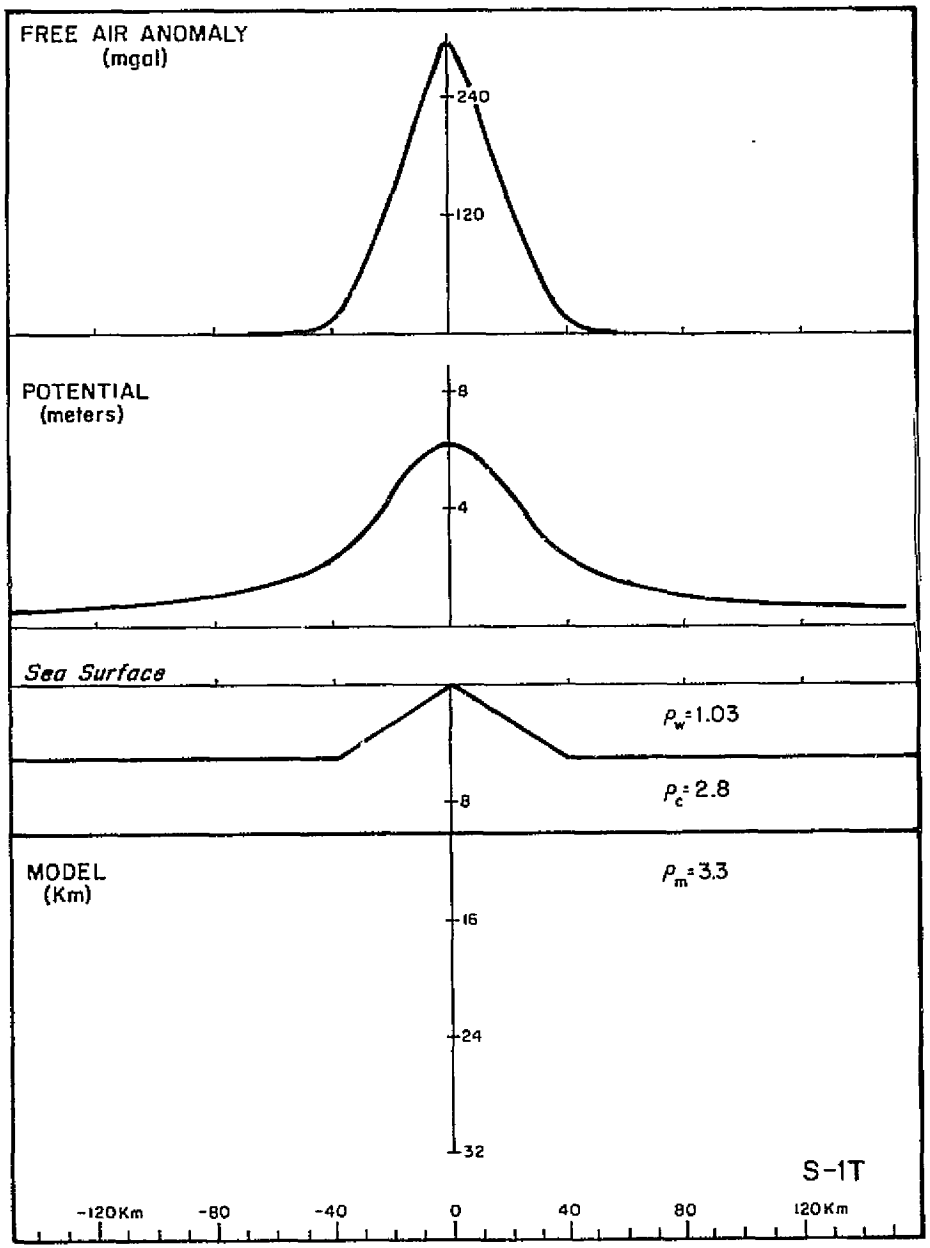
FREE AIR ANOMALY
(mgal)
240
120
POTENTIAL
(meters)
8
4
Sea Surface
ρ_w=1.03
ρ_c=2.8
8
MODEL
(Km)
ρ_m=3.3
16
24
32
S-1T
-120Km
-80
-40
0
40
80
120Km

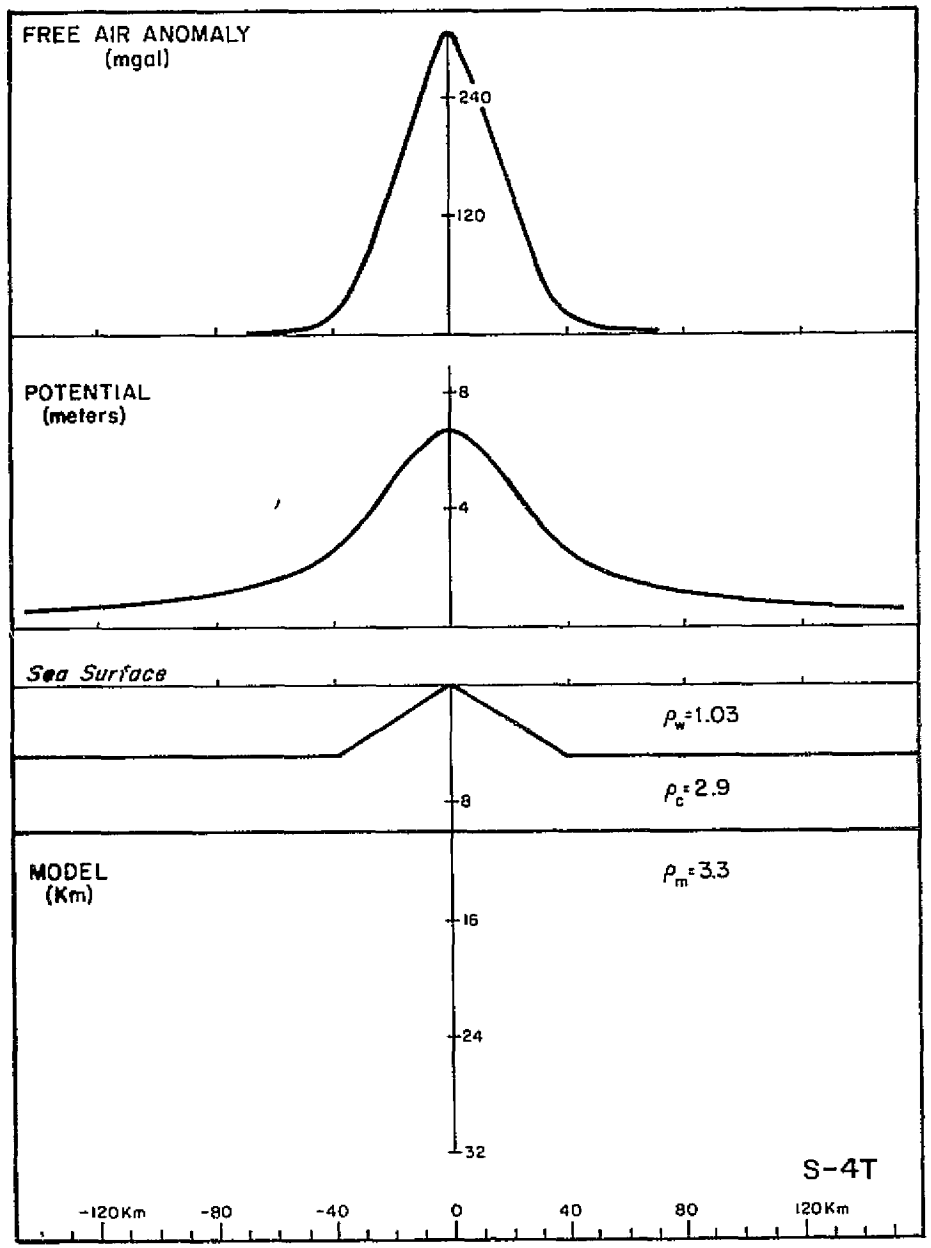
FREE AIR ANOMALY
(mgal)
240
120
POTENTIAL
(meters)
8
4
Sea Surface
ρ_w=1.03
ρ_c=2.9
8
MODEL
(Km)
ρ_m=3.3
16
24
32
S-4T
-120Km
-80
-40
0
40
80
120Km

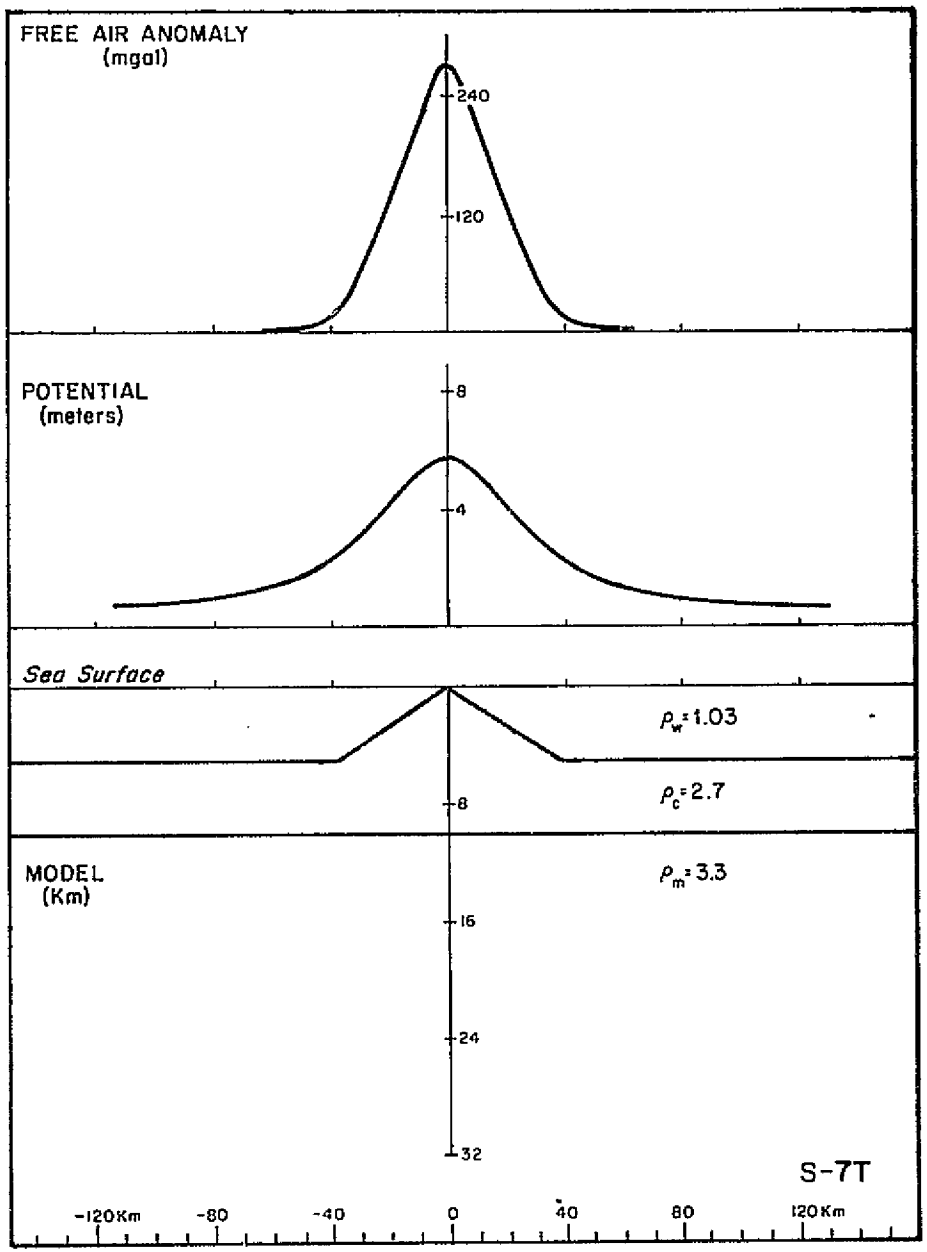
FREE AIR ANOMALY
(mgal)
240
120
POTENTIAL
(meters)
8
4
Sea Surface
ρ_w=1.03
ρ_c=2.7
8
MODEL
(Km)
ρ_m=3.3
16
24
32
S-7T
-120Km
-80
-40
0
40
80
120Km

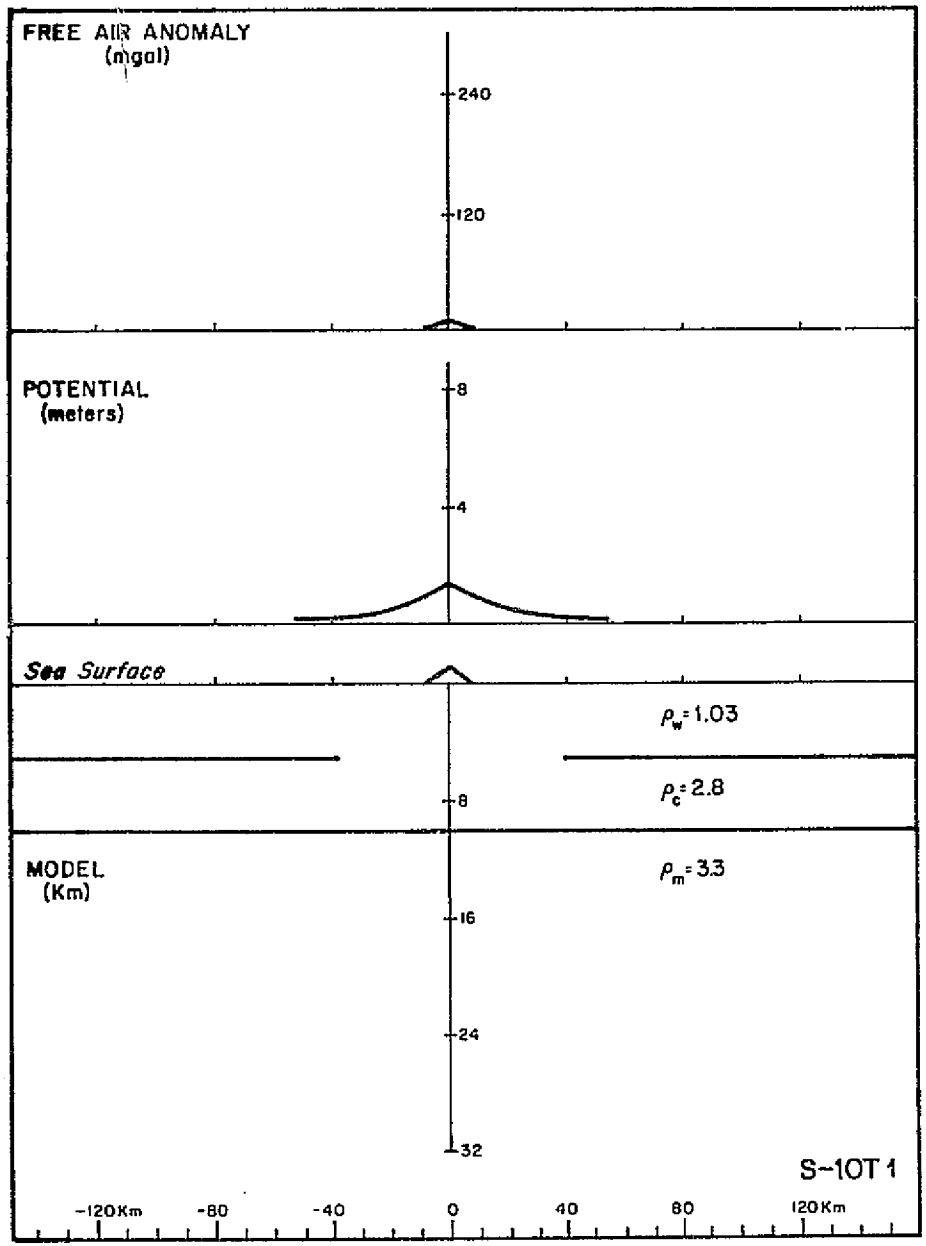
FREE AIR ANOMALY
(mgal)
240
120
POTENTIAL
(meters)
8
4
Sea Surface
ρ_w=1.03
ρ_c=2.8
8
MODEL
(Km)
ρ_m=3.3
16
24
32
S-10T 1
-120Km
-80
-40
0
40
80
120Km

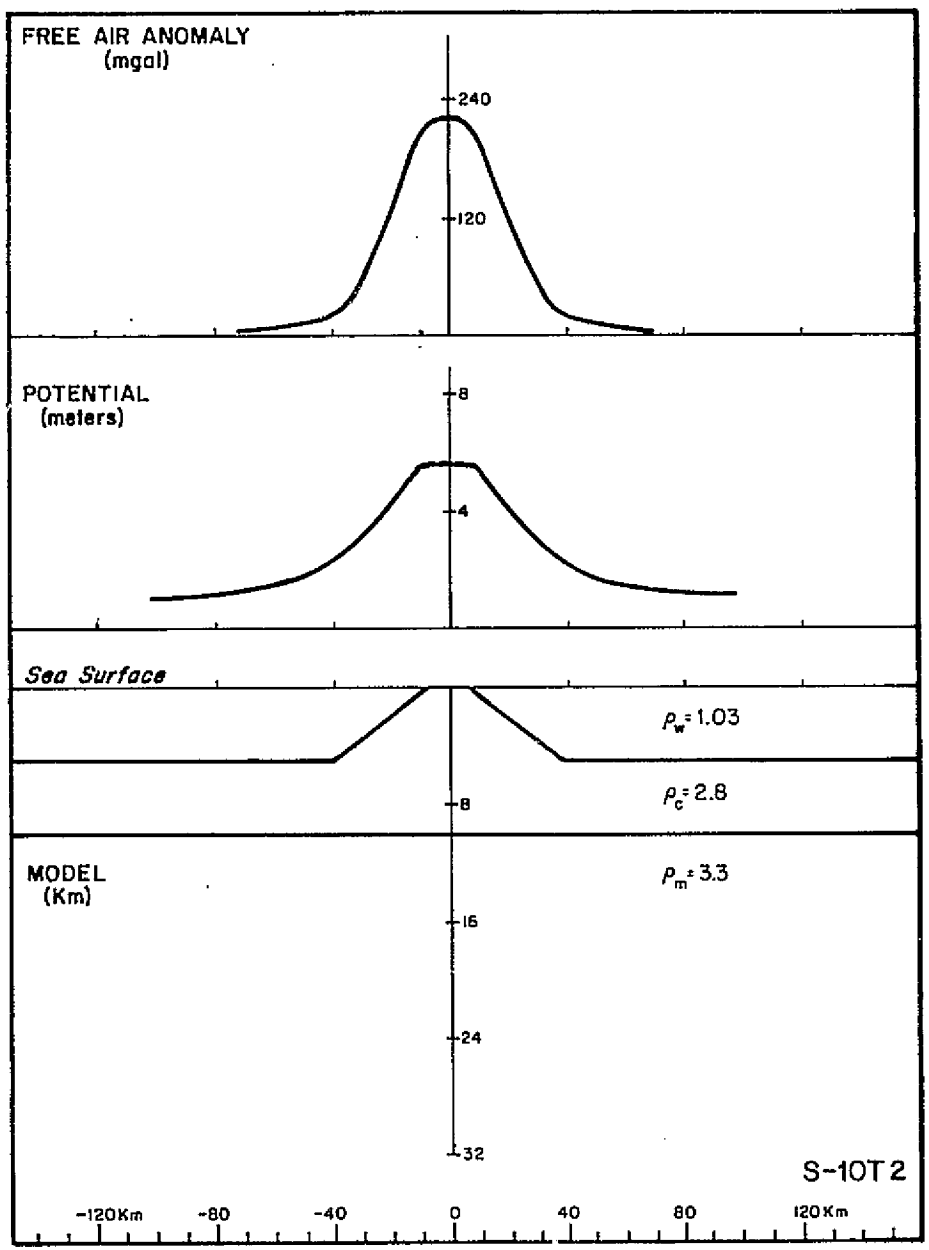
FREE AIR ANOMALY
(mgal)
240
120
POTENTIAL
(meters)
8
4
Sea Surface
ρ_w=1.03
ρ_c=2.8
8
MODEL
(Km)
ρ_m=3.3
16
24
32
S-10T2
-120Km
-80
-40
0
40
80
120Km

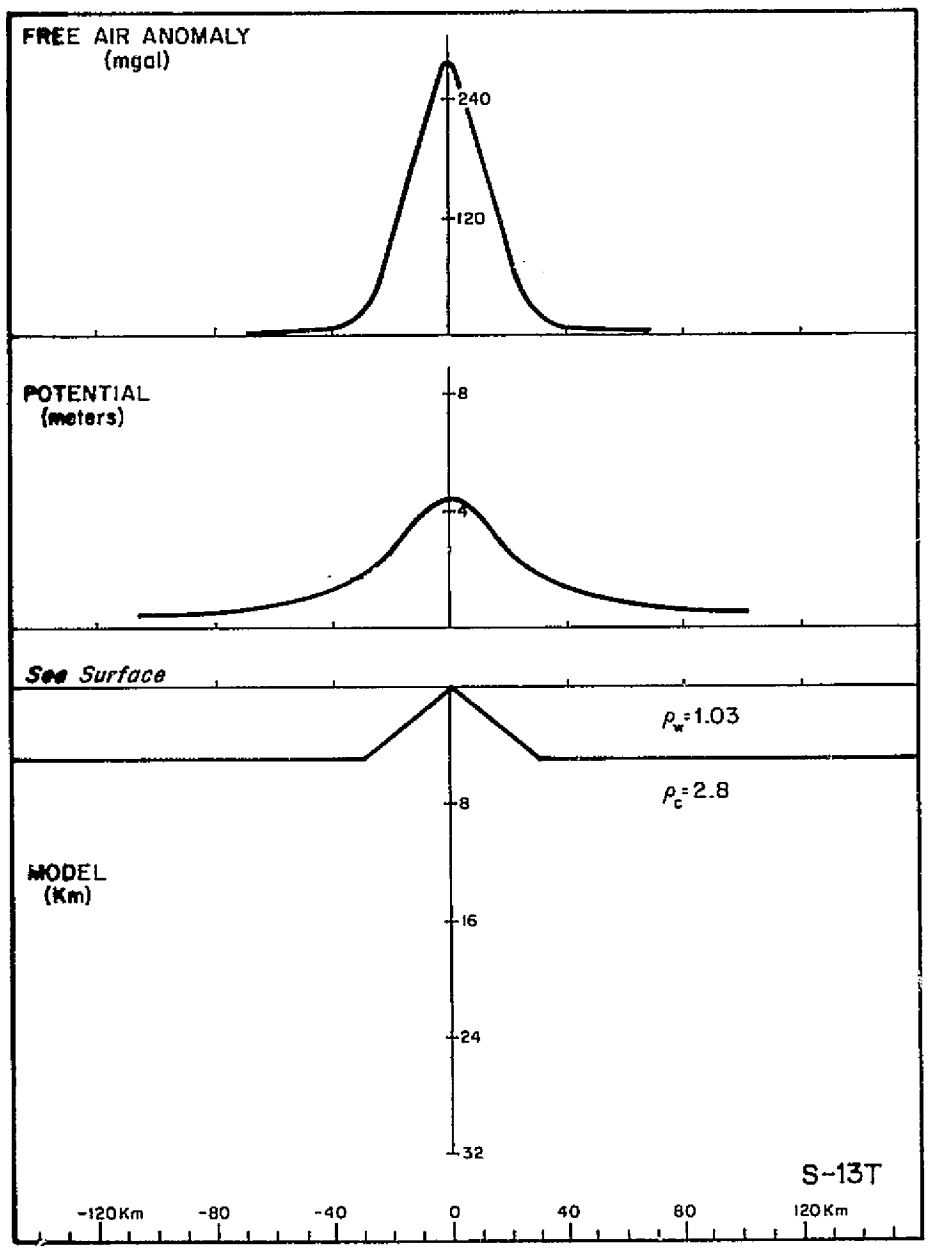
FREE AIR ANOMALY
(mgal)
240
120
POTENTIAL
(meters)
8
4
Sea Surface
ρ_w=1.03
ρ_c=2.8
8
MODEL
(Km)
16
24
32
S-13T
-120Km
-80
-40
0
40
80
120Km

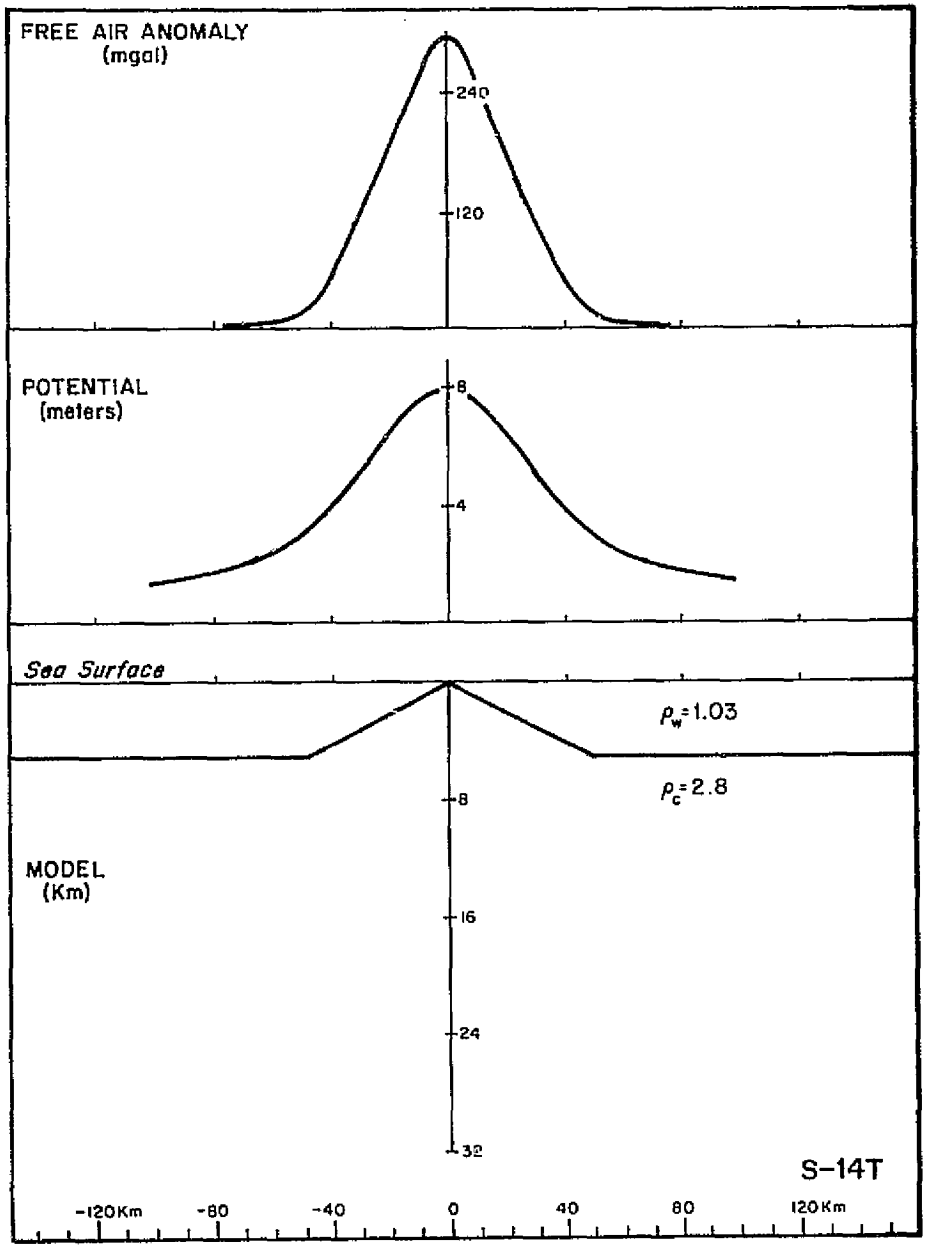
FREE AIR ANOMALY
(mgal)
240
120
POTENTIAL
(meters)
8
4
Sea Surface
ρ_w=1.03
ρ_c=2.8
MODEL
(Km)
8
16
24
32
S-14T
-120Km
-80
-40
0
40
80
120Km

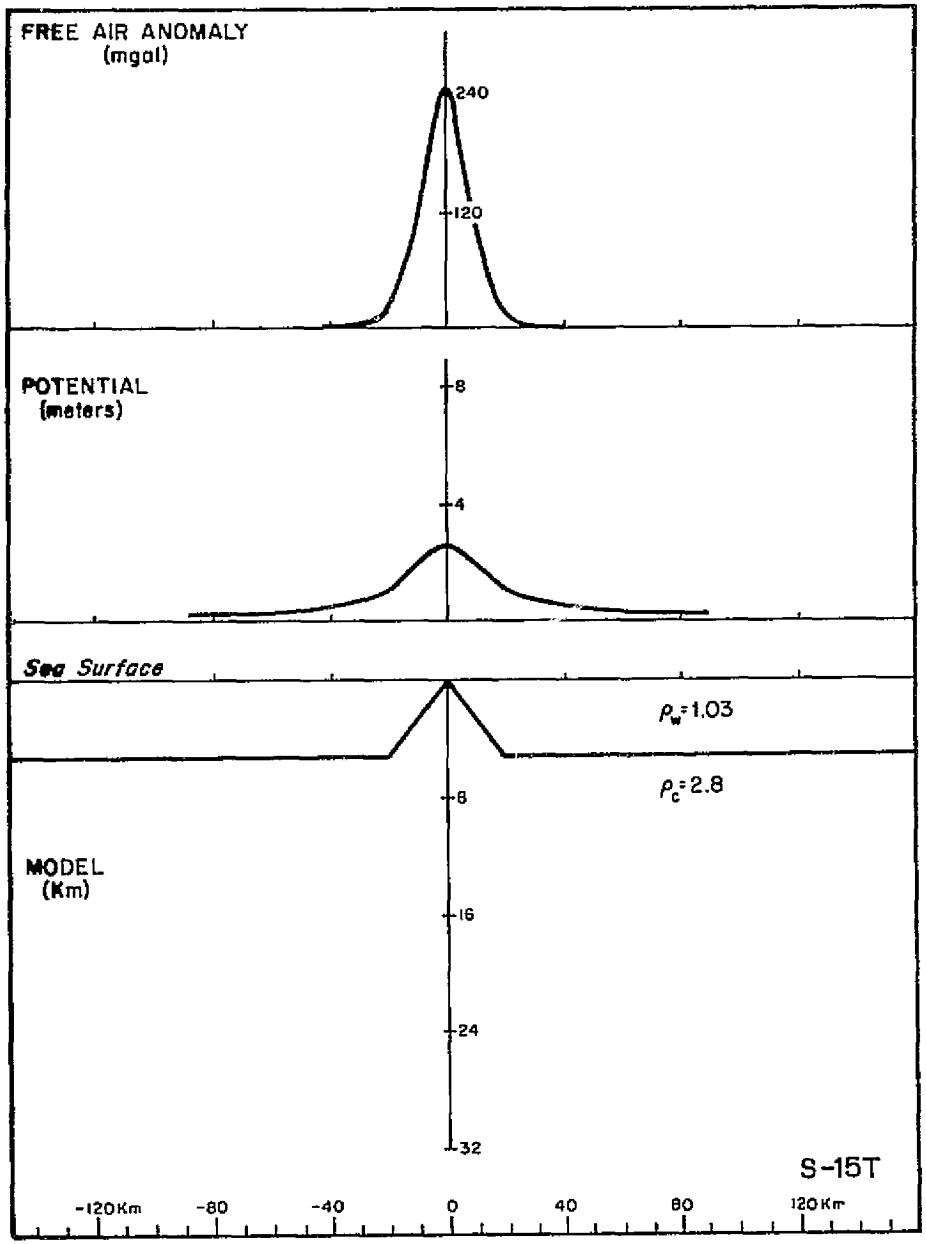
FREE AIR ANOMALY
(mgal)
240
120
POTENTIAL
(meters)
8
4
Sea Surface
ρ_w=1.03
ρ_c=2.8
MODEL
(Km)
8
16
24
32
S-15T
-120Km
-80
-40
0
40
80
120Km

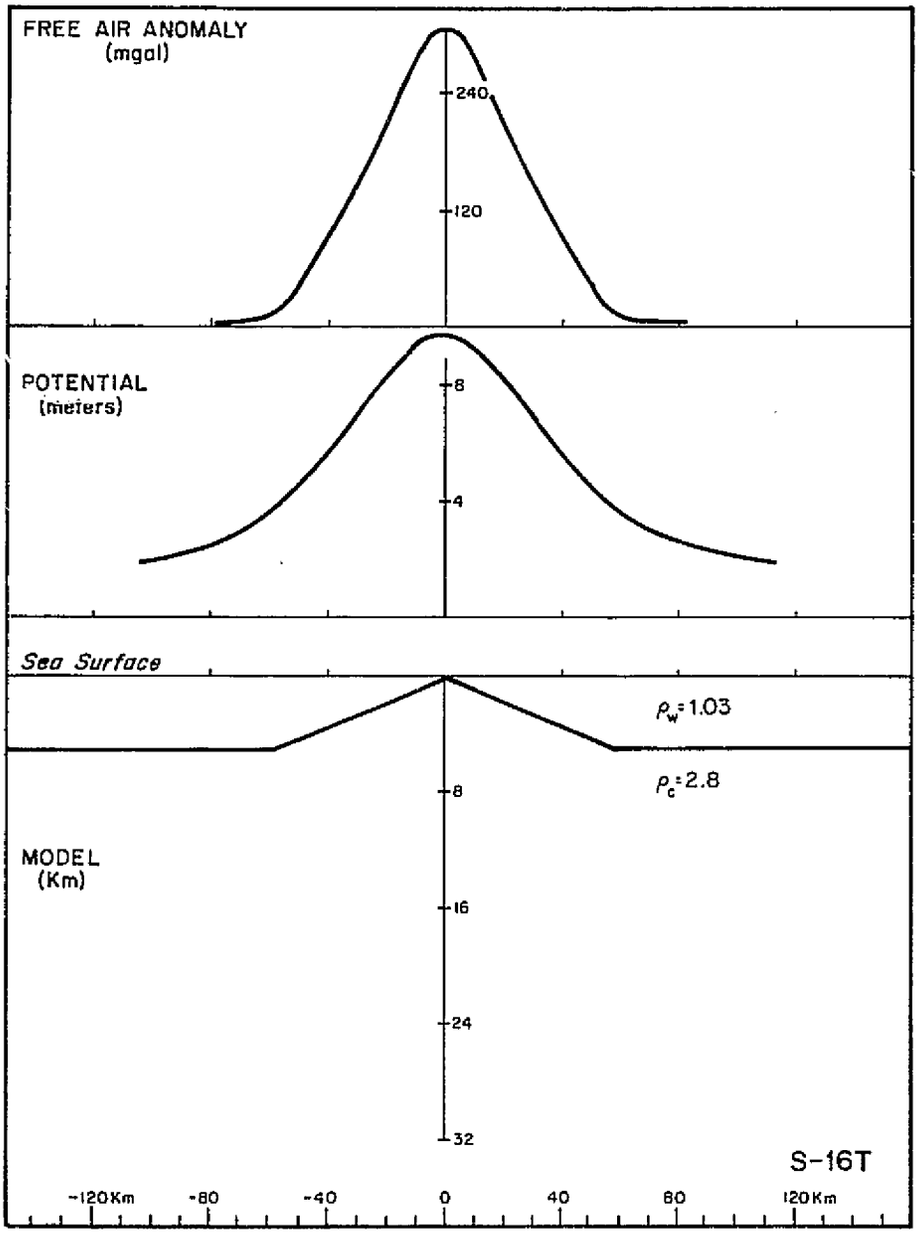
FREE AIR ANOMALY
(mgal)
240
120
POTENTIAL
(meters)
8
4
Sea Surface
ρ_w=1.03
ρ_c=2.8
8
MODEL
(Km)
16
24
32
S-16T
-120Km
-80
-40
0
40
80
120Km

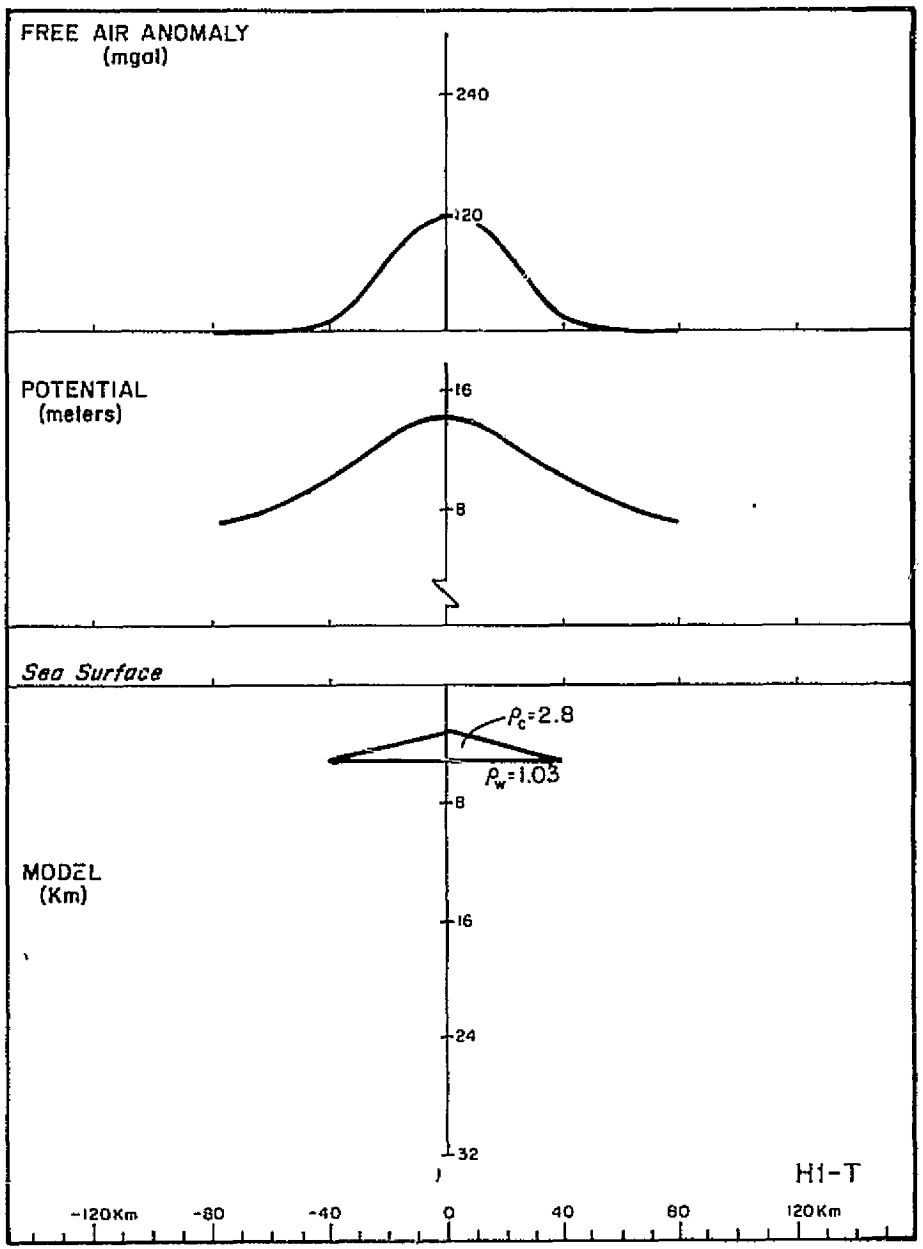
FREE AIR ANOMALY
(mgal)
240
120
POTENTIAL
(meters)
16
8
Sea Surface
ρ_c=2.8
ρ_w=1.03
8
MODEL
(Km)
16
24
32
H1-T
-120Km
-80
-40
0
40
80
120Km

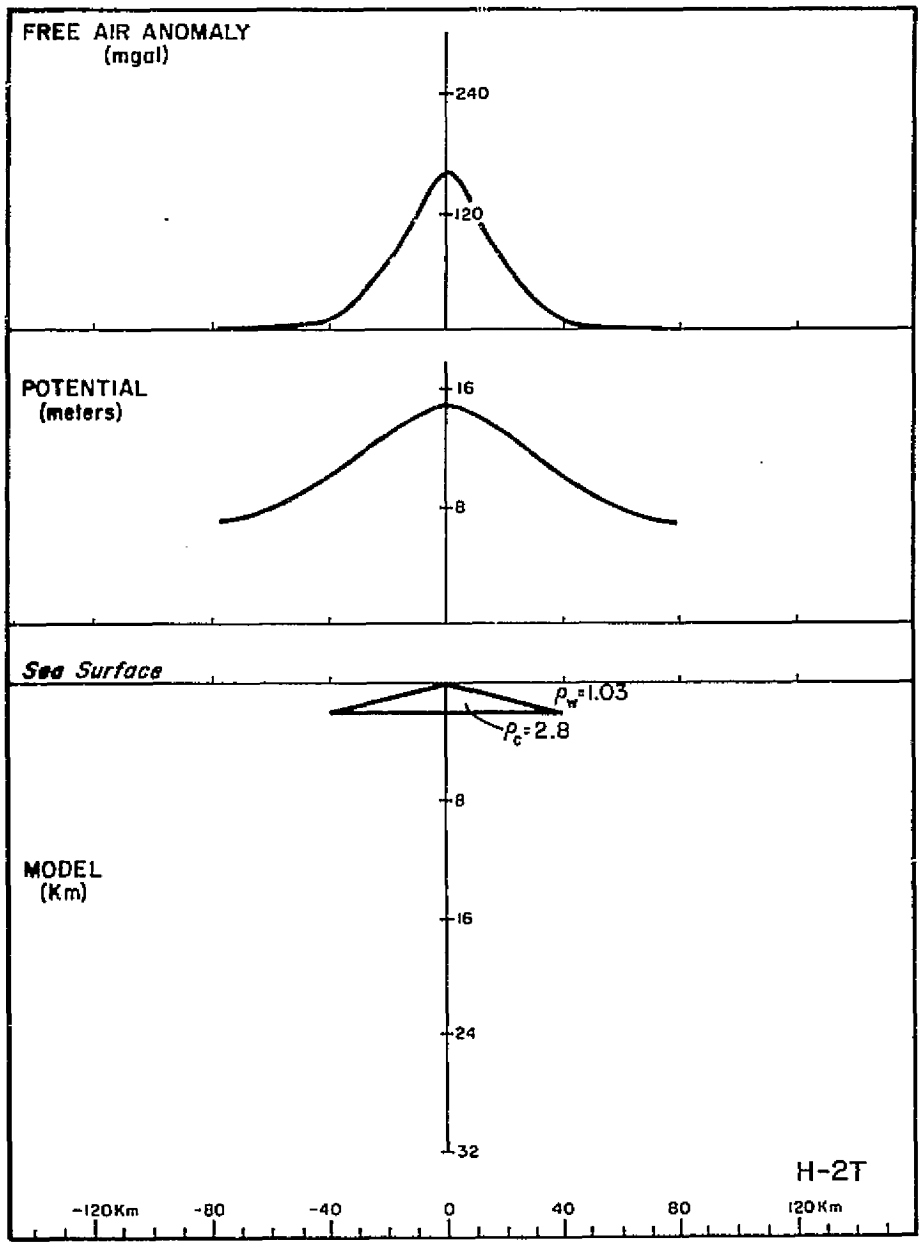
FREE AIR ANOMALY
(mgal)
240
120
POTENTIAL
(meters)
16
8
Sea Surface
ρ_w=1.03
ρ_c=2.8
8
MODEL
(Km)
16
24
32
H-2T
-120Km
-80
-40
0
40
80
120Km

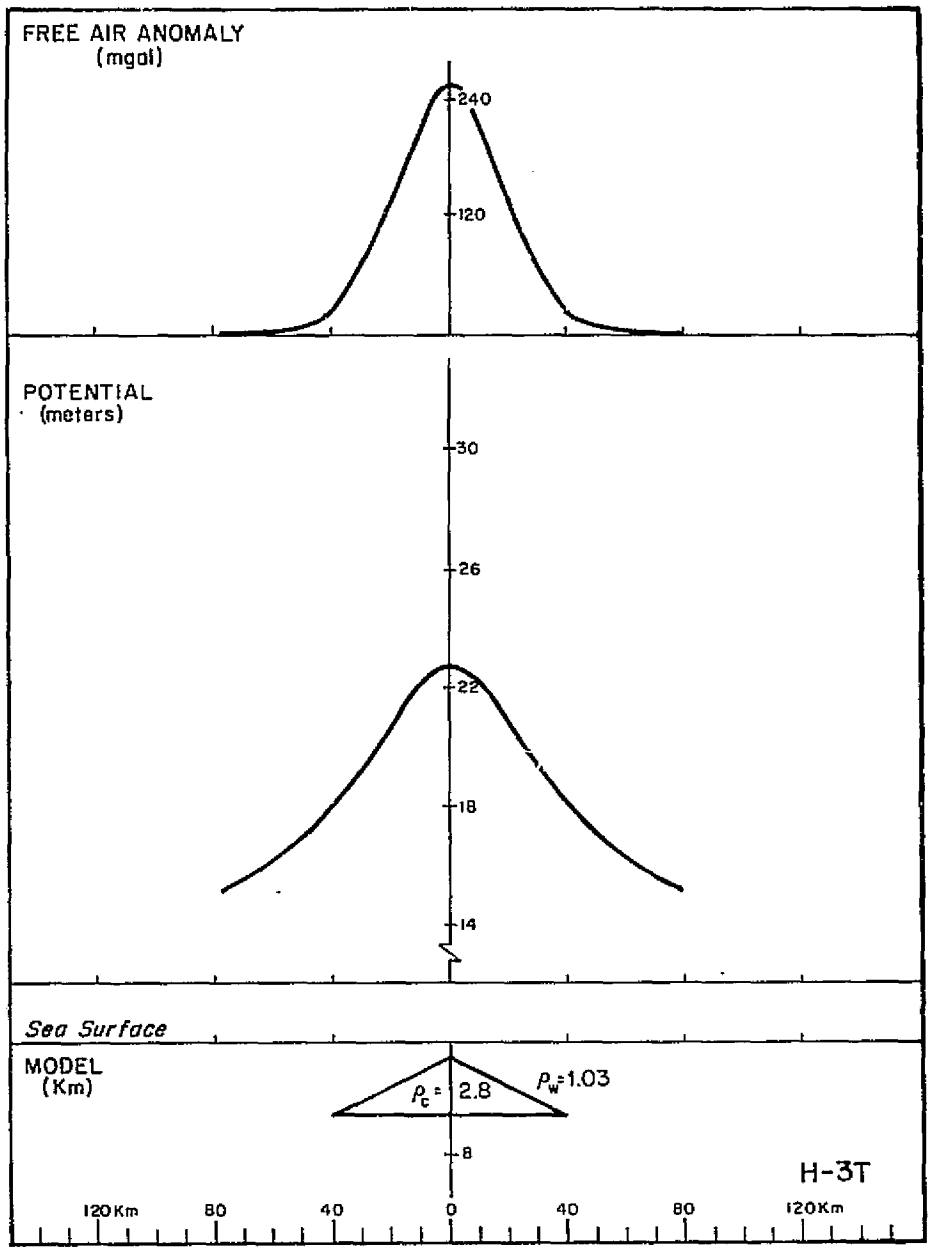
FREE AIR ANOMALY
(mgal)
240
120
POTENTIAL
(meters)
30
26
22
18
14
Sea Surface
MODEL
(Km)
ρ_c = 2.8
ρ_w=1.03
8
H-3T
120Km
80
40
0
40
80
120Km

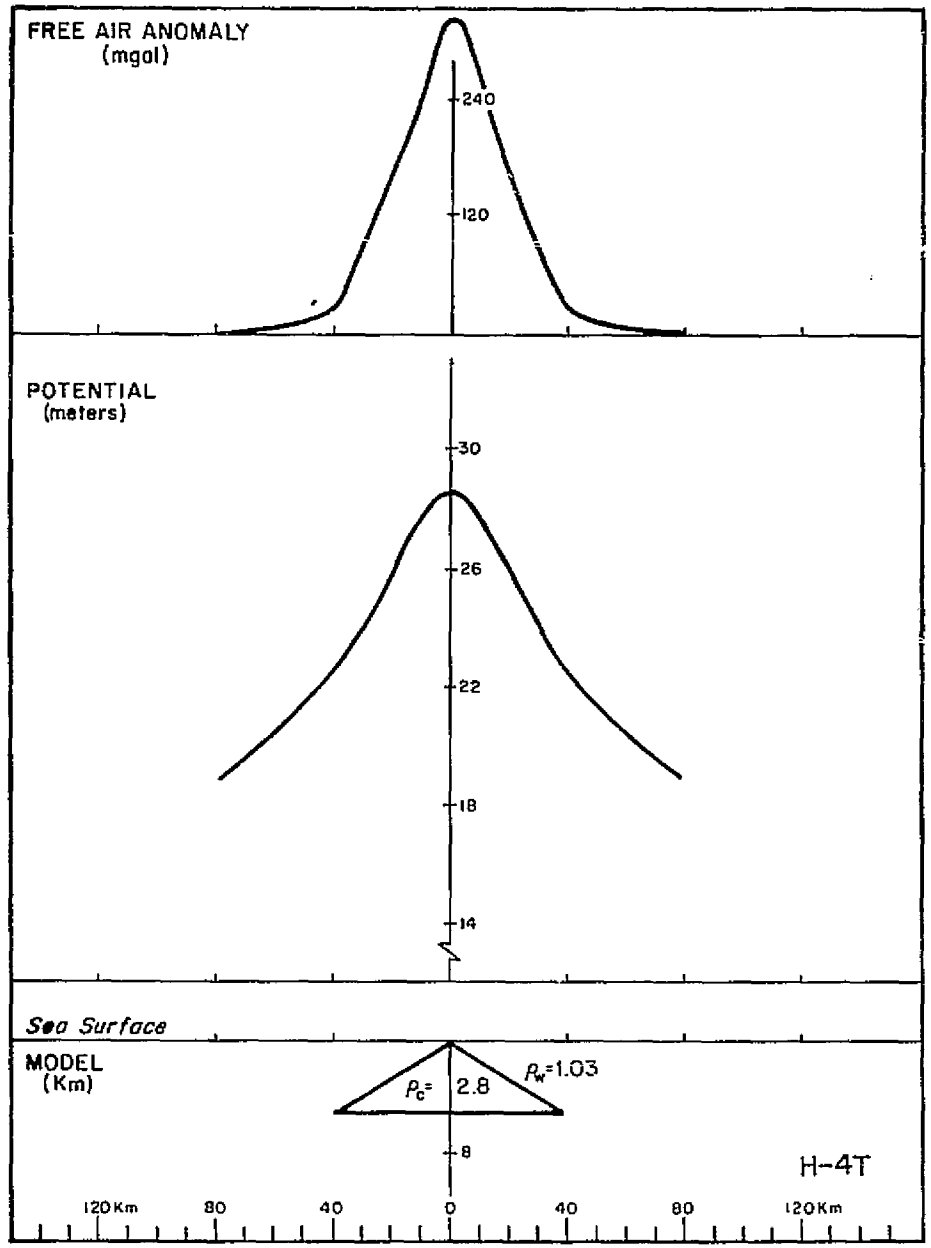
FREE AIR ANOMALY
(mgal)
240
120
POTENTIAL
(meters)
30
26
22
18
14
Sea Surface
MODEL
(Km)
ρ_c= 2.8
ρ_w=1.03
8
H-4T
120Km
80
40
0
40
80
120Km

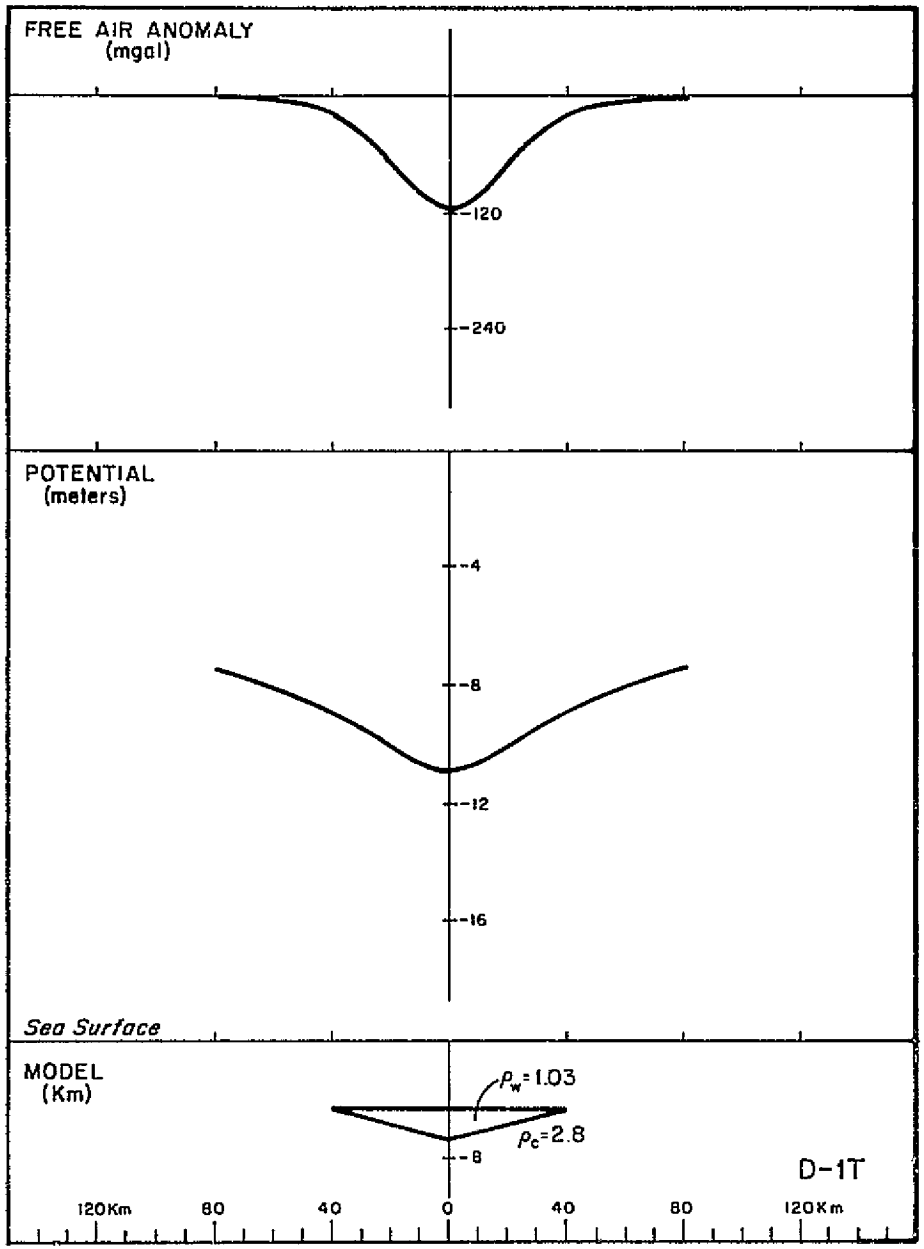
FREE AIR ANOMALY
(mgal)
-120
-240
POTENTIAL
(meters)
-4
-8
-12
-16
Sea Surface
MODEL
(Km)
ρ_w=1.03
ρ_c=2.8
-8
D-1T
120Km
80
40
0
40
80
120Km

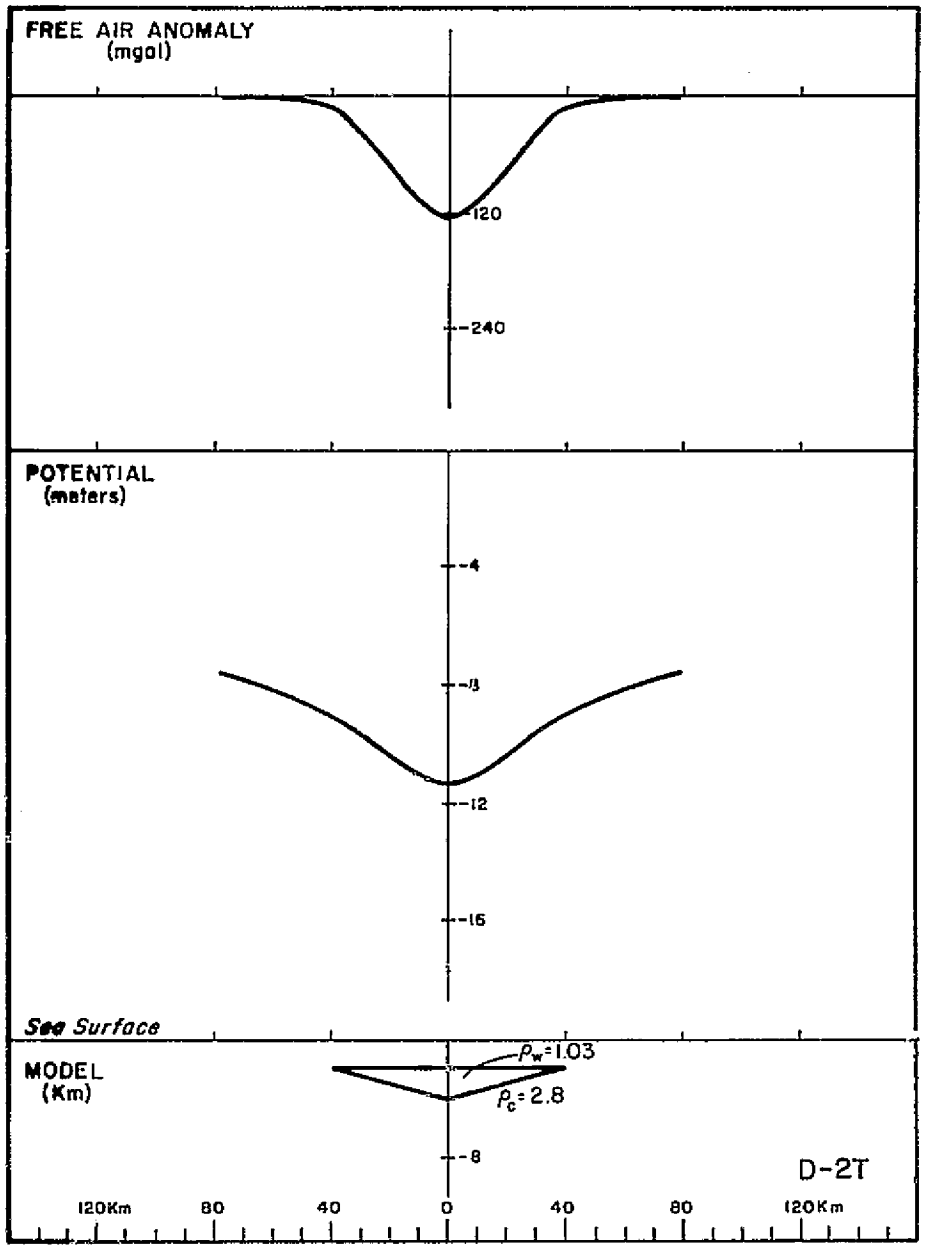
FREE AIR ANOMALY
(mgal)
-120
-240
POTENTIAL
(meters)
-4
-8
-12
-16
Sea Surface
MODEL
(Km)
ρ_w=1.03
ρ_c=2.8
-8
D-2T
120Km
80
40
0
40
80
120Km

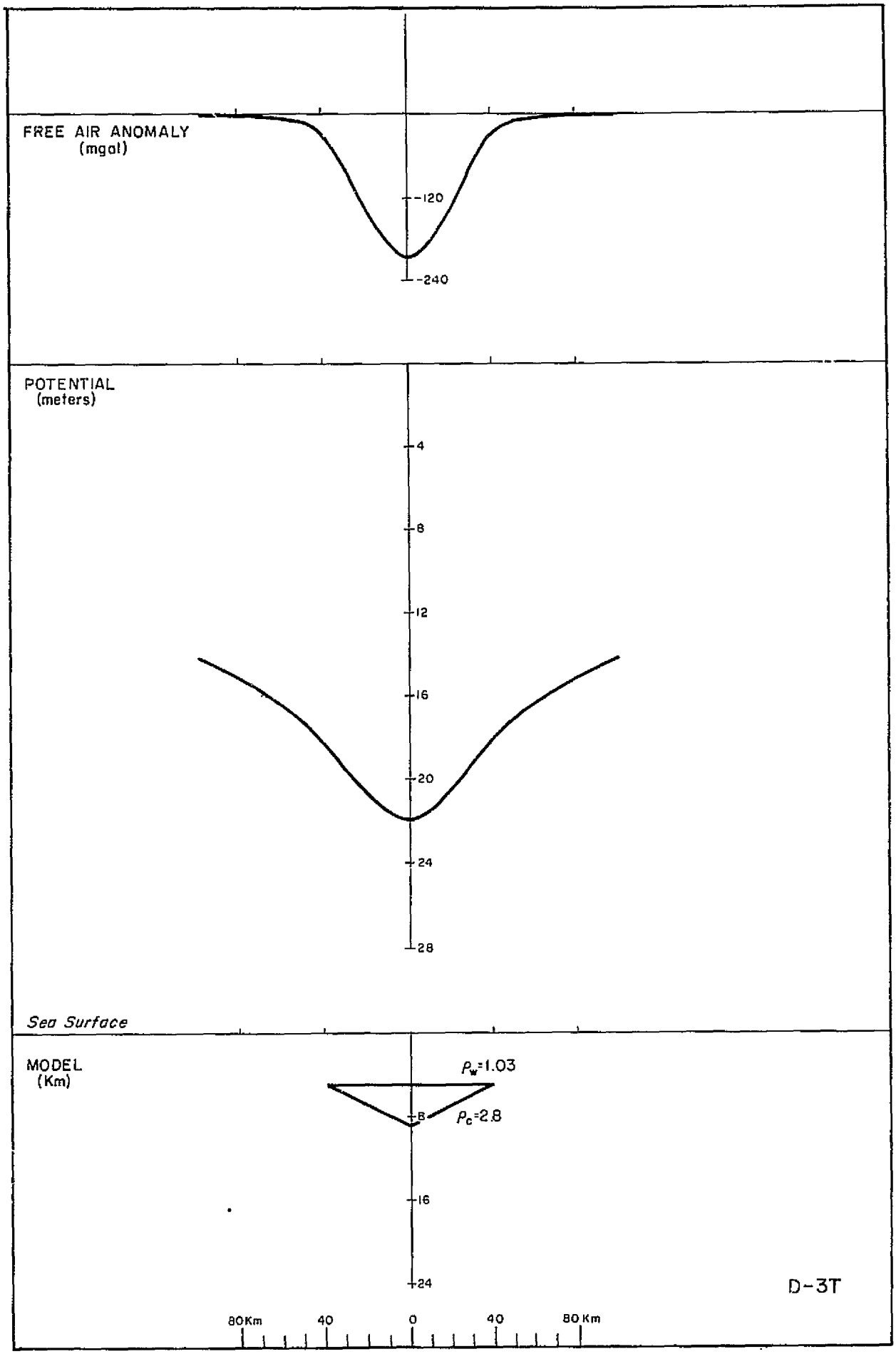
FREE AIR ANOMALY
(mgal)
-120
-240
POTENTIAL
(meters)
4
8
12
16
20
24
28
Sea Surface
MODEL
(Km)
ρ_w=1.03
8
ρ_c=2.8
16
24
D-3T
80Km
40
0
40
80 Km

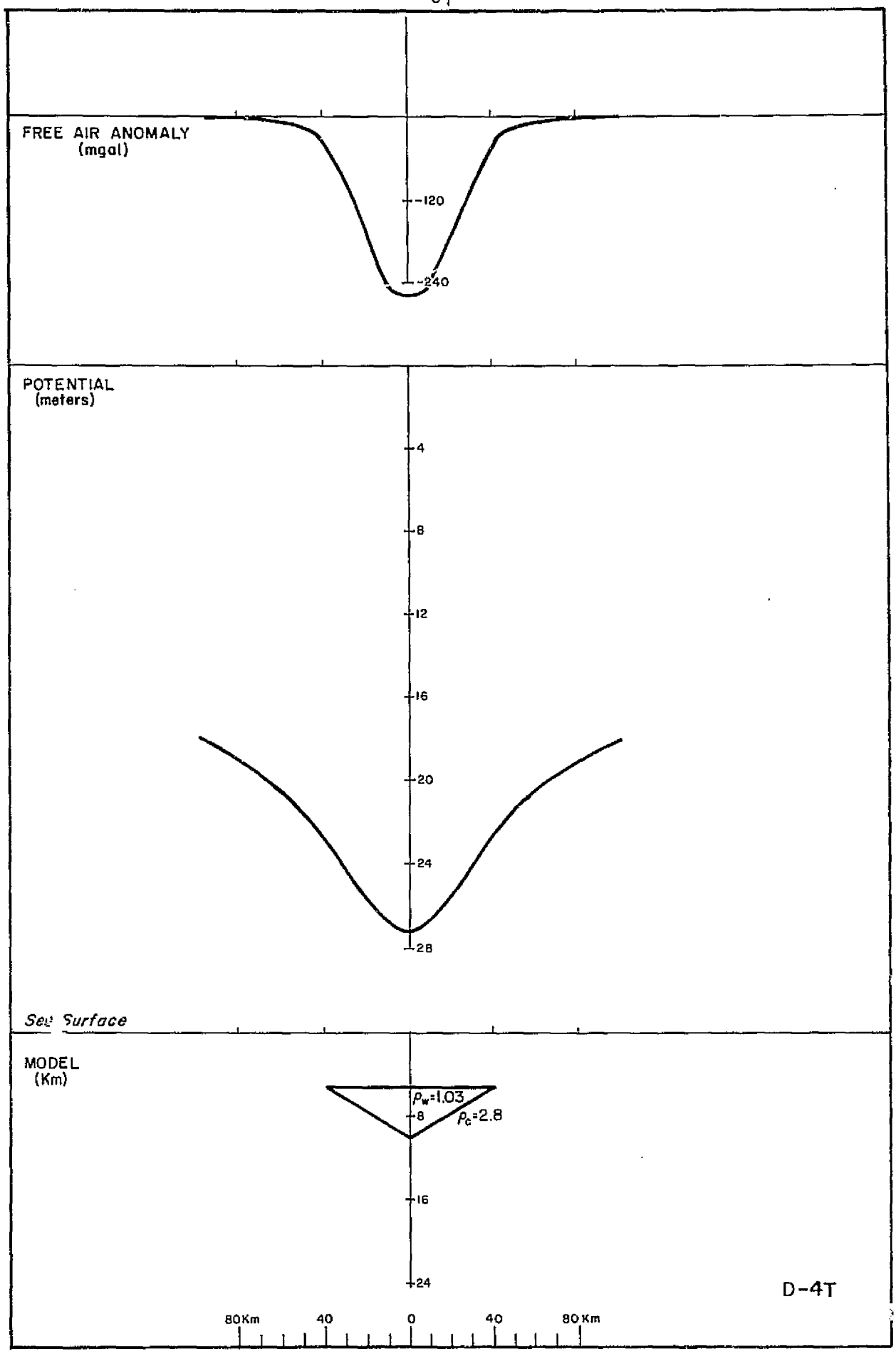
FREE AIR ANOMALY
(mgal)
-120
-240
POTENTIAL
(meters)
4
8
12
16
20
24
28
Sea Surface
MODEL
(Km)
ρ_w=1.03
8
ρ_c=2.8
16
24
D-4T
80Km
40
0
40
80Km

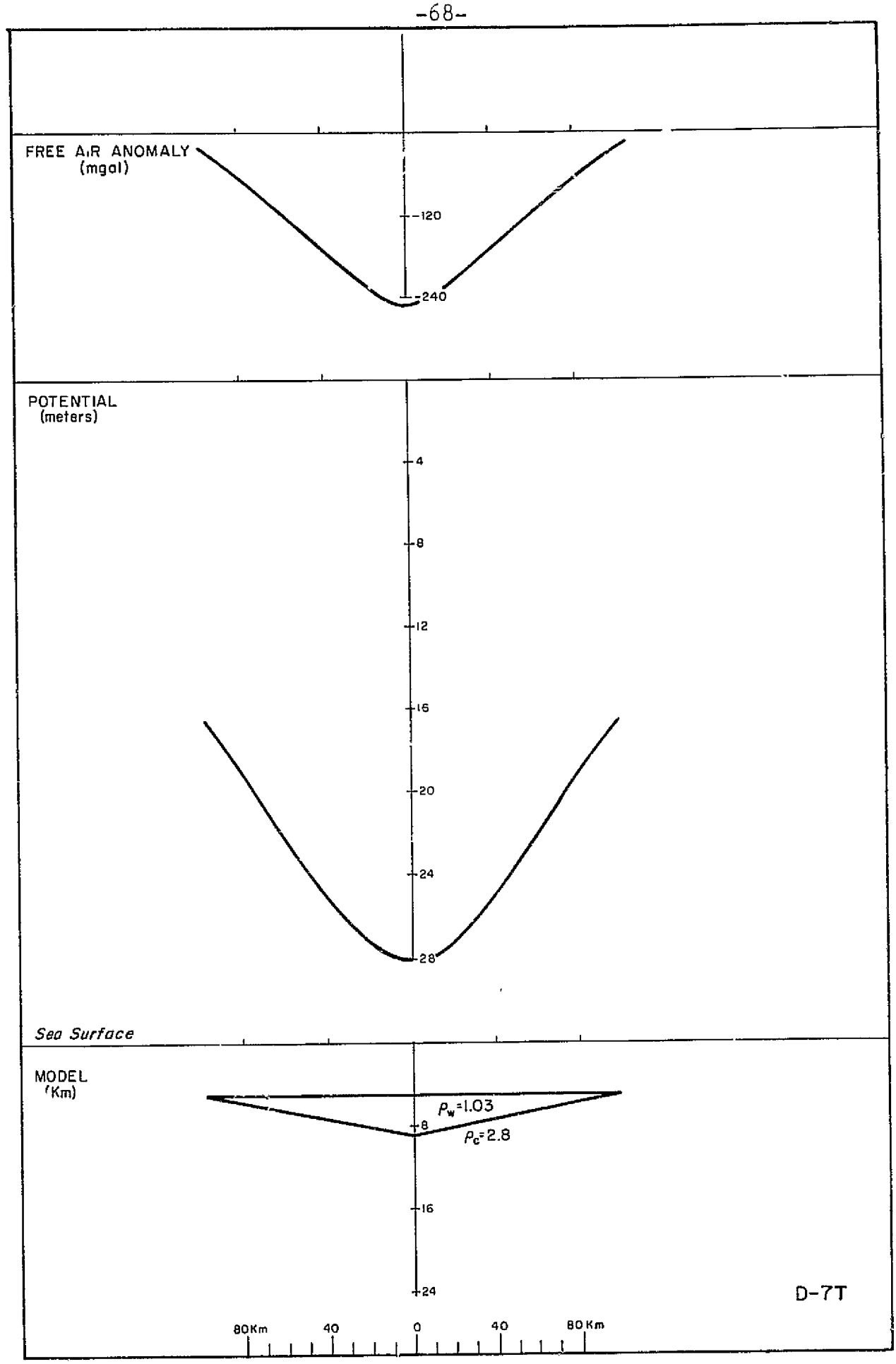
FREE AIR ANOMALY
(mgal)
-120
-240
POTENTIAL
(meters)
4
8
12
16
20
24
28
Sea Surface
MODEL
(Km)
ρ_w=1.03
8
ρ_c=2.8
16
24
D-7T
80Km
40
0
40
80Km

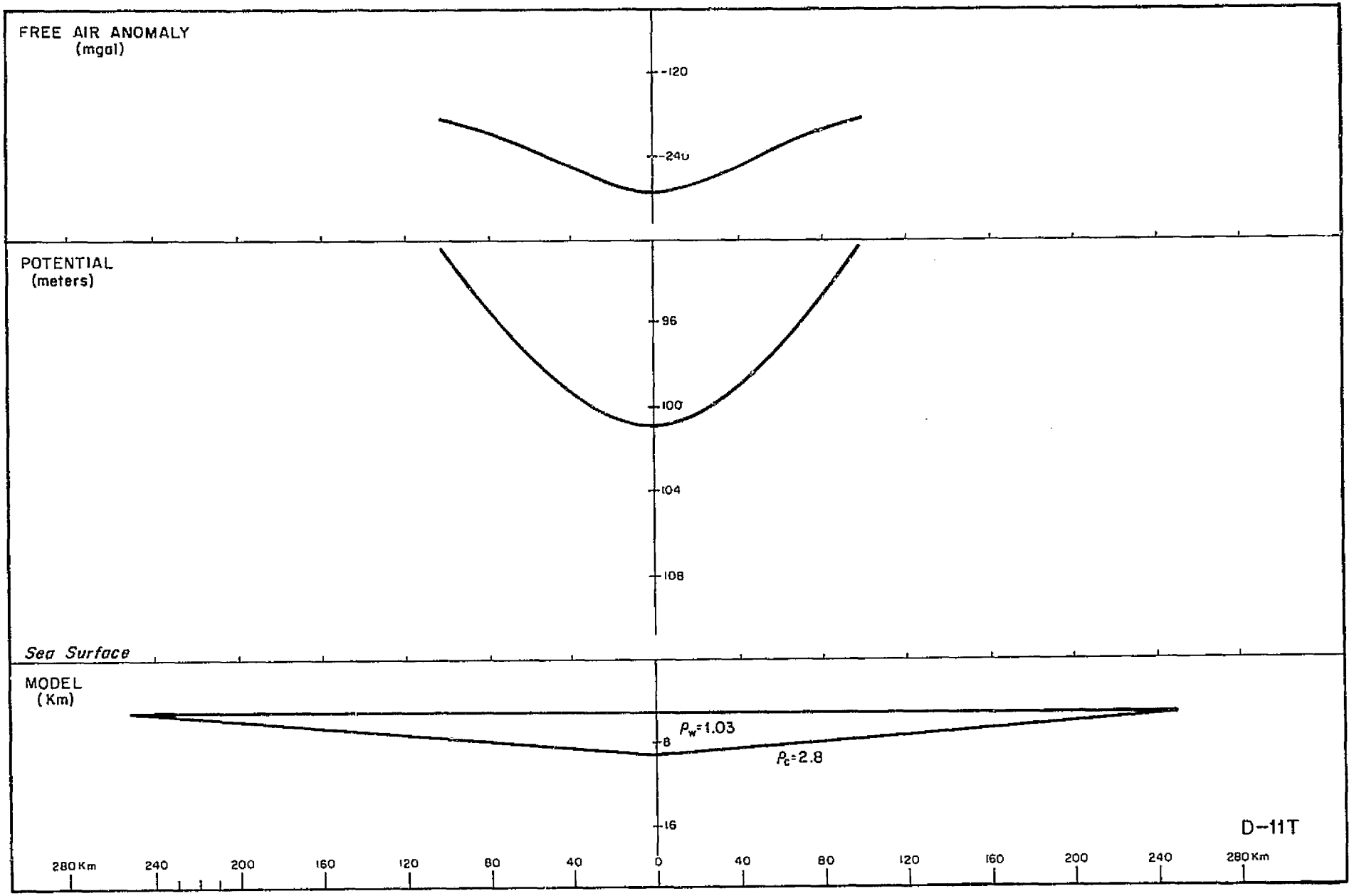
FREE AIR ANOMALY
(mgal)
-120
-240
POTENTIAL
(meters)
96
100
104
108
Sea Surface
MODEL
(Km)
P_w=1.03
P_c=2.8
8
16
D-11T
280 Km
240
200
160
120
80
40
0
40
80
120
160
200
240
280 Km

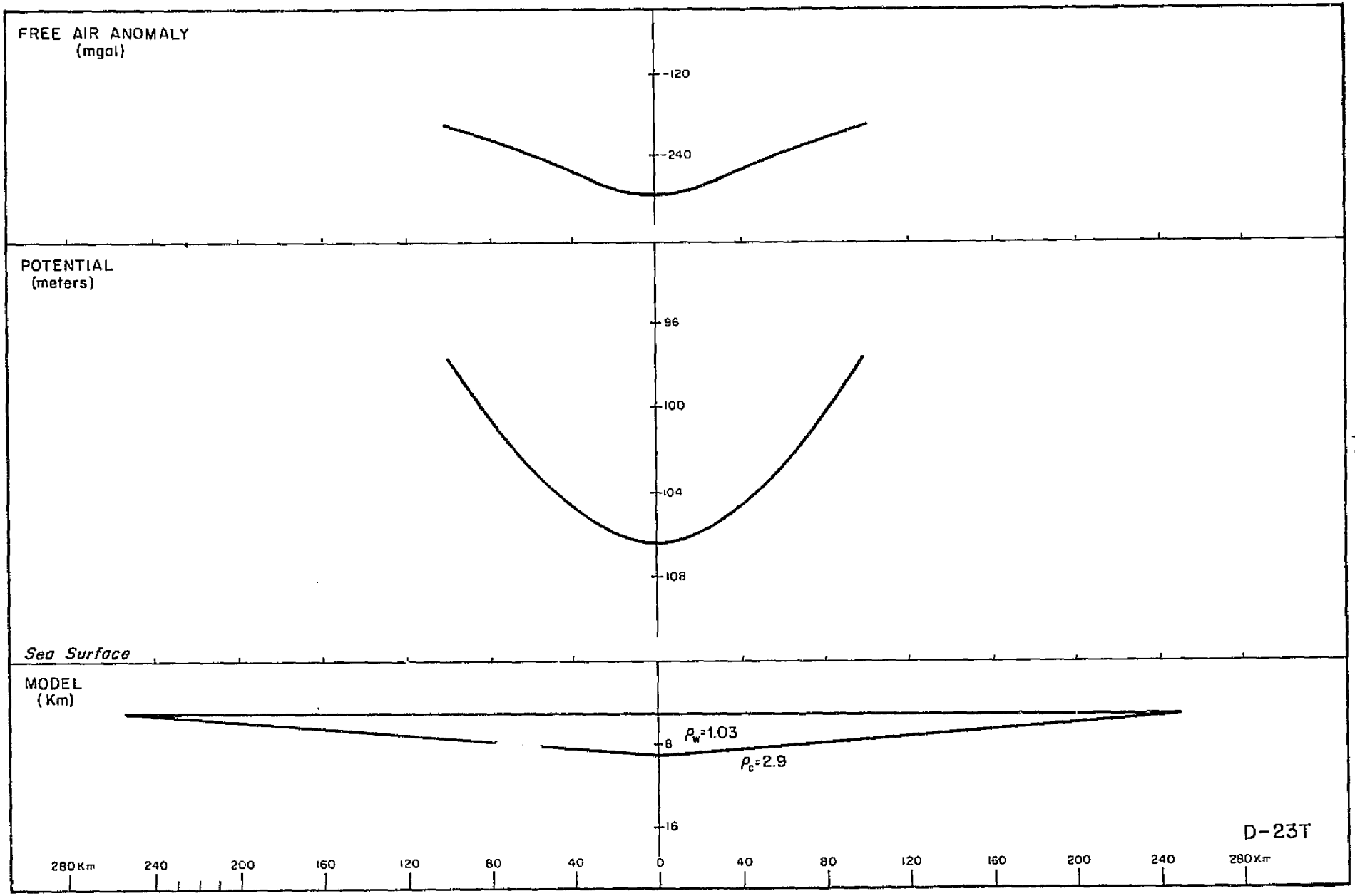
FREE AIR ANOMALY
(mgal)
-120
-240
POTENTIAL
(meters)
96
100
104
108
Sea Surface
MODEL
(Km)
8
ρ_w=1.03
ρ_c=2.9
16
D-23T
280Km
240
200
160
120
80
40
0
40
80
120
160
200
240
280Km

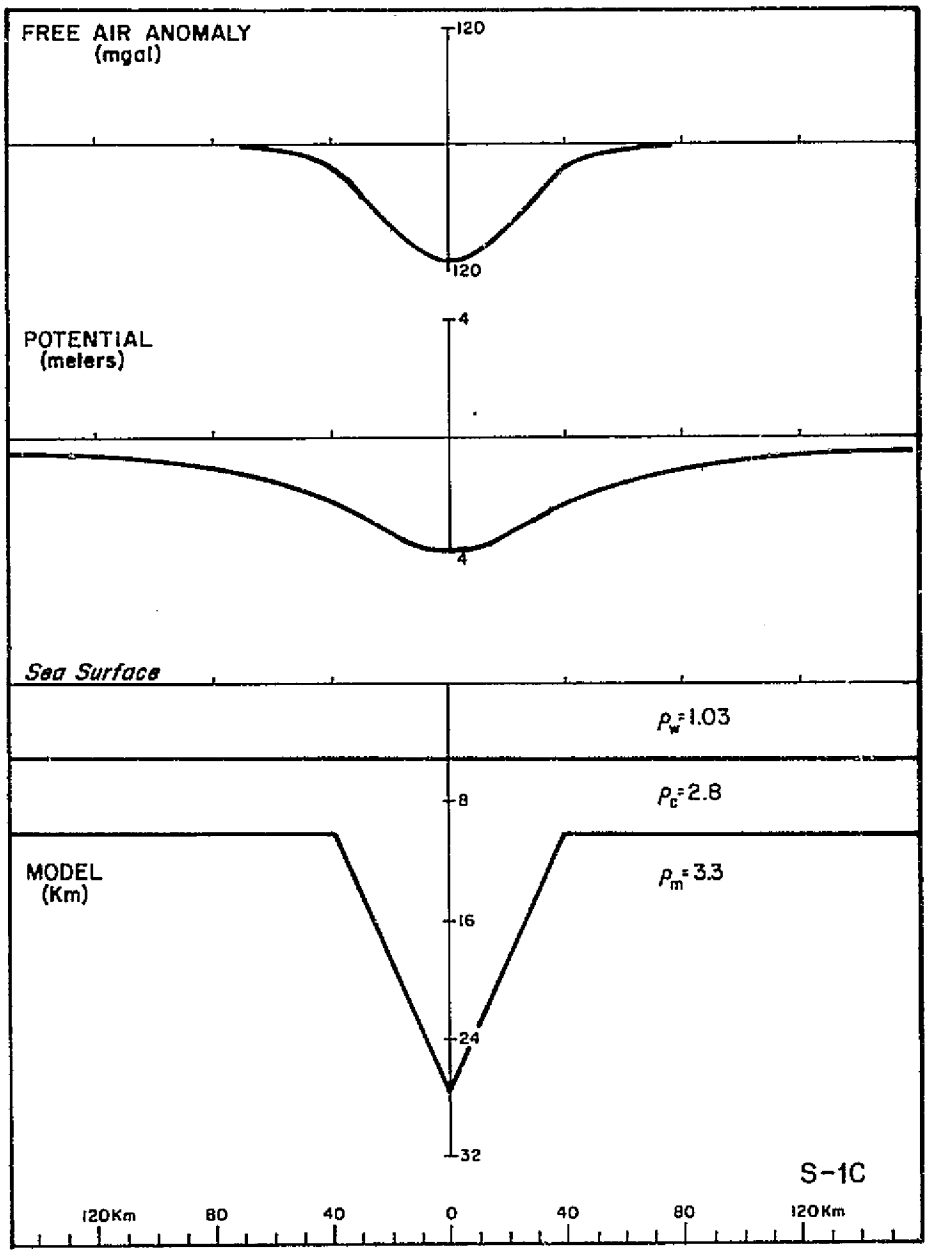
FREE AIR ANOMALY
(mgal)
120
120
POTENTIAL
(meters)
4
4
Sea Surface
ρ_w=1.03
ρ_c=2.8
ρ_m=3.3
MODEL
(Km)
8
16
24
32
S-1C
120Km
80
40
0
40
80
120Km

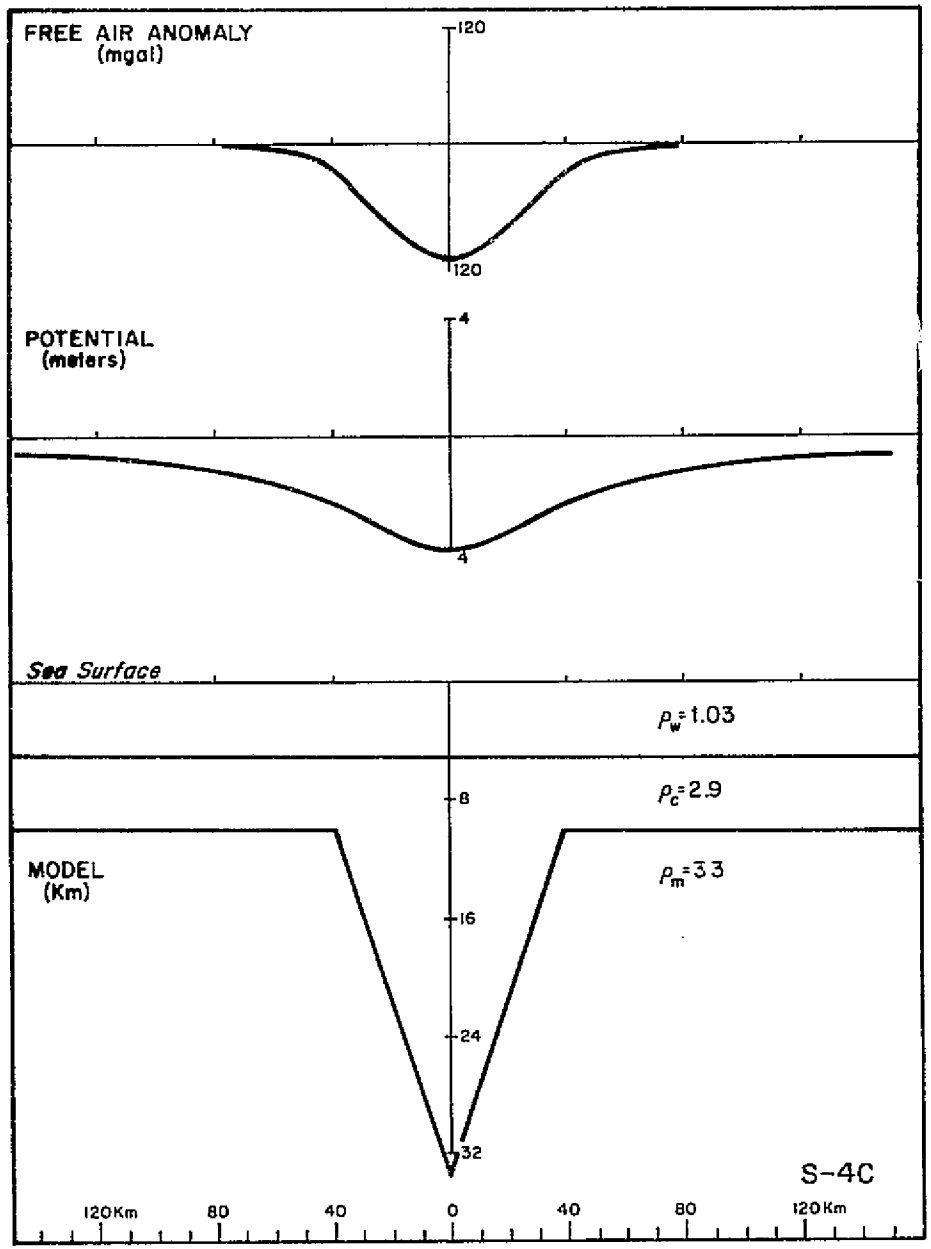
FREE AIR ANOMALY
(mgal)
120
120
POTENTIAL
(meters)
4
4
Sea Surface
ρ_w=1.03
ρ_c=2.9
ρ_m=3.3
MODEL
(Km)
8
16
24
32
S-4C
120Km
80
40
0
40
80
120Km

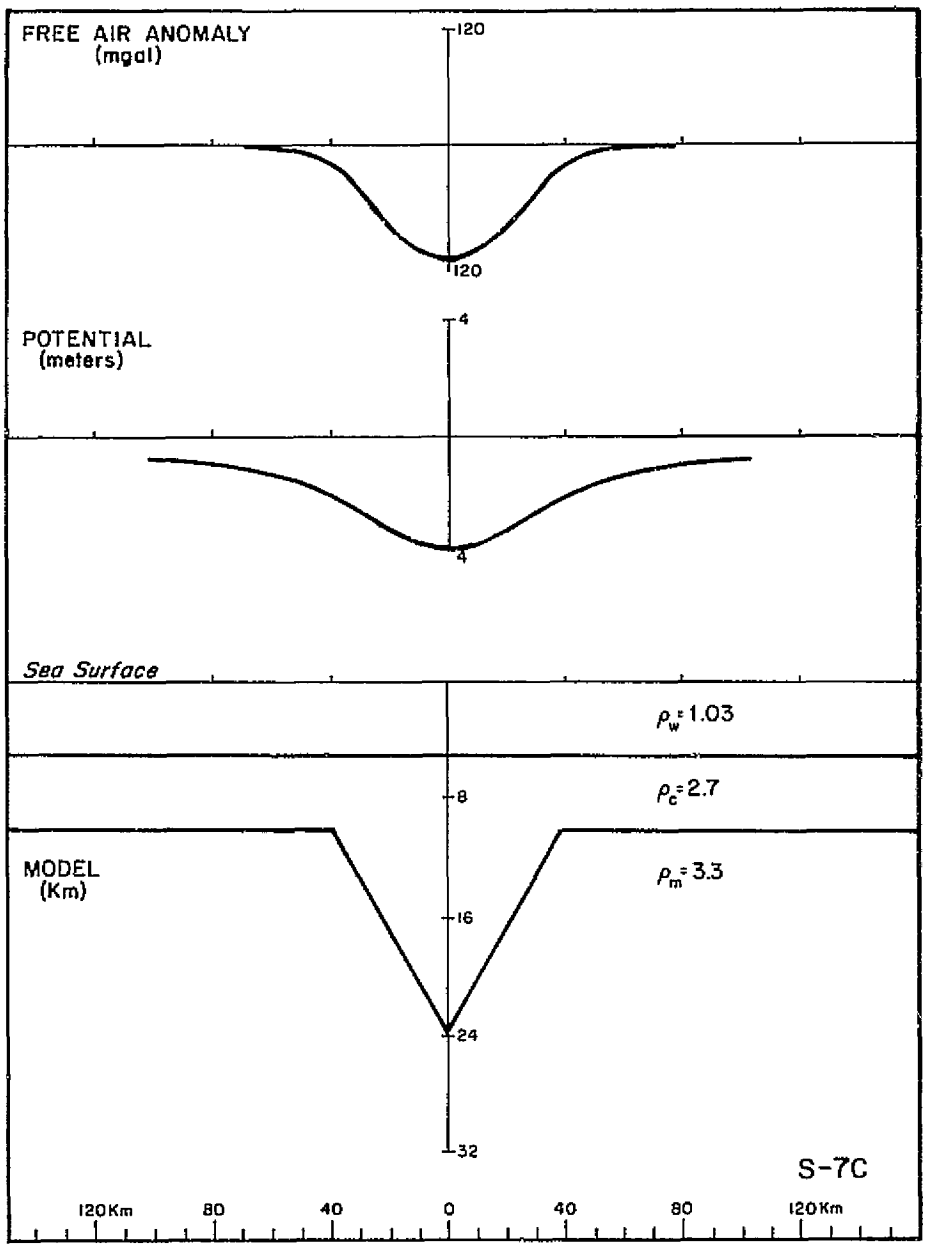
FREE AIR ANOMALY
(mgal)
120
120
POTENTIAL
(meters)
4
4
Sea Surface
ρ_w=1.03
ρ_c=2.7
ρ_m=3.3
MODEL
(Km)
8
16
24
32
S-7C
120Km
80
40
0
40
80
120Km

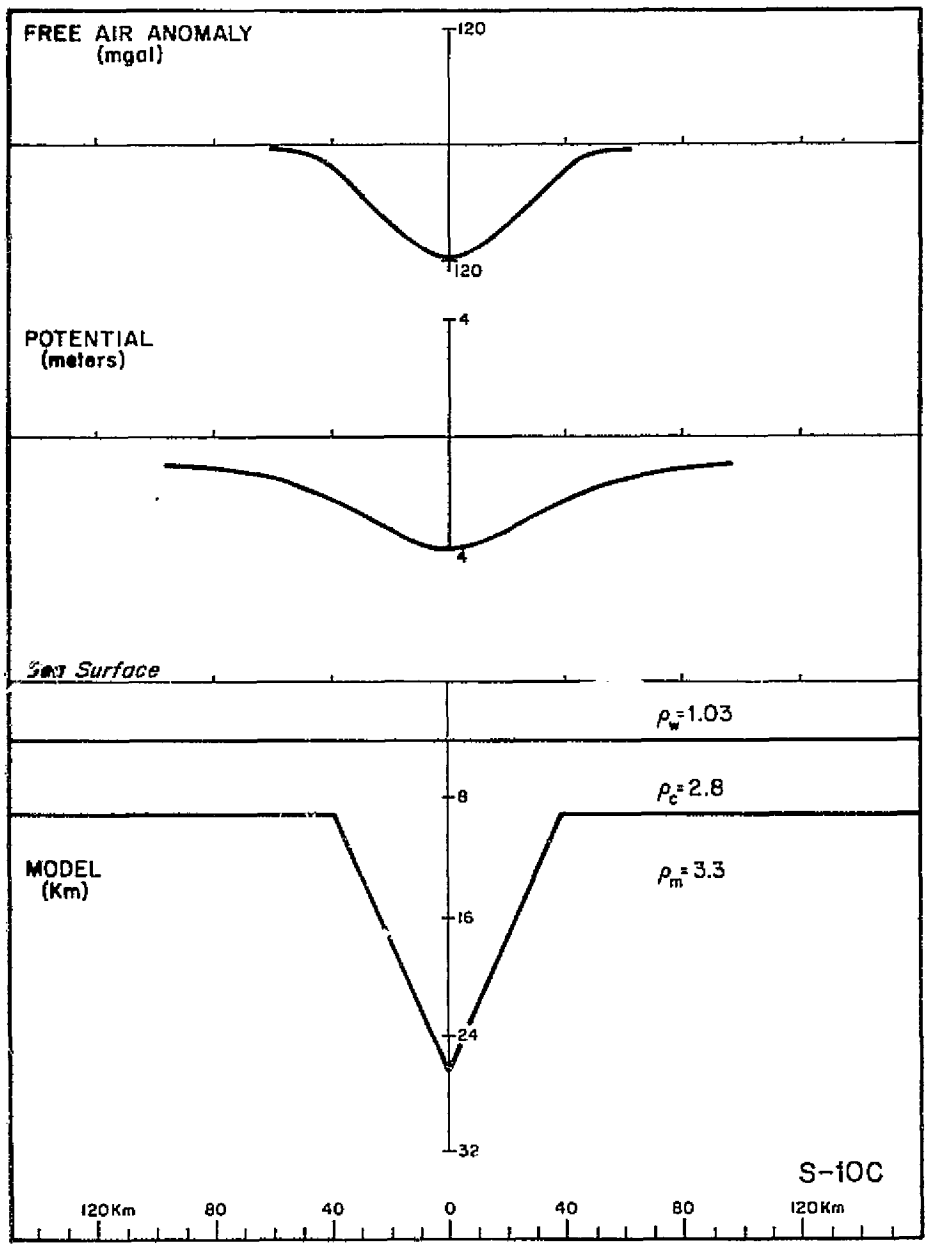
FREE AIR ANOMALY
(mgal)
120
120
POTENTIAL
(meters)
4
4
Sea Surface
ρ_w=1.03
ρ_c=2.8
ρ_m=3.3
MODEL
(Km)
8
16
24
32
S-10C
120Km
80
40
0
40
80
120Km

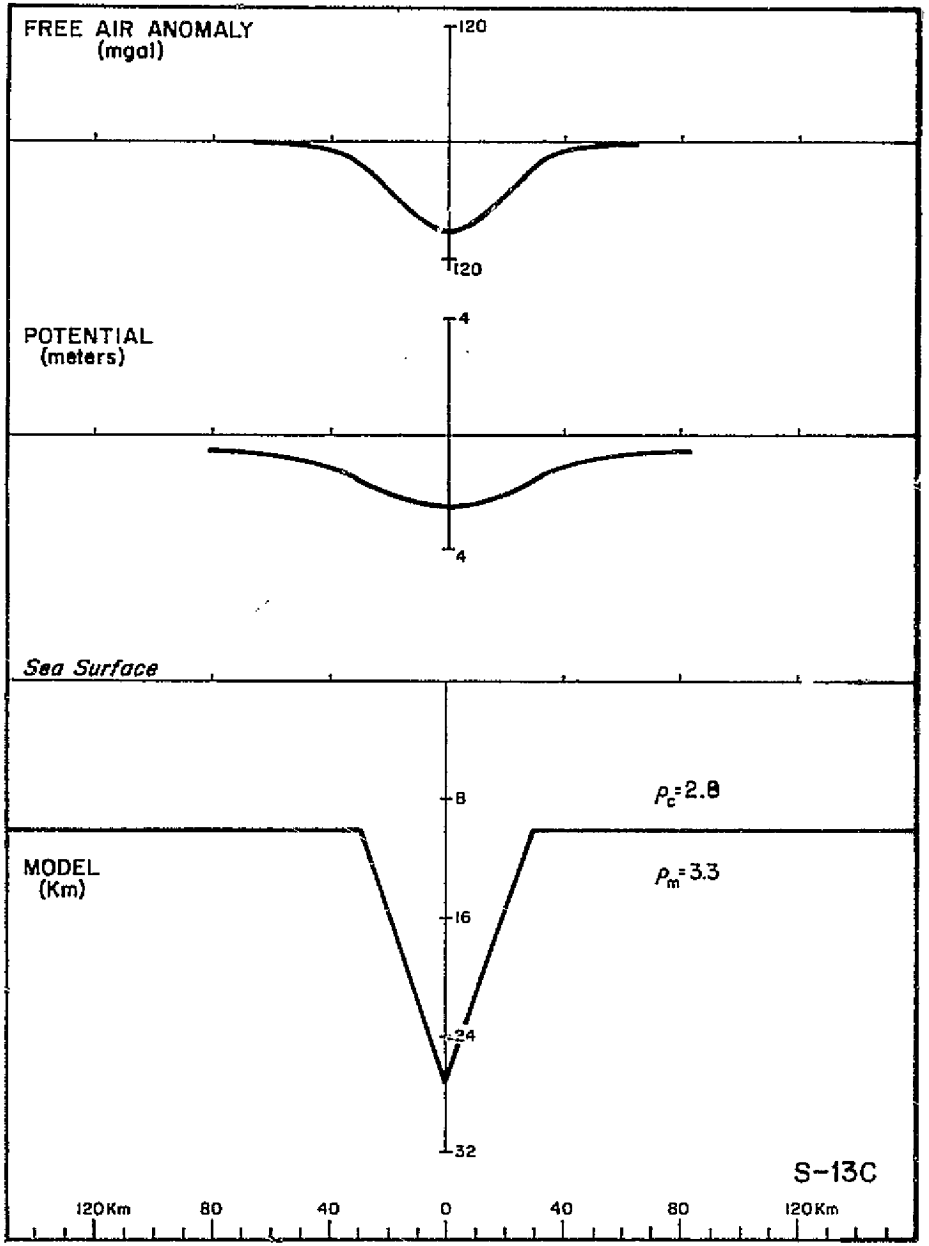
FREE AIR ANOMALY
(mgal)
120
120
POTENTIAL
(meters)
4
4
Sea Surface
8
16
24
32
ρ_c=2.8
ρ_m=3.3
MODEL
(Km)
S-13C
120Km
80
40
0
40
80
120Km

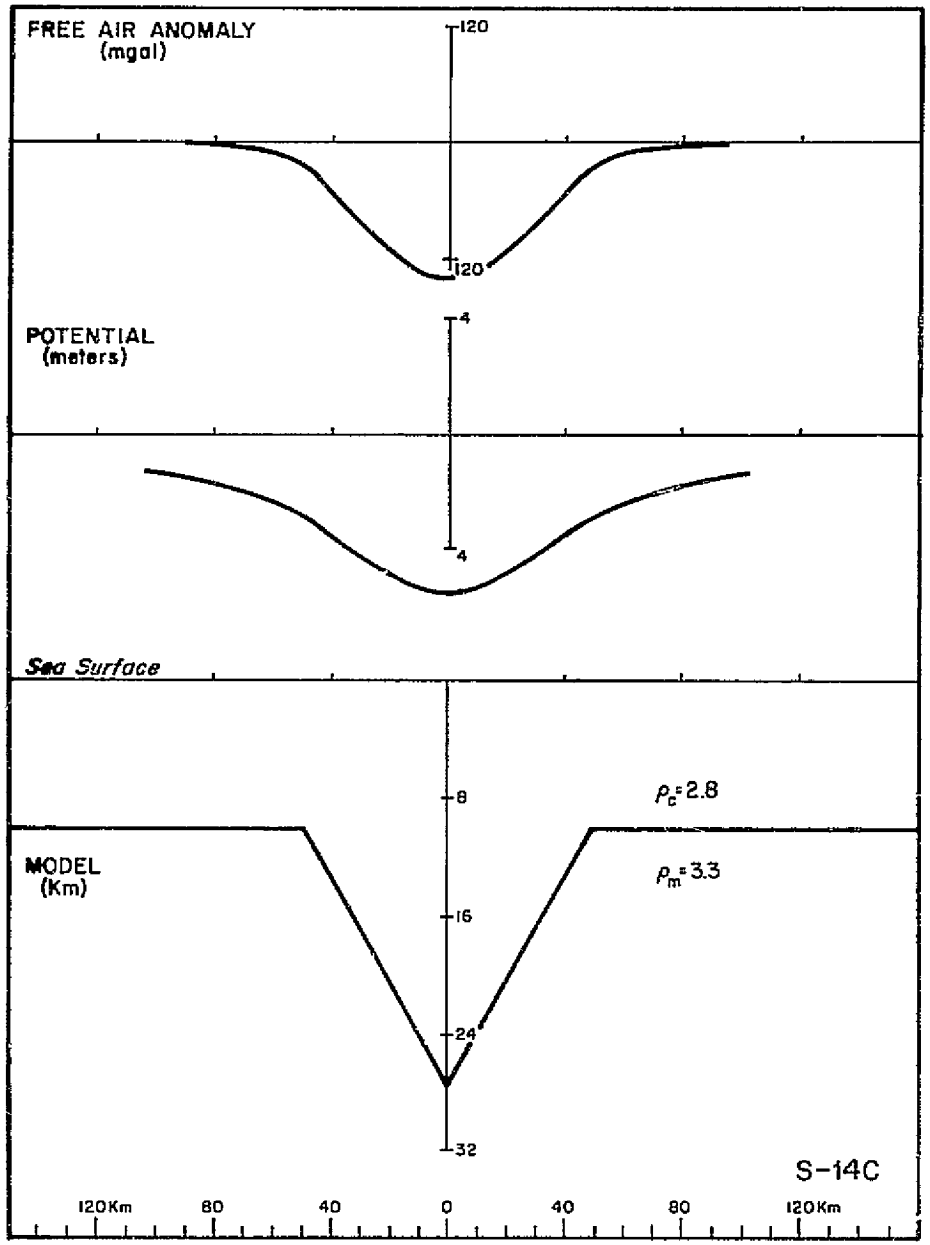
FREE AIR ANOMALY
(mgal)
120
120
POTENTIAL
(meters)
4
4
Sea Surface
8
16
24
32
ρ_c=2.8
ρ_m=3.3
MODEL
(Km)
S-14C
120Km
80
40
0
40
80
120Km

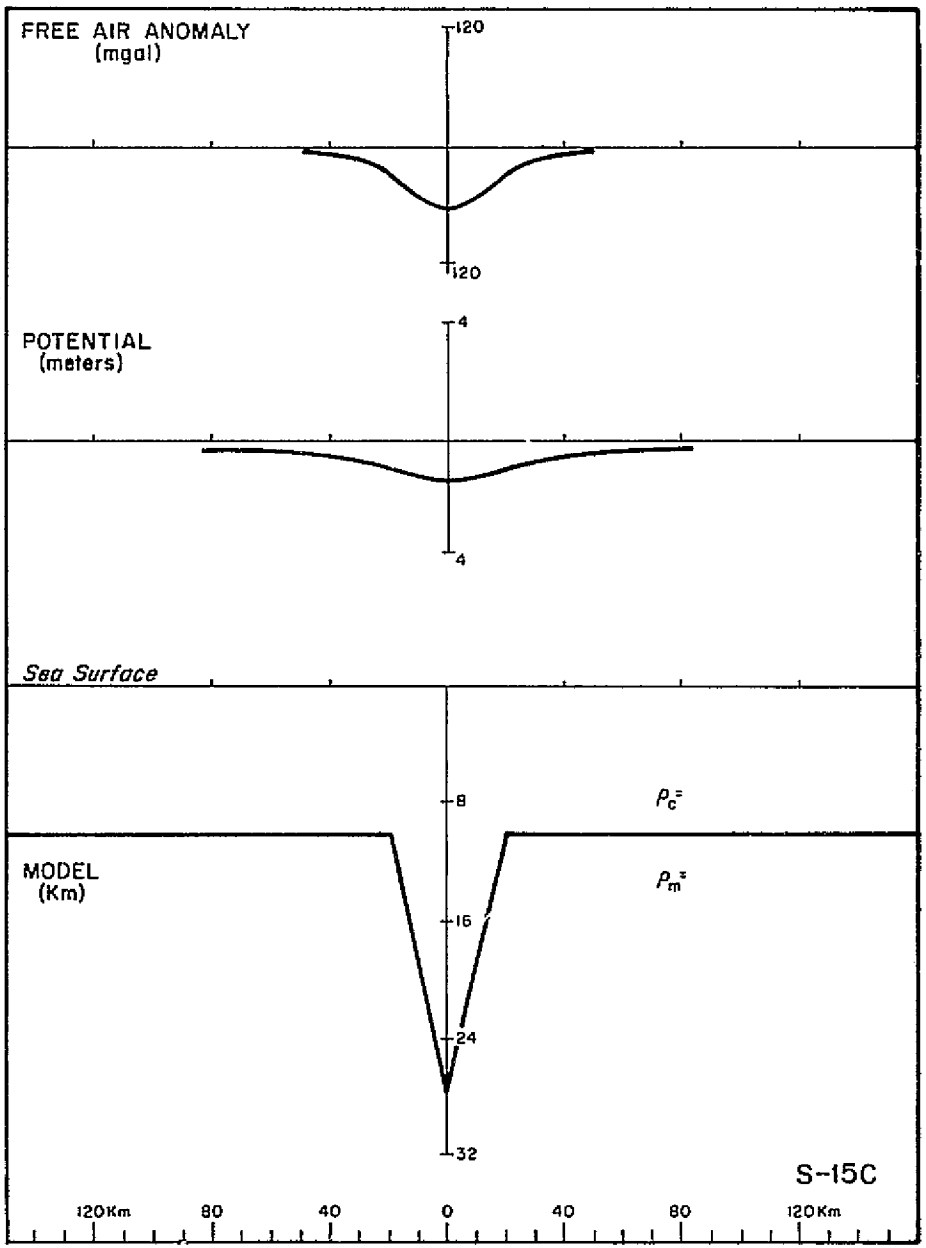
FREE AIR ANOMALY
(mgal)
120
120
POTENTIAL
(meters)
4
4
Sea Surface
8
ρ_c=
MODEL
(Km)
ρ_m=
16
24
32
S-15C
120Km
80
40
0
40
80
120Km

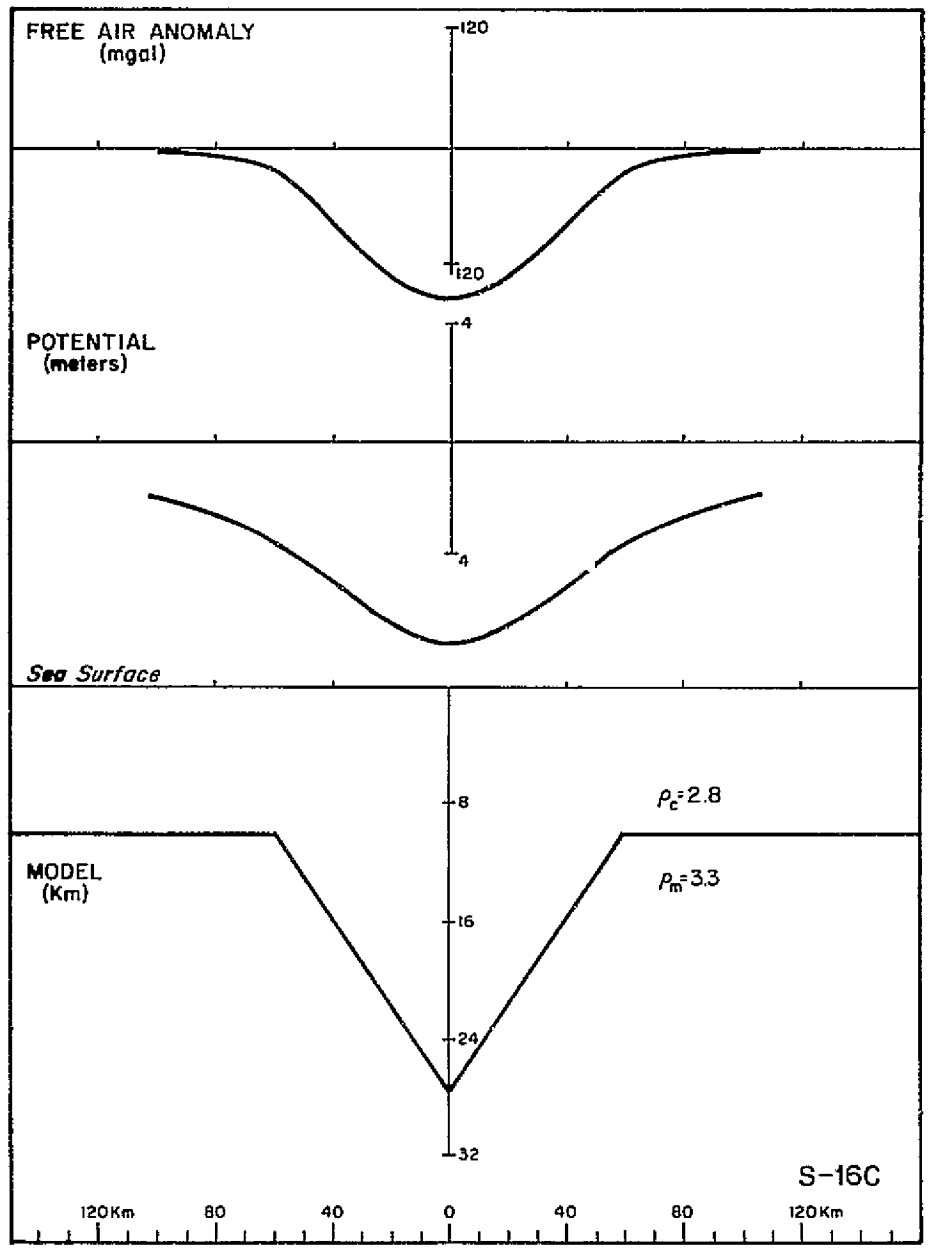
FREE AIR ANOMALY
(mgal)
120
120
POTENTIAL
(meters)
4
4
Sea Surface
8
ρ_c=2.8
MODEL
(Km)
ρ_m=3.3
16
24
32
S-16C
120Km
80
40
0
40
80
120Km